Practical approach to XANES data analysis:

*How to understand **local atomic structure, coordination chemistry** and **electronic state** from XANES spectra*

Carlo Meneghini

carlo.meneghini@uniroma3.it

"Gilberto Vlaic" XVII School on Synchrotron Radiation: Fundamentals, Methods and Applications

Muggia (Italy), 16 - 26 September 2024

XAFS is a *local sensitive*, *chemical selective* **probe**

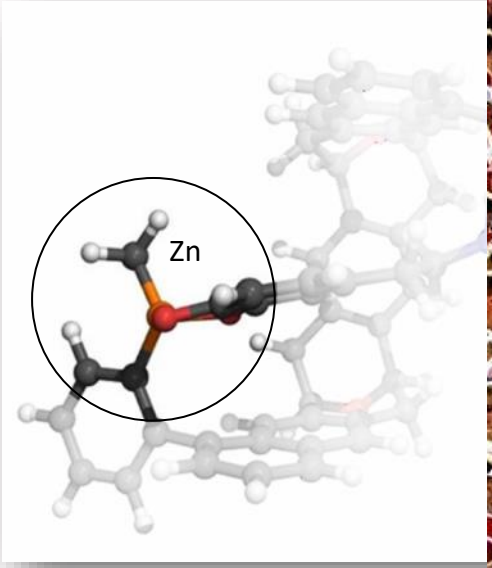

Subjective (Absorber) point of view of the local atomic structure in your sample

XAFS is a *local sensitive*, *chemical selective* **probe**

which can provide **structural**, **electronic** and even **magnetic** information abouot specific elements (absorbers)

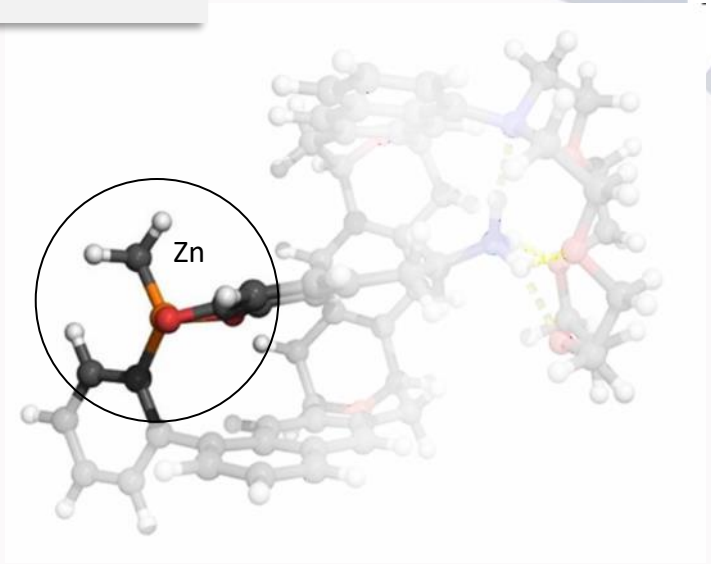

- Applicable to materials in **any aggregation state:** gas, liquid, solid, single crystals, powders, amorphous, nanostructures, etc....
- Measurable from **bulk** to the highest **diluted** samples (micro- and nano-molar)
- **Versatile** (bulk, surfaces, layered structures, quantum structures, etc...)
- (*relatively*) **simple** experimental set-up and easy data collection
- **Fast** (*min*) and **ultrafast** (*ps*) data collection
- **Directional sensitivity** (polarized XAS): structural anisotropy
- **Element selective Magnetic** state sensitive (**XMCD**)

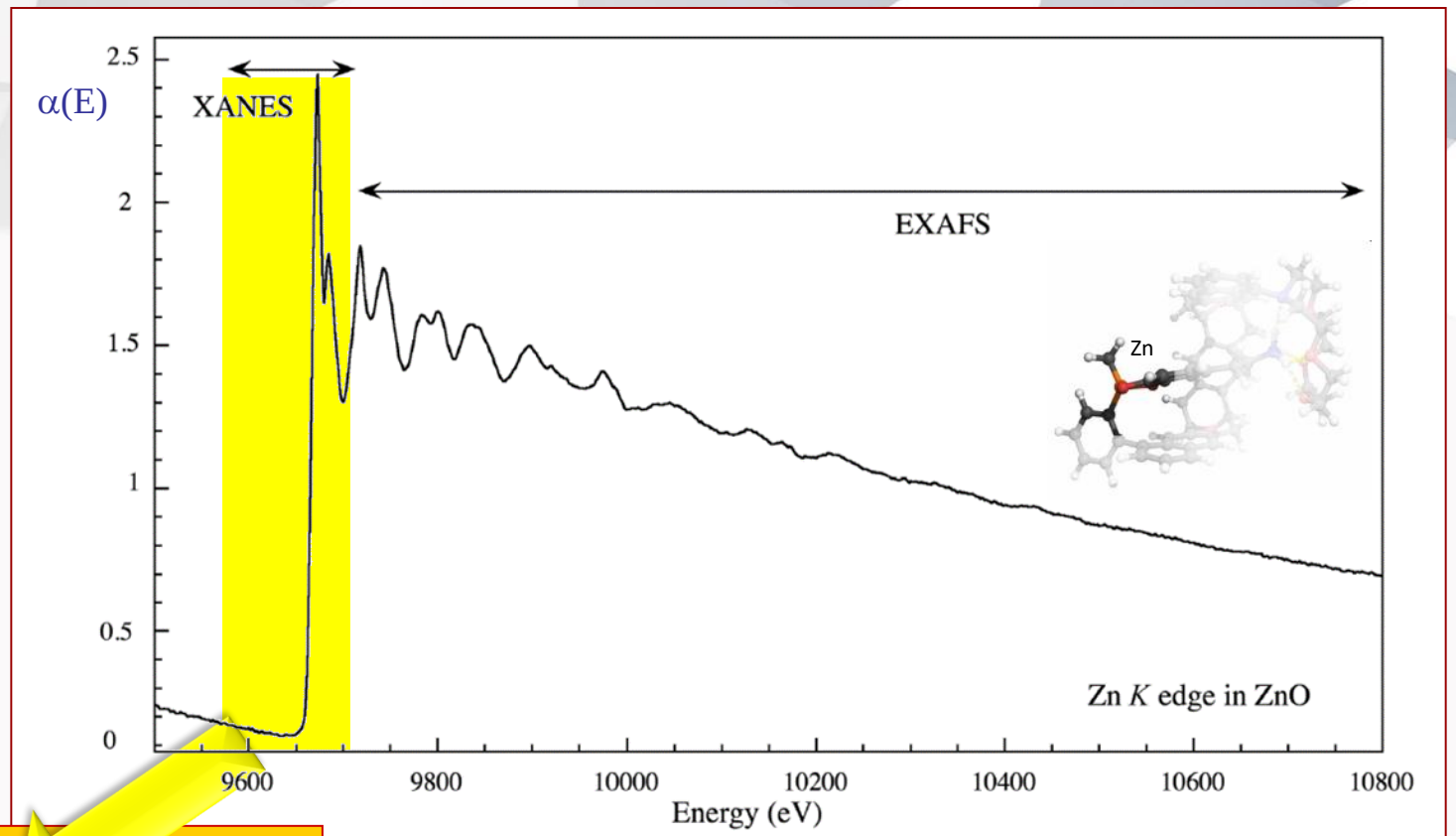

XANES region:

- **lack of an analytical expression**
- long computation time
- **Good theoreticians and data analysis skills**

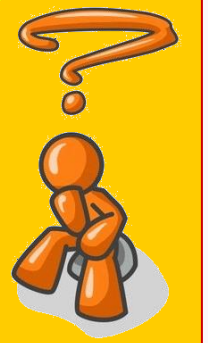

EXAFS region: simple analytical formula suited for data fitting and ***easy*** structural refinement

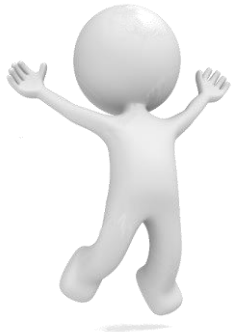

$$\chi(k) = \frac{1}{k}\sum_j A_j(k,R_j)\sin\left(2kR_j + \phi_j(k)\right)$$

$$A_j(k,R_j) = \frac{S_o^2 N_j}{R_j^2}\left|f_j(k,R_j)\right| e^{-2k^2\sigma_j^2} e^{-\frac{2R_j}{\lambda}}$$

Advantages of XANES based probes

Compared to EXAFS

- XANES signal is **higher** than EXAFS
- Weaker damping due to **structural disorder**
- Restricted **energy range**
- Simpler/faster data collection
- **sensitive to**
  - **Electronic structure** (empty DoS)
  - symmetry of the coordination geometry

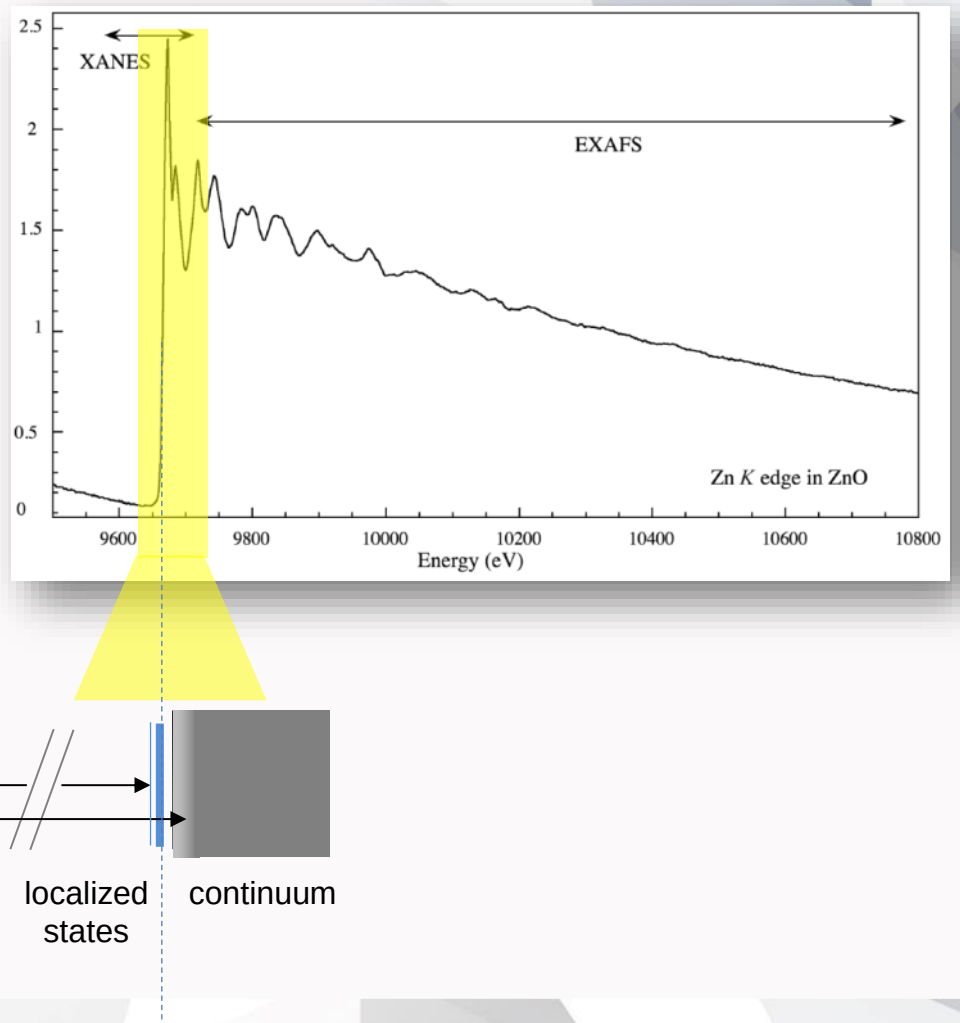

XANES signal is dense of electronic, structural and magnetic and information

XANES signal is stronger than EXAFS:

- less sensitive to data statistics, sample quality, beam intensity,
- can be measured on less concentrated samples,
- can be measured faster than EXAFS (time resolved experiments)

Damping of XANES signal due to structural disorder is weak:

- Extreme conditions experiments: High **T**, High **P**, High **H**....

Electronic structure (DoS) and structural topology:

- XANES features are especially sensitive to the valence state, coordination chemistry, ligand symmetry of the absorber.
- Can be used as fingerprint for chemical speciation in mixtures and inhomogeneous systems.

Restricted energy range around the edge:

- Measurements at low energies (Si, S, Cl, ...)
- Fast data collection (time resolved XAS)
- XANES Microprobes (mapping) with sub-micrometer resolution

Chemical selective Magnetic information

- X ray Magnetic Circular Dichroism (XMCD) signal is an element specific probe for magnetism
- Sum rules at $L_{2,3}$ edges allow distinguishing orbital and spin contributions to the magnetic moment of the photoabsorber

XANES theory is complex

- lack of an analytical expression
- long computation time
- Good theoreticians and data analysis skills

XANES signal is prone to *(relatively)* simple interpretation for *(relatively)* easy and fast (semi-)quantitative analysis

Deeper into the XANES region

XANES signal is prone to *(relatively)* simple interpretation for *(relatively)* easy and fast (semi-)quantitative analysis

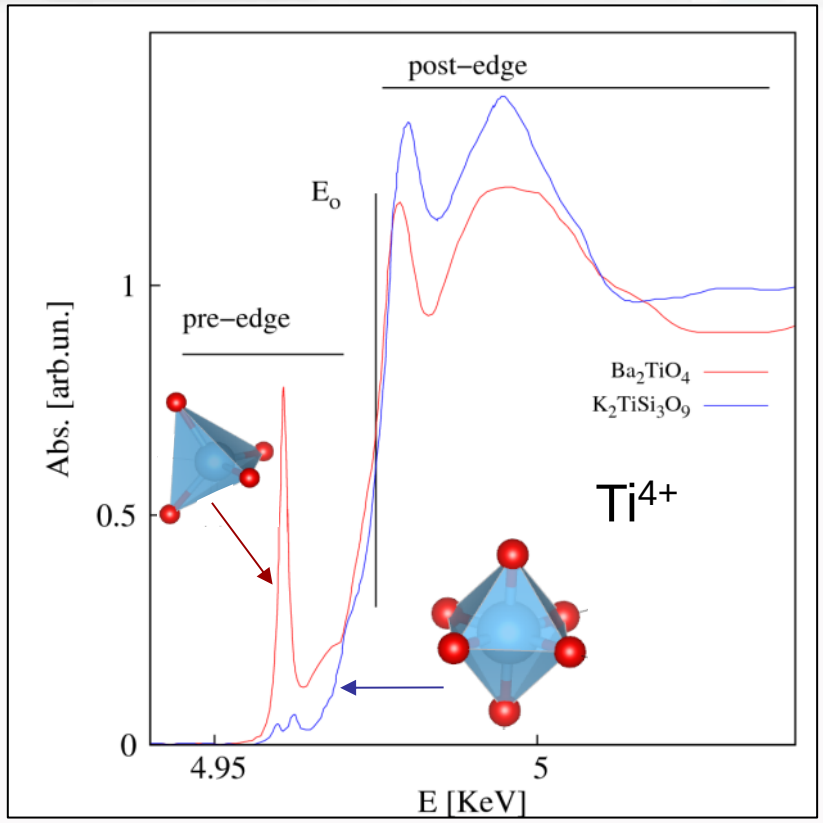

Local symmetry and XANES in Ti^{4+} compounds

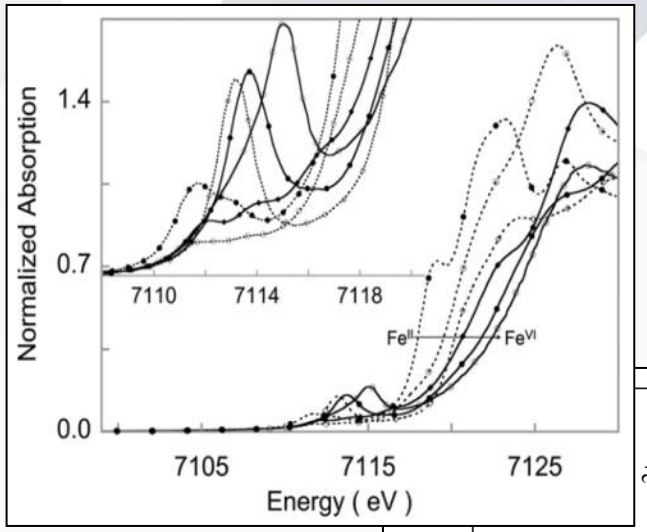

Fe K edges: representative XANES Fe in complexes

R. Sarangi, Coord. Chem. Rev. **257** 459–472 (2013)

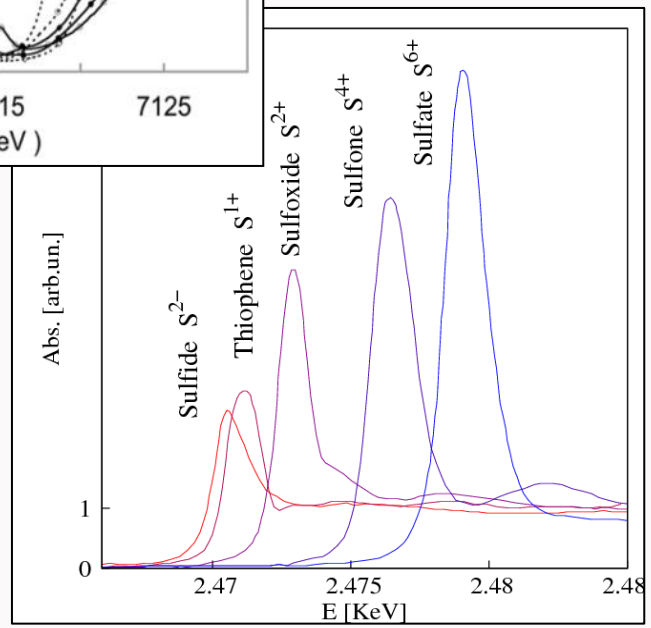

Sulphur K edges: chemical shift as a function of valence state of S-ions

XANES **features** are strongly related to the coordination chemistry & geometry: Number, kind and symmetry of the ligands

Edge position depends on the **oxidation state** of the absorber

XANES regions

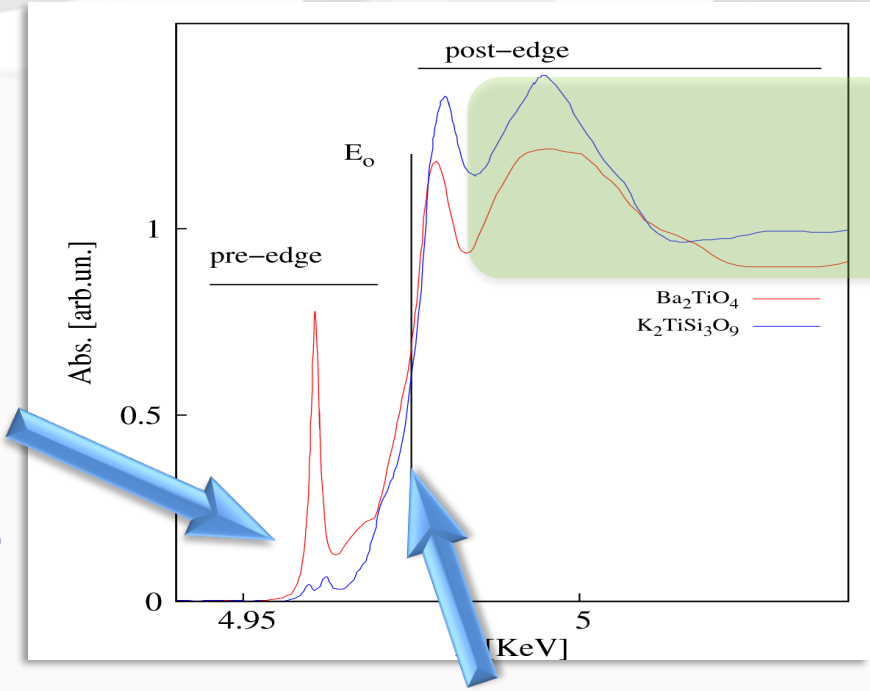

Pre-edge

caused by electronic transitions to **empty bound states** near the Fermi level.

electronic state and local coordination geometry around the absorber

Post-edge (XANES)

full multiple scattering (FMS)

Edge (E_o)

the onset of **continuous states**

E_o is a function of the absorber oxidation state.
It may increase by several eV per oxidation unit

Early research

The Pre-edge region

- Below the ionization continuum, transitions to bound states occur
- Each transition has a defined lines shape determined by the core-hole lifetime(Lorentzian) convoluted with the x-ray energy resolution (Gaussian)

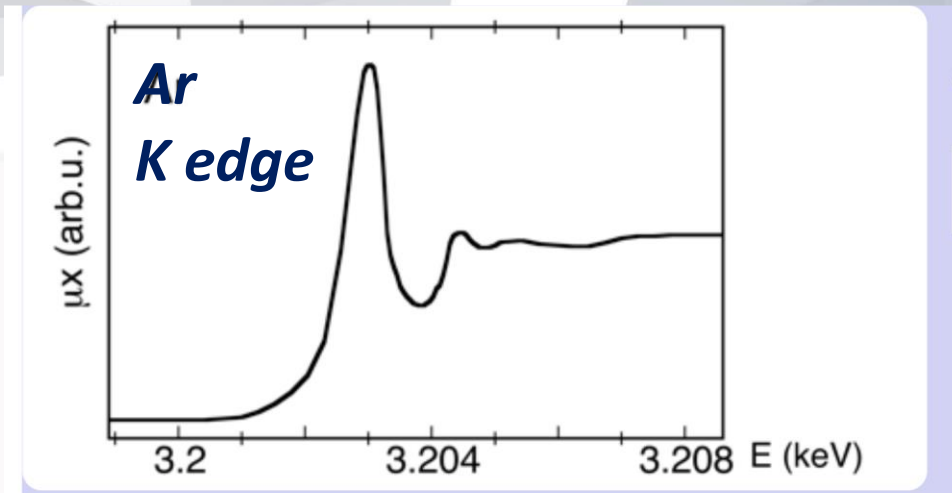

Experiment

L. G. Parratt,
Phys. Rev. 56, 295 (1939)

Energy resolution ~ 0.6 eV

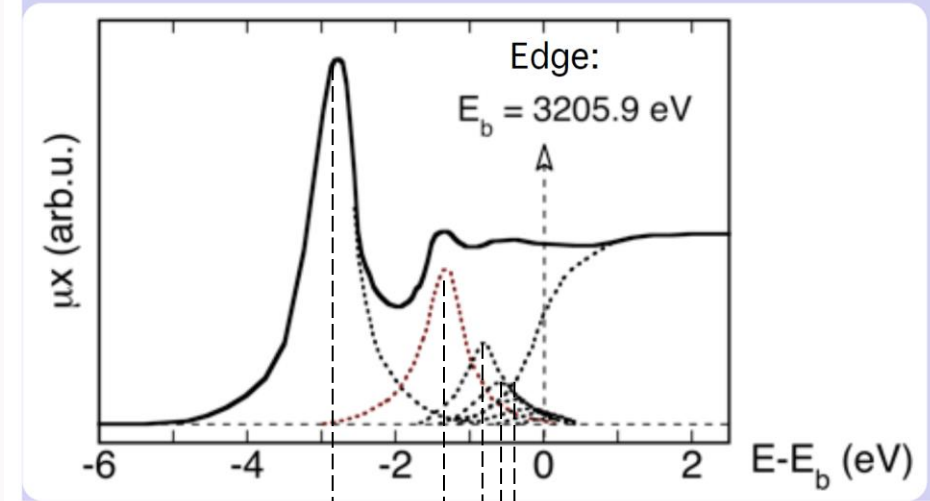

Interpretation:
- Rydberg levels
- edge to continuum

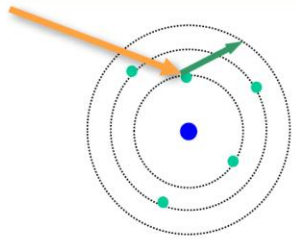

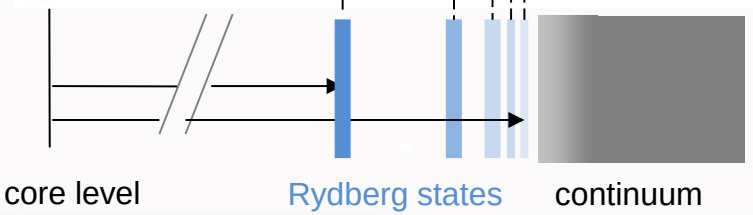

The Pre-edge region

electronic transitions to **empty bound states** near the Fermi level.

XANES signal is complementary to the **XPS**, probing the occupied density of states.

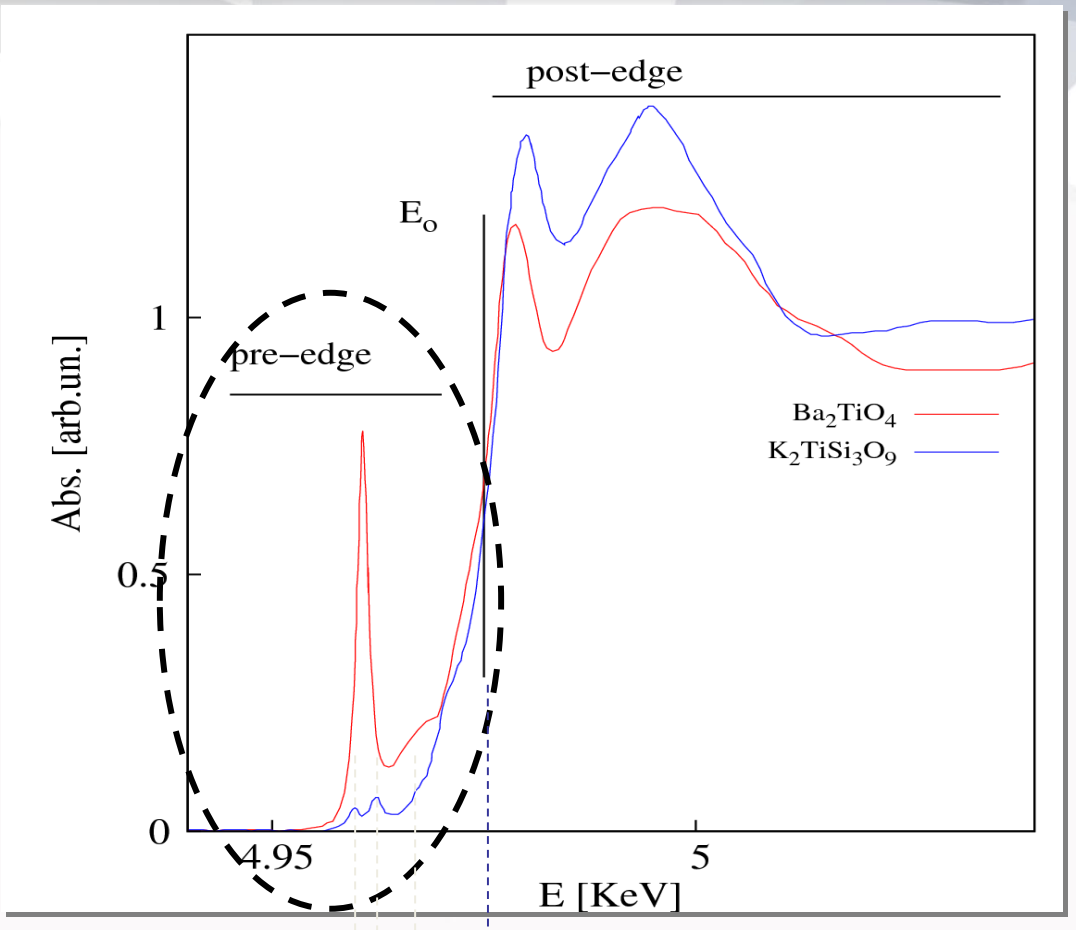

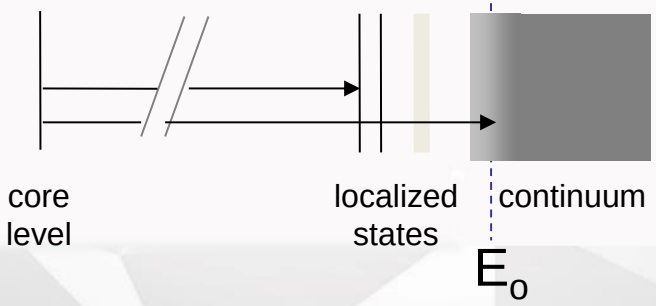

Empty state density

K *pre-edges* in 3d metal oxides: intensity *vs* empty electronic states

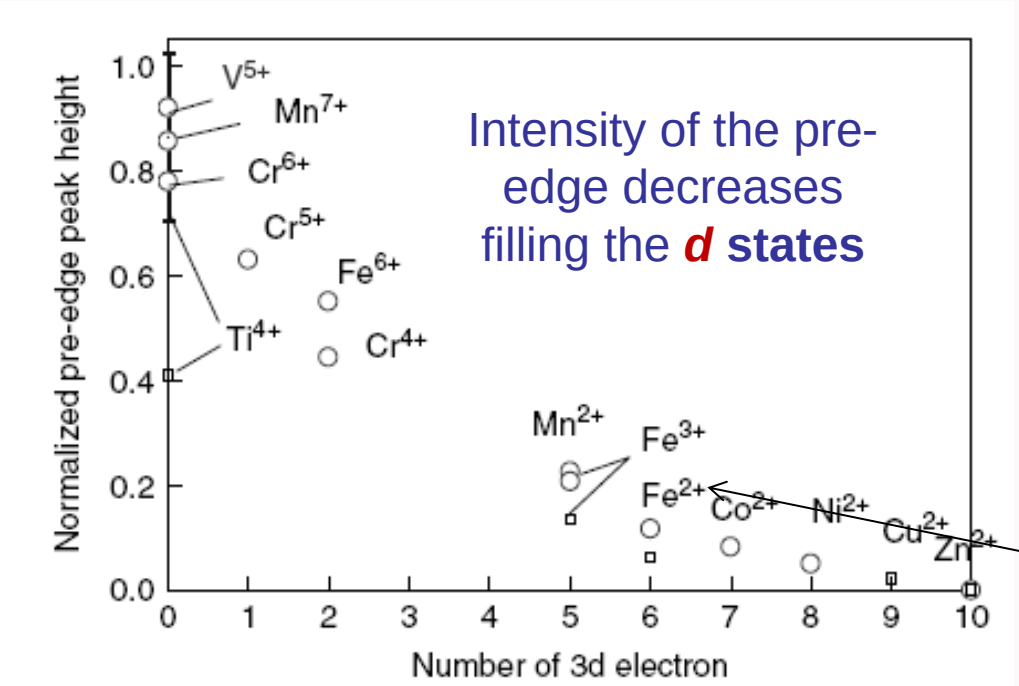

Example:
Pseudo Tetrahedral Metal Complexes ***M*(B(3-isopropyl-pyrazol-1-yl)4)2**

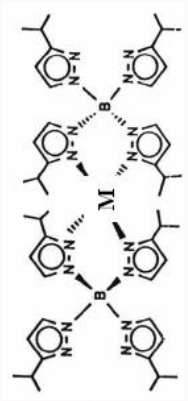

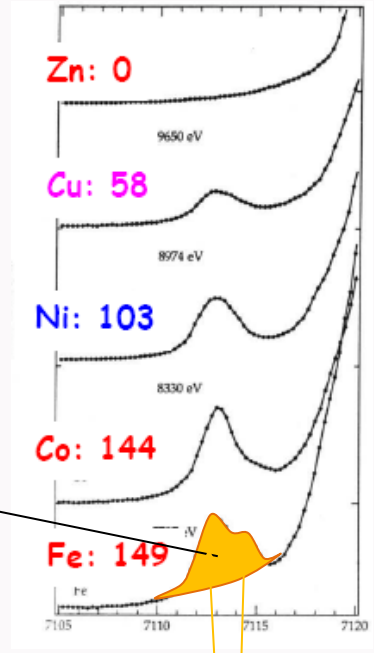

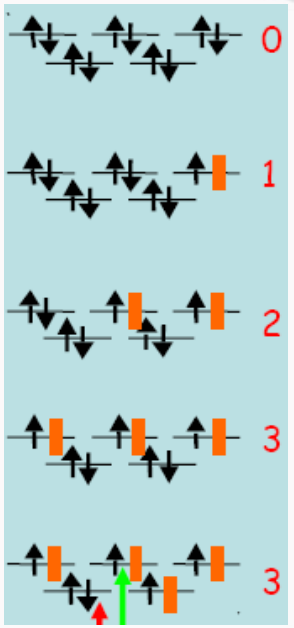

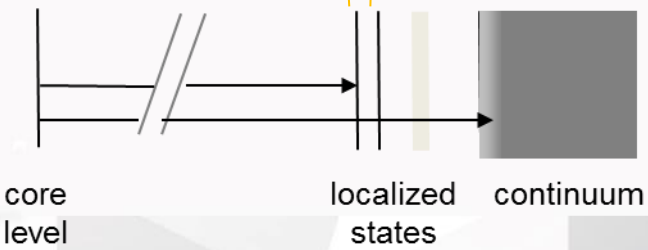

Pre-edge features are caused by electronic transitions (***mainly dipole***) to empty states close to the Fermi level.

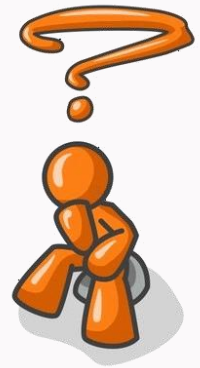

But...
These are 3d states!

Fe K edges in minerals

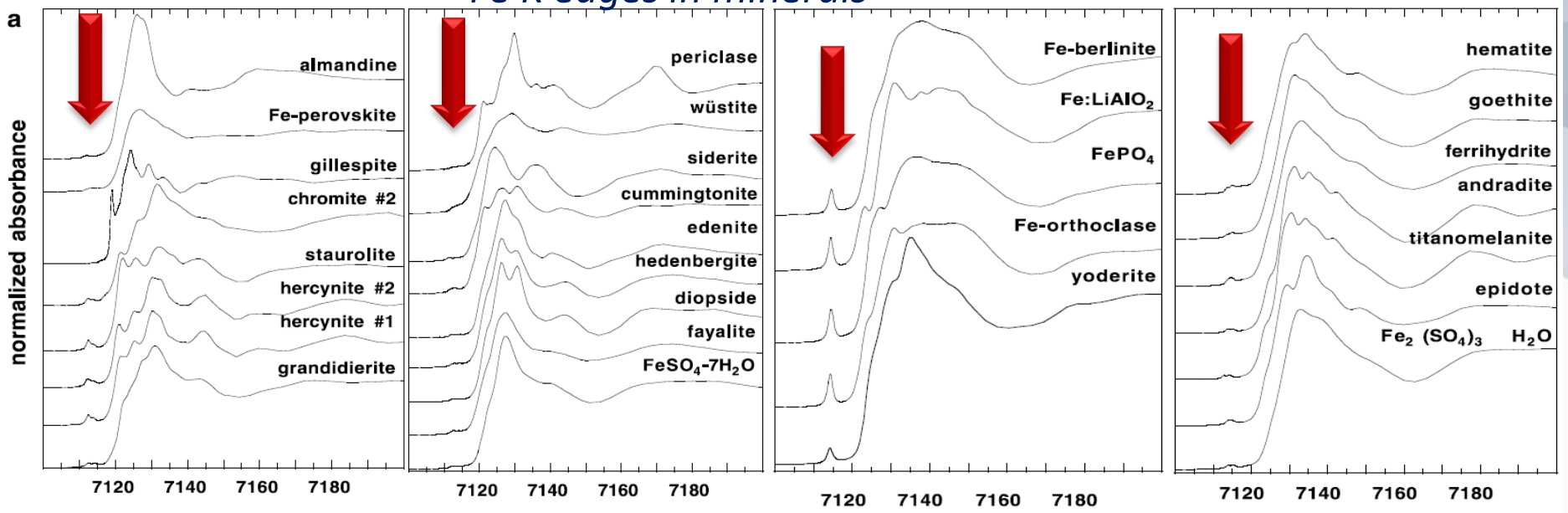

Fe^{2+} in 4, 5, 6 coord. sites | Fe^{2+} in 6 coord. sites | Fe^{3+} in 4, 5 coord. sites | Fe^{3+} in 6 coord. sites

M. Wilke, F. Farges et al. *American Mineralogist, Volume 86, pages 714–730, 2001*

Fe K pre-edge may be different as a function of Fe **oxidation** state **and coordination** number

Ti K edge spectra in Ti^{4+} compounds

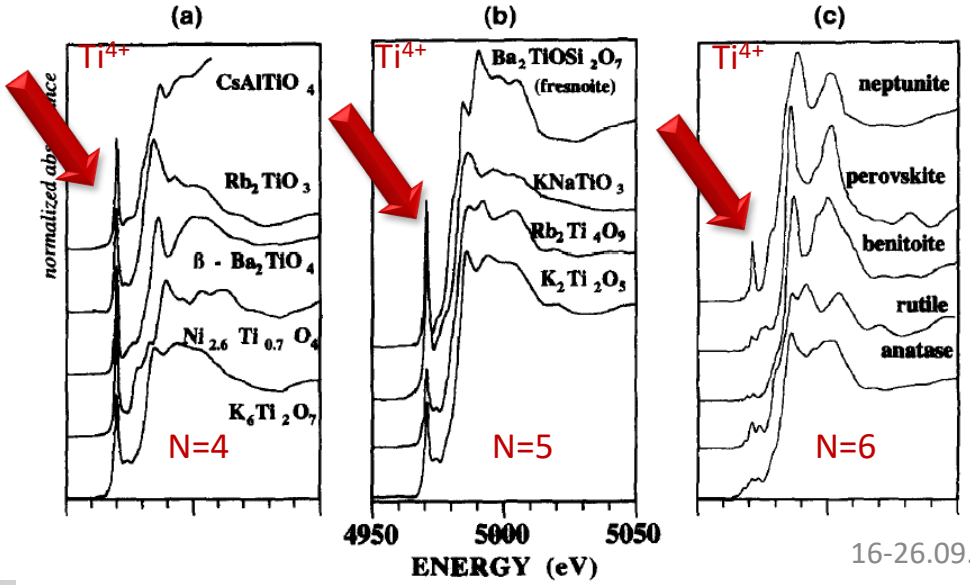

Ti K pre-edge peak in **4-**, **5-** and **6-**fold coordinated **Ti^{4+}** compounds have **different shape**

6. Farges F, Brown GE, Rehr JJ. *Geochim. Cosmochim. Acta* 1996; 60: 3023.

Pre-edge features come from transitions to bound electronic levels below the continuum threshold

Ti K edge

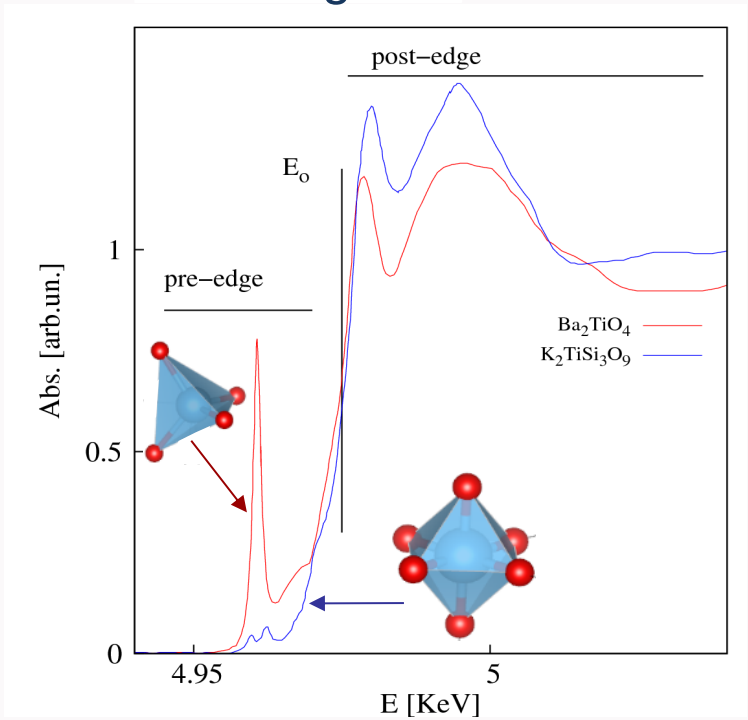

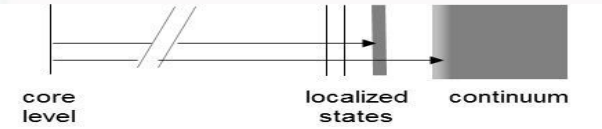

The XANES features of the same ions, even in the same oxidation state, **may behave** differently in different compounds…

… as a function of the absorber **oxidation state** and **coordination geometry**

The XANES features are **fingerprints for specific compounds**

Cu K edge

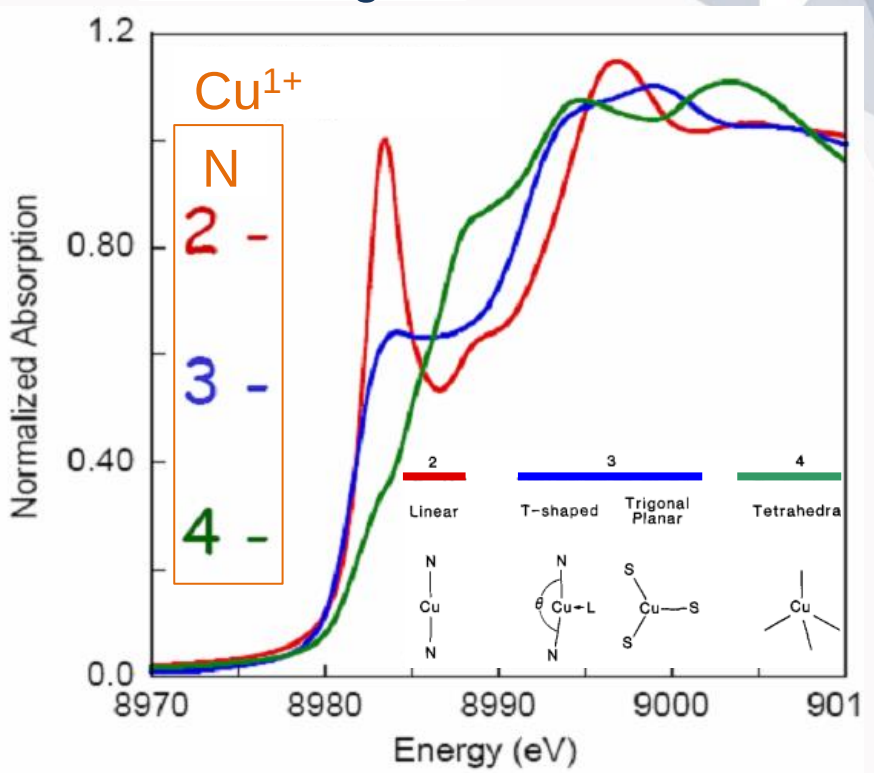

R. Sarangi, Coord. Chem. Rev. **257** 459–472 (2013)

pre-edge features (Fe examples)

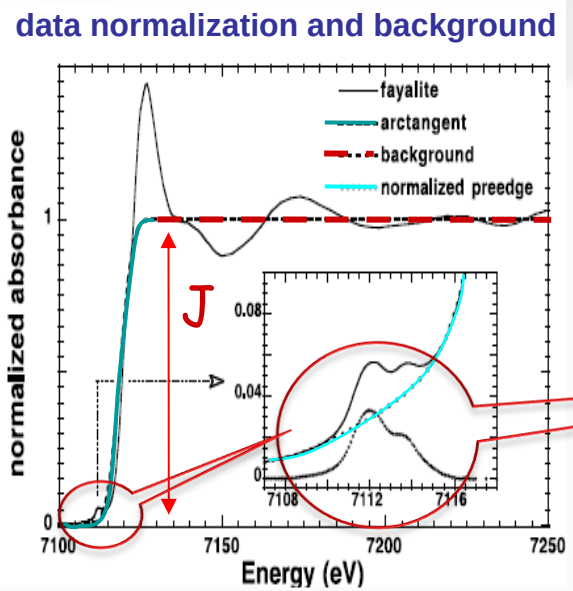

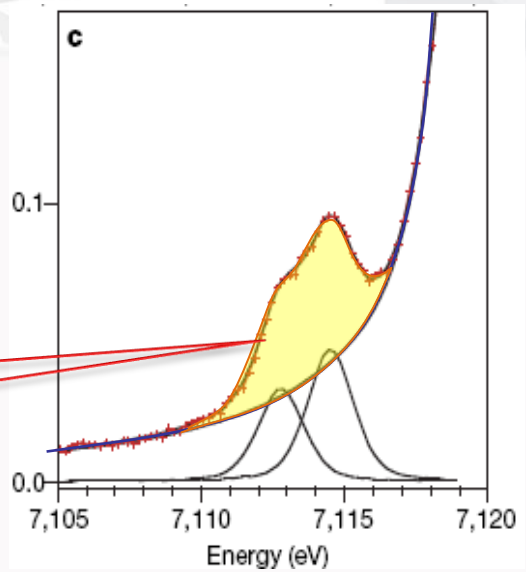

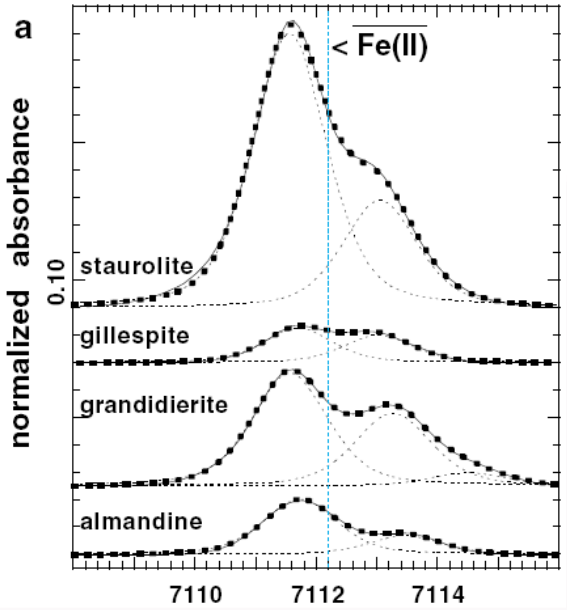

normalization: Jump = 1

Arctangent or Sigmoid: transitions to continuum states,

peaks: transitions to localized states

Pseudo-Voigt shaped peaks take into account for the convolution of true peak shape (Lorentzian contribution) with the experimental energy resolution (Gaussian contribution)

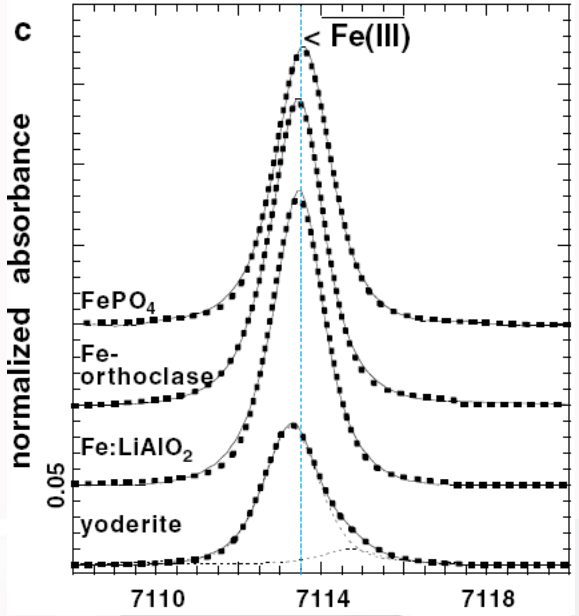

M. Wilke, F. Farges et al.

American Mineralogist, Volume 86, pages 714–730, 2001

The Iron case: the average valence and coordination chemistry from the pre-edge peak shape/position

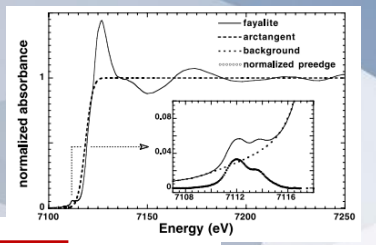

American Mineralogist, Volume 86, pages 714–730, 2001

Oxidation state and coordination of Fe in minerals: An Fe *K*-XANES spectroscopic study

MAX WILKE,[1,*] FRANÇOIS FARGES,[1,2] PIERRE-EMMANUEL PETIT,[3] GORDON E. BROWN JR.,[2,4] AND FRANÇOIS MARTIN[5]

900 cit. (sept.2019, Scholar Google)

Fe^{2+}

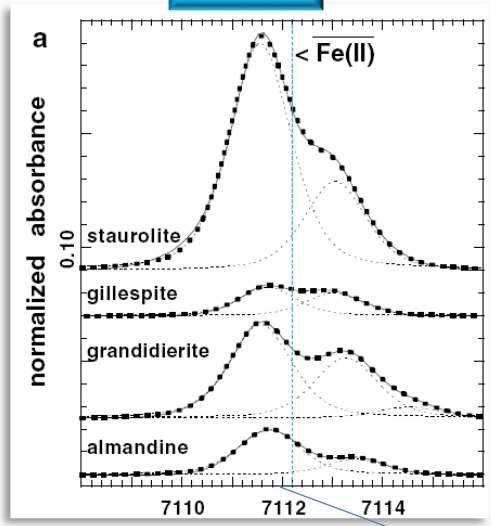

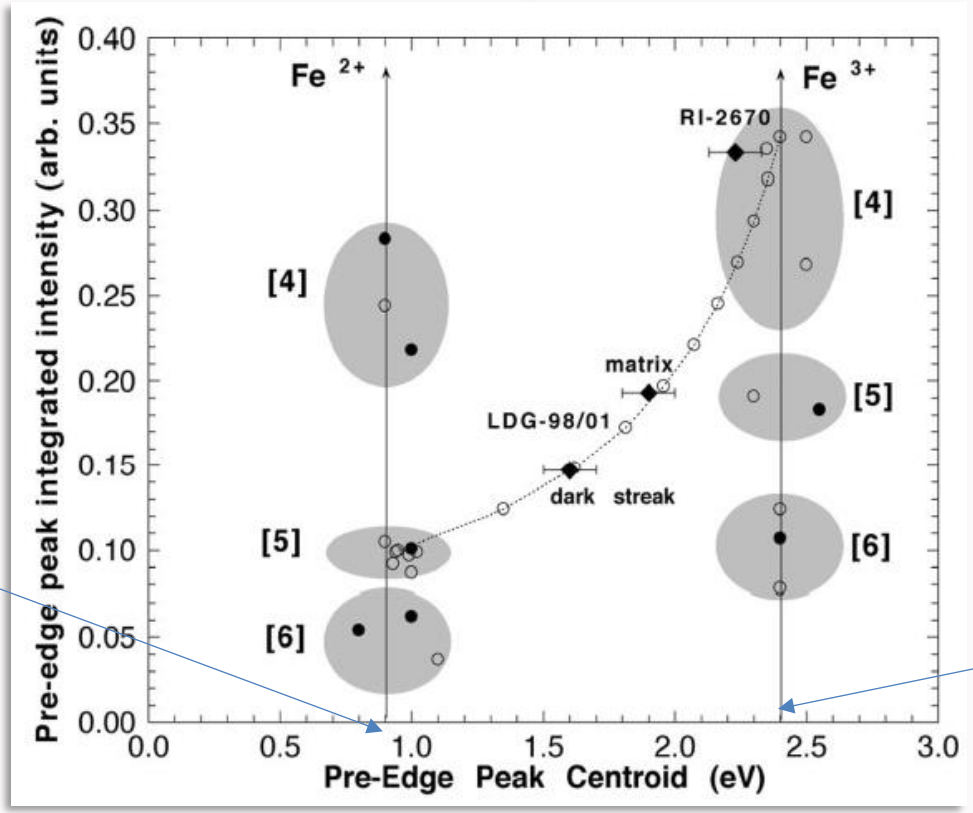

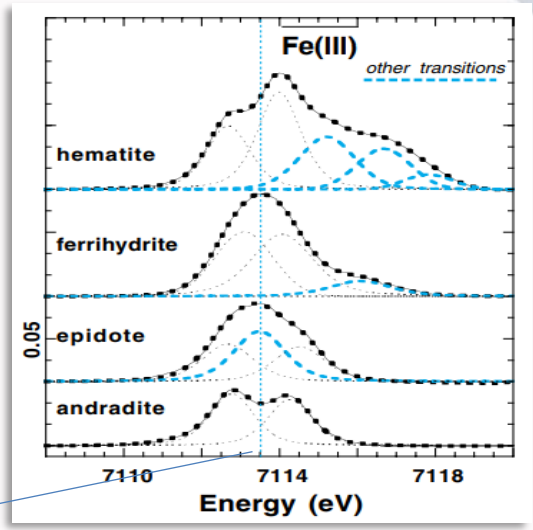

Fe^{3+}

Pre-edge…

Area → average Fe **coordination number**

Centroid → average Fe **valence**

The case of Fe in metallo-proteins: Ibuprofen/warfarin induce V to VI Fe coordination transition in HSA

Biophysics

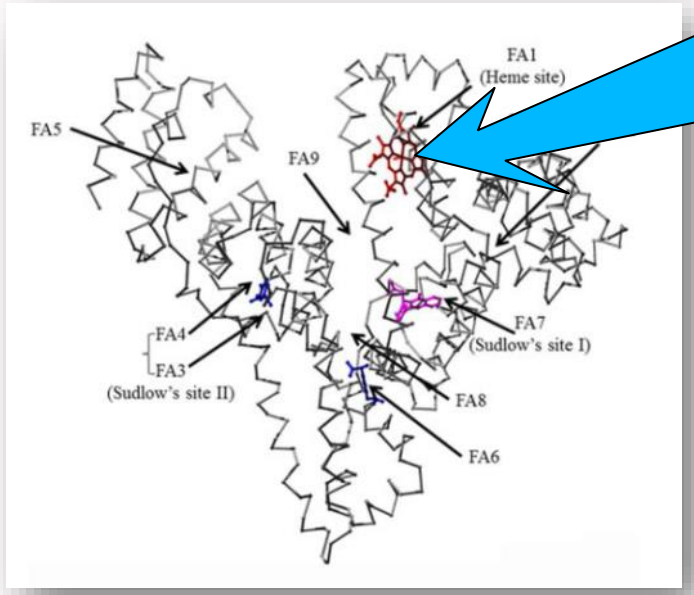

Human Serum Albumin

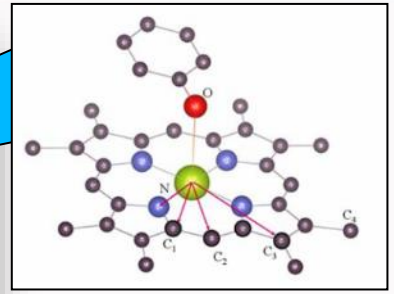

Heme (Fe) site

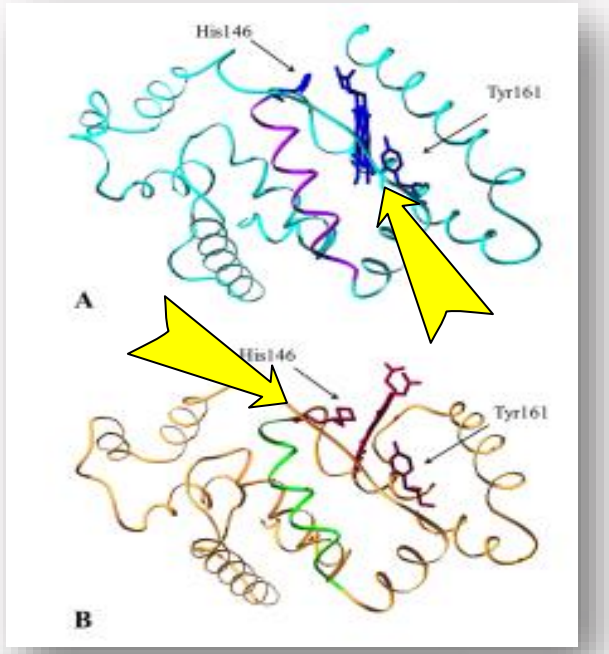

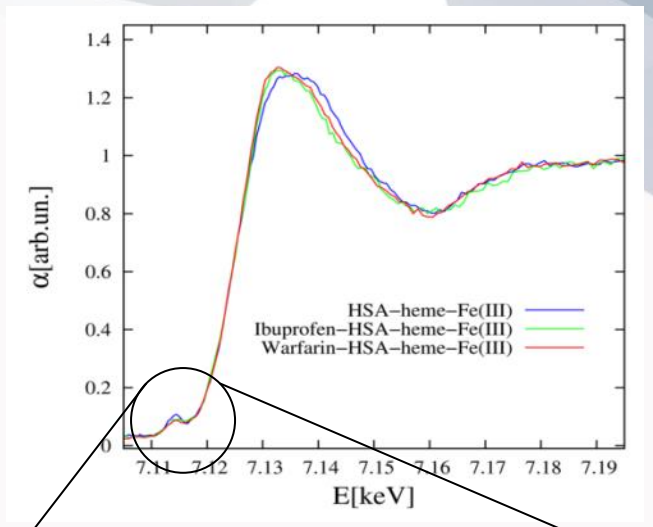

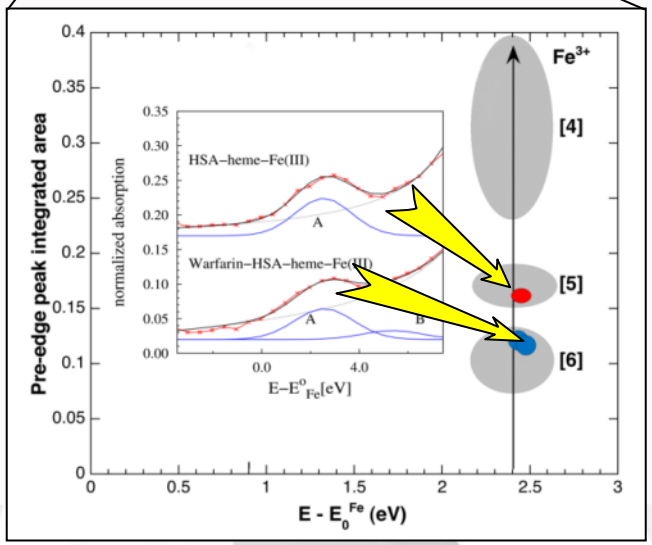

OPEN ACCESS Freely available online PLOS ONE

The Five-To-Six-Coordination Transition of Ferric Human Serum Heme-Albumin Is Allosterically-Modulated by Ibuprofen and Warfarin: A Combined XAS and MD Study

Carlo Meneghini[1*], Loris Leboffe[1,2*], Monica Bionducci[1], Gabriella Fanali[3], Massimiliano Meli[4], Giorgio Colombo[4], Mauro Fasano[3], Paolo Ascenzi[2,5*], Settimio Mobilio[1]

Fe in archaean rocks

Geophysics

Geolgy

reference samples with different Fe^{3+} over total Fe (ΣFe) content

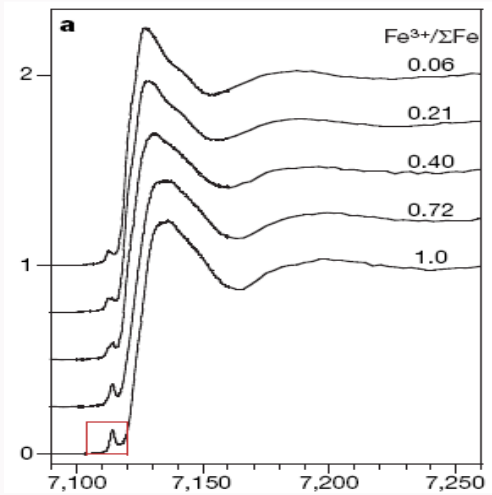

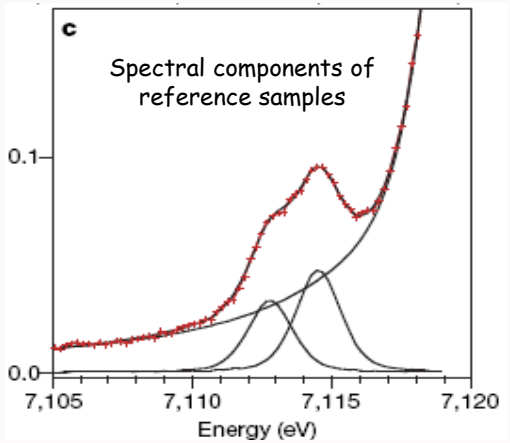

Andrew J. Berry

Vol 455|16 October 2008|doi:10.1038/nature07377

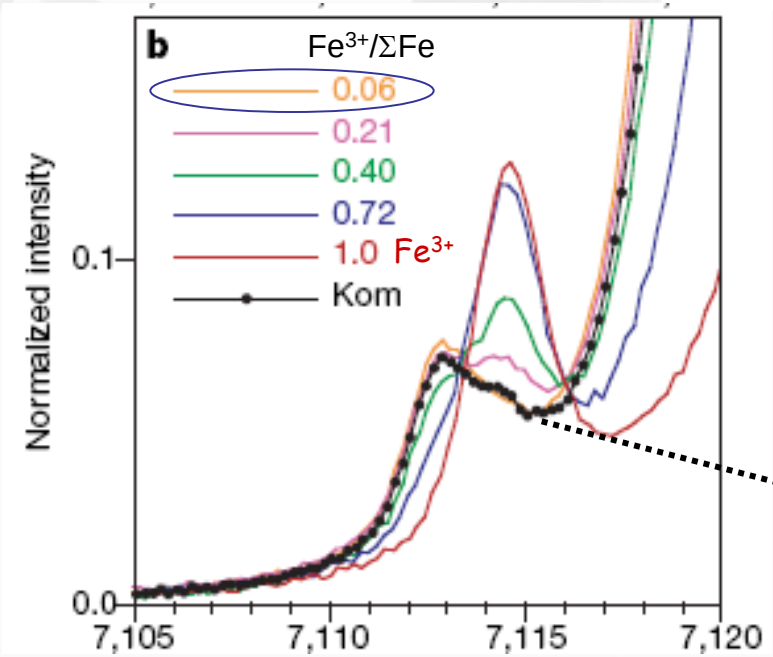

Samples: small inclusions (D~15 μm) of Belingwe komatiite in olivine minerals

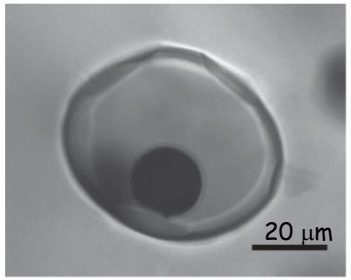

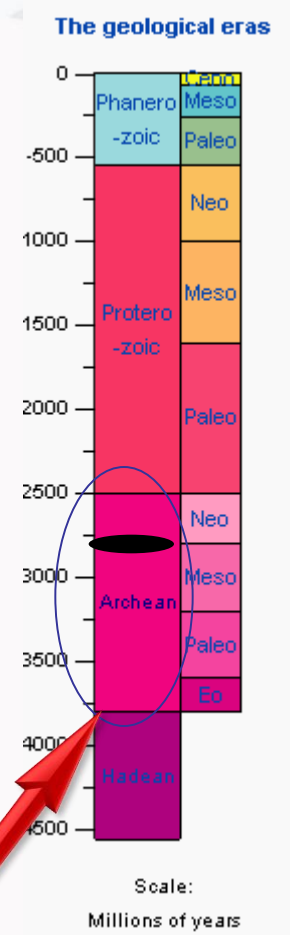

Our results support the identification of the Belingwe komatiite as a product of high mantle temperatures (~1,700 °C), rather tha melting under hydrous conditions (3–5-wt% water), confirm g the existence of anomalously hot mantle in the Archaean era.

Ti: *the average **valence** and **coordination** chemistry*

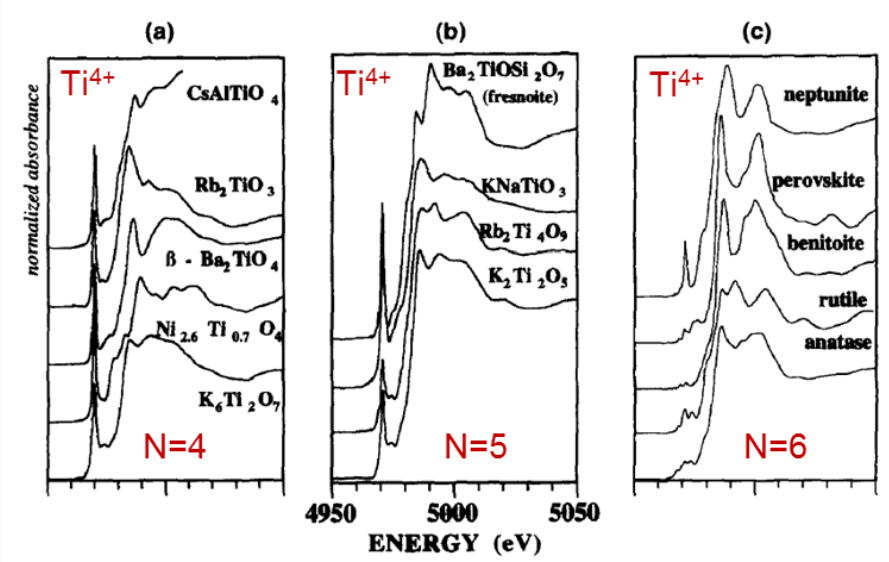

coordination number and **valence state** from the position & area of the pre-edge peaks

6. Farges F, Brown GE, Rehr JJ. *Geochim. Cosmochim. Acta* 1996; 60: 3023.

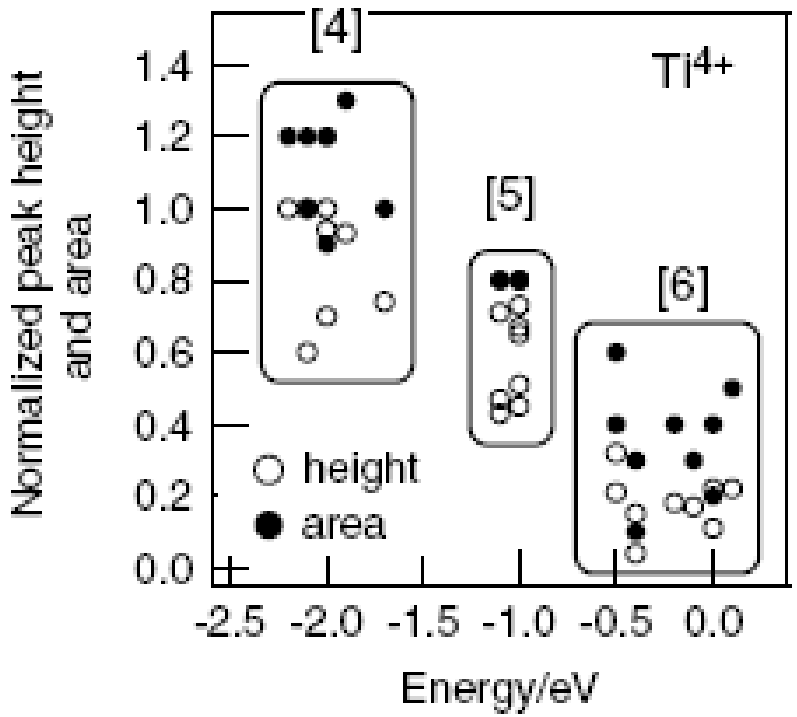

Ti pre-edge main peak intensity and area as a function of coordination number

.... and **Vanadium**

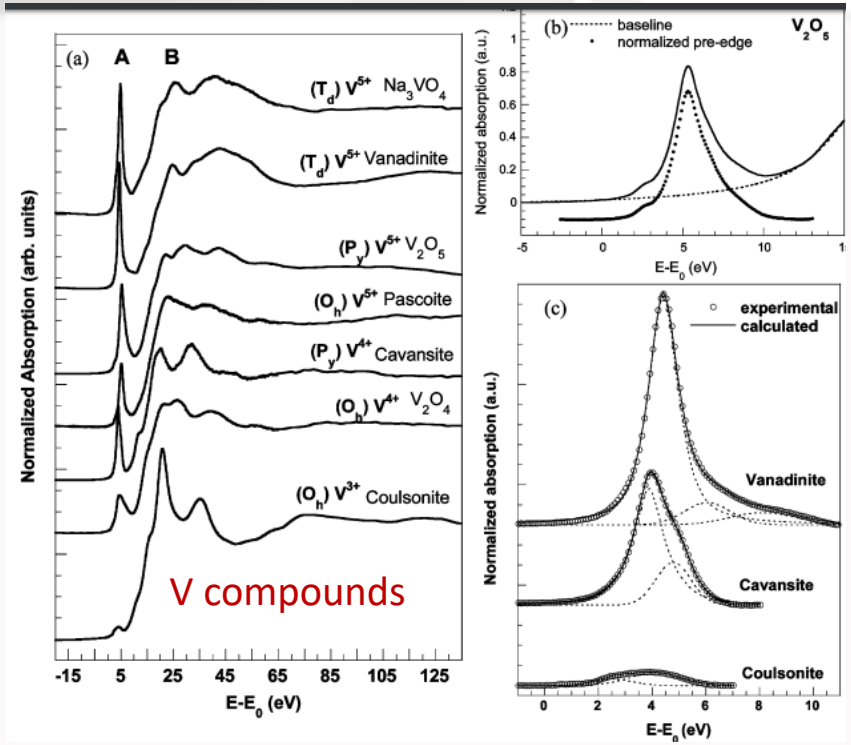

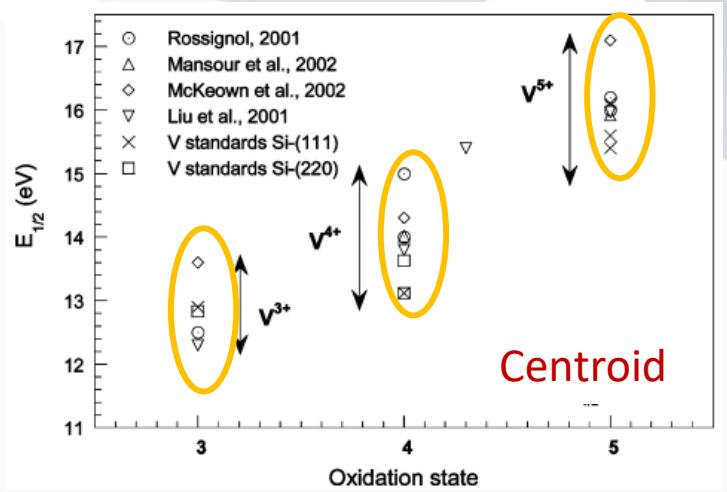

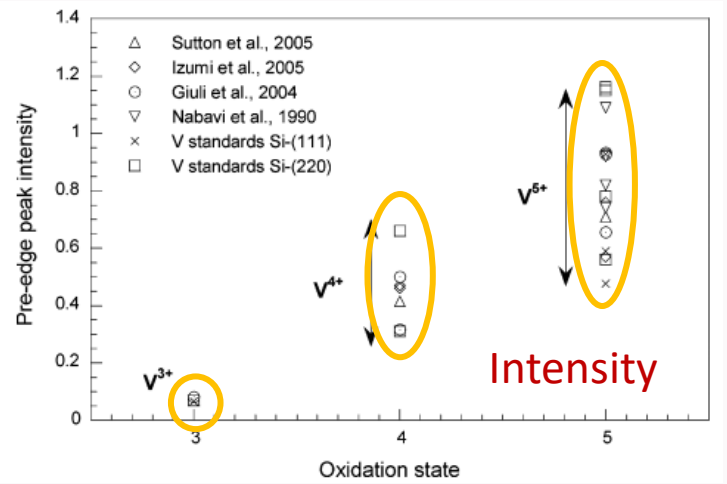

J. Phys. Chem. B **2007**, *111*, 5101−5110 **5101**

New Methodological Approach for the Vanadium K-Edge X-ray Absorption Near-Edge Structure Interpretation: Application to the Speciation of Vanadium in Oxide Phases from Steel Slag

Perrine Chaurand,*,† Jérôme Rose,† Valérie Briois,‡ Murielle Salome,§ Olivier Proux,||

K edges of 3d metal oxides: the origin of the pre-edge features

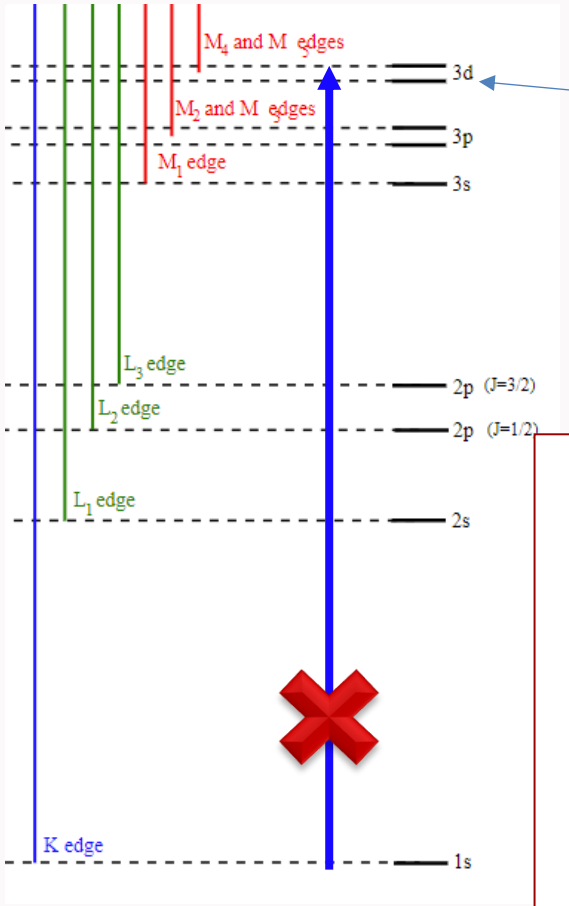

But...
These **are**
3d states!

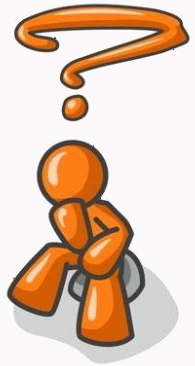

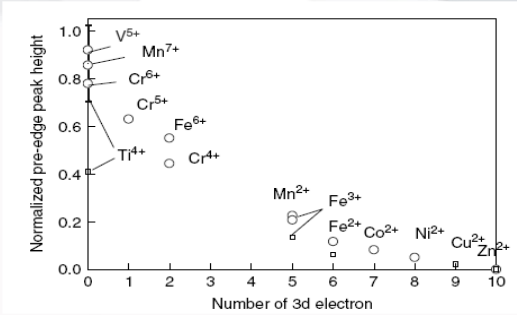

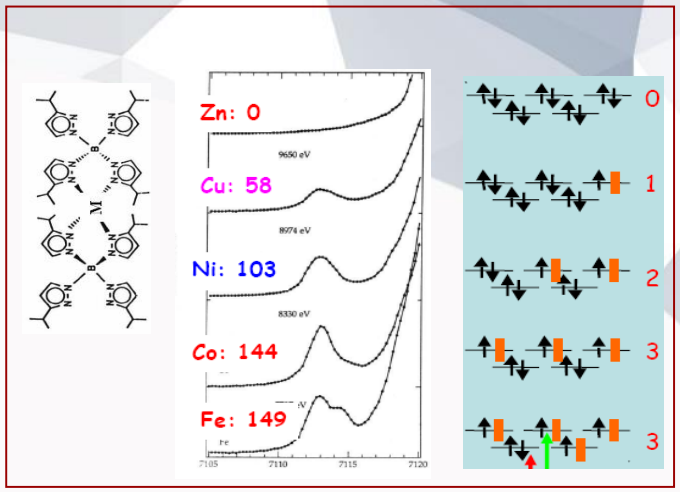

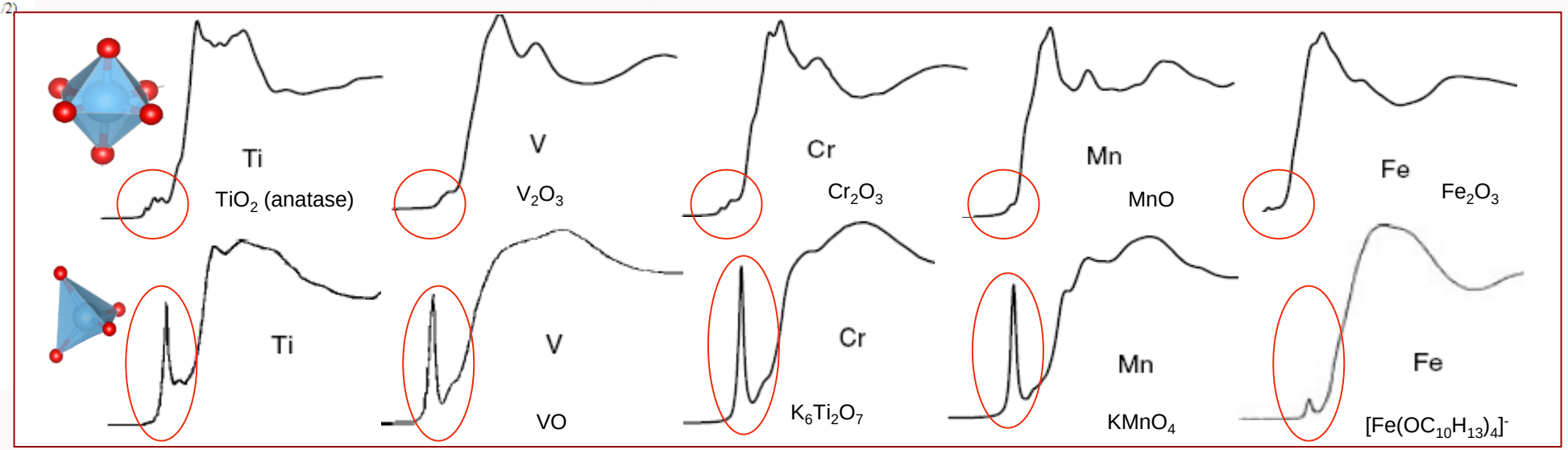

K edge + dipole selection rules = s → p transitions

$I_{s\to d}$ (quadrupole) ~ **10^{-2}** $I_{s\to p}$ (dipole)

crystalline field splitting of *d* atomic orbitals

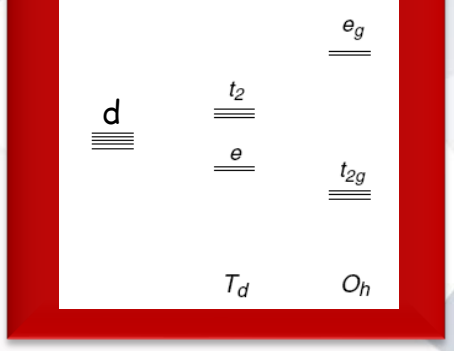

Hybridization mixes *p-d* states allowing for dipole allowed transitions to *empty p-components* of hybrid *pd* levels

Table 1. Lists of irreducible representations and the relating functions in T_d, O_h, and D_{4h} point groups

	T_d	
	p	d
A_1		$x^2+y^2+z^2$
A_2		
E		$(2z^2-x^2-y^2, x^2-y^2)$
T_1	(R_x, R_y, R_z)	
T_2	(x, y, z)	(xz, yz, xy)
	O_h	
	p	d
A_{1g}		$x^2+y^2+z^2$
A_{2g}		
E_g		$(2z^2-x^2-y^2, x^2-y^2)$
T_{1g}	(R_x, R_y, R_z)	
T_{2g}		(xz, yz, xy)
A_{1u}		
A_{2u}		
E_u		
T_{1u}	(x, y, z)	
T_{2u}		

Yamamoto *X-Ray Spectrom.* 2008; **37**: 572–584

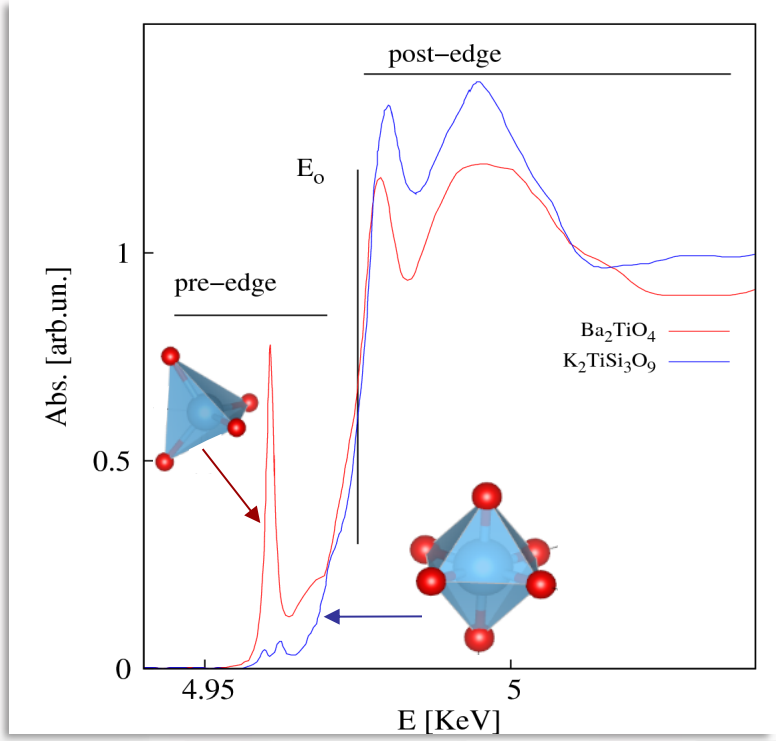

p-d *mixing and sensitivity to local symmetry of TiO_6 units*

Off centre displacement and **stretching** of the octahedron decreases the local symmetry (non-centro-symmetric) allowing **some degree of *p-d* mixing**, this affects the pre-edge peaks intensity

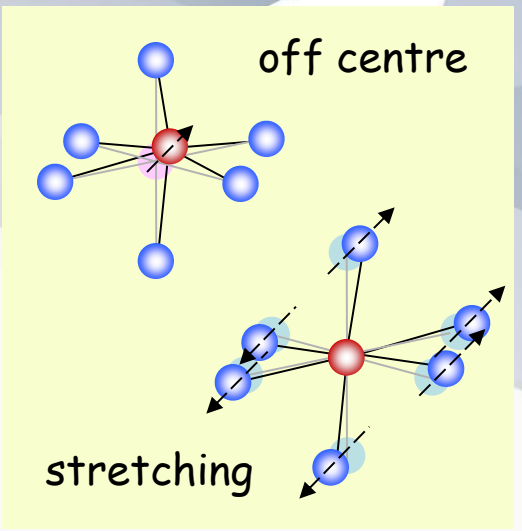

Regular TiO_6

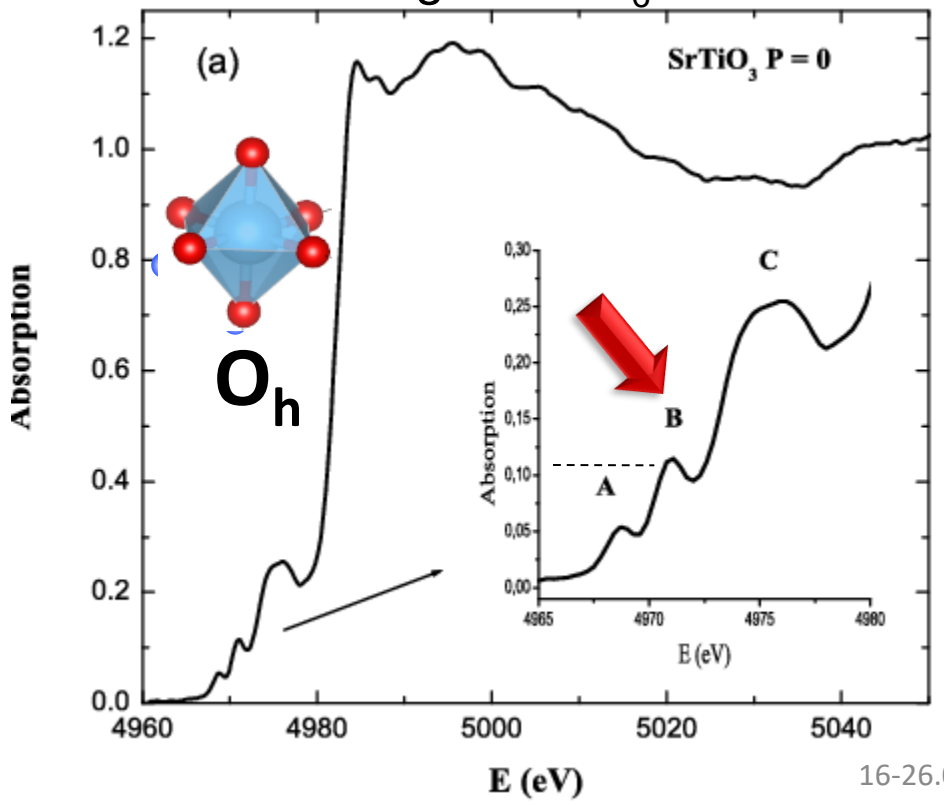

Distorted TiO_6

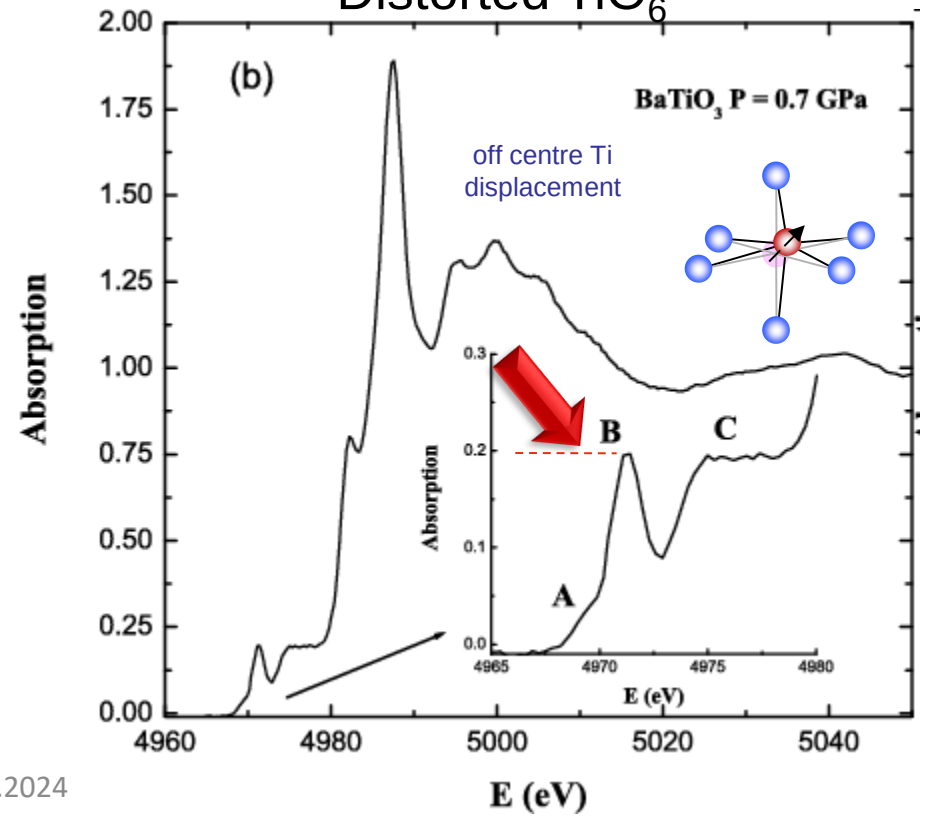

O_h

Example: hydrostatic pressure reduces TiO_6 distortions in $BaTiO_3$ and suppress ferroelectricity

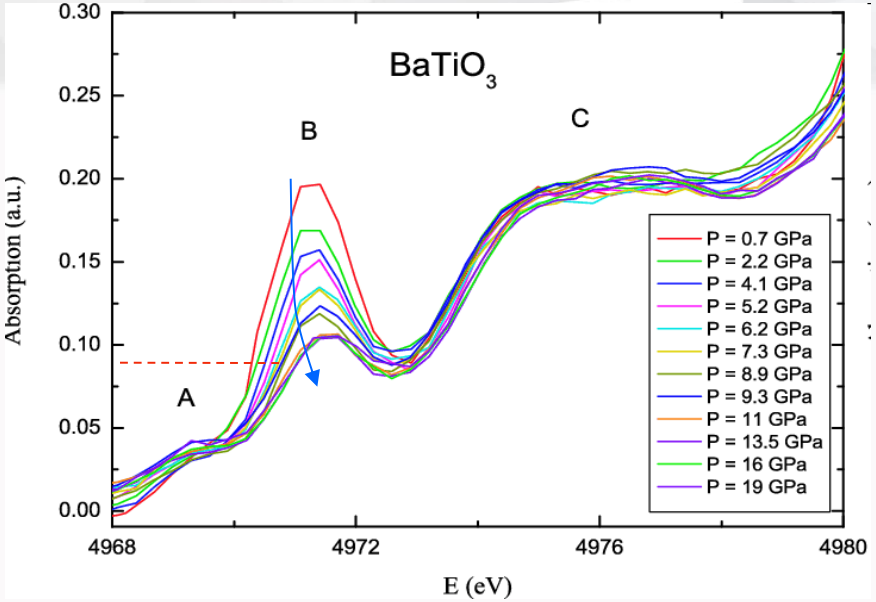

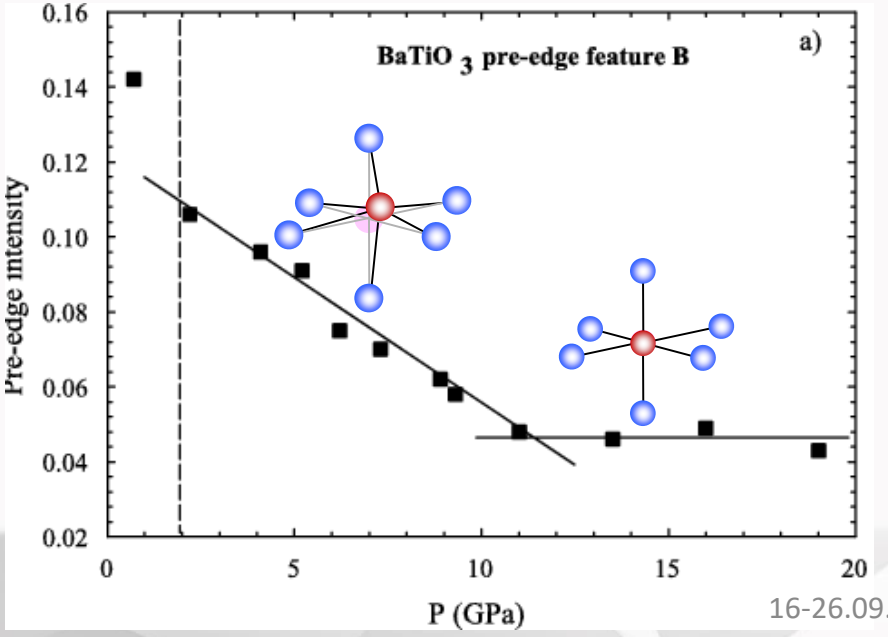

The decrease of B peak intensity signals the reduction of Ti atom displacement.

Above 10 GPa Ti must be at the center of a regular oxygen octahedron,

the hybridization of the Ti 3*d* electronic states with the 2*p* electronic states of the surrounding oxygen is at the minimum

Europhys. Lett., **74** (4), pp. 706–711 (2006)
DOI: 10.1209/epl/i2006-10020-2 J. P. Itié et al.

The Edge region:
Shape and position

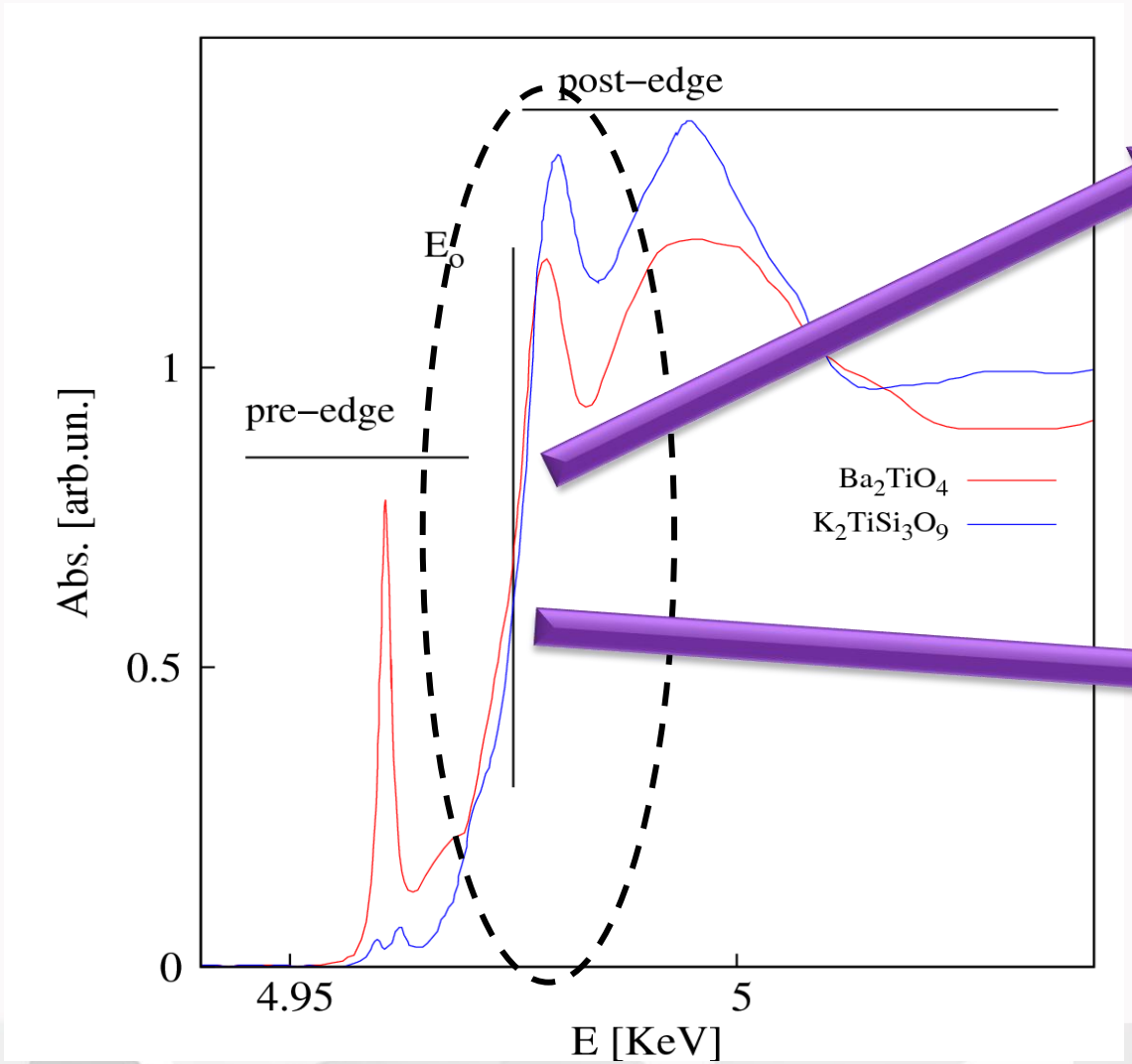

The edge position

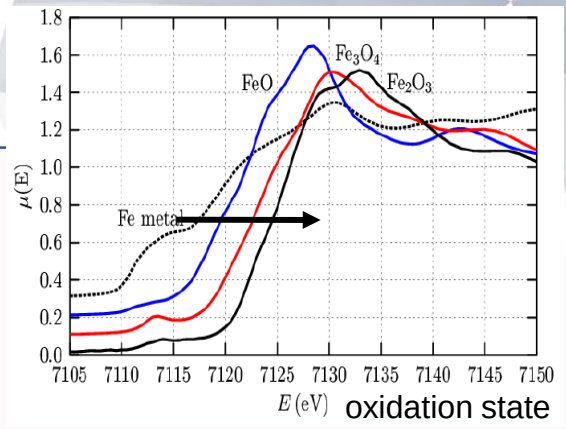

The shape of the edge

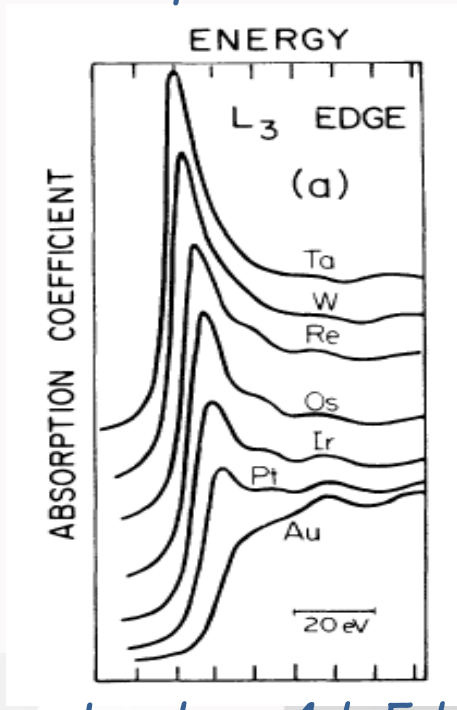

L edges 4d, 5d

The chemical shift (edge position) reveals the absorber oxidation state...

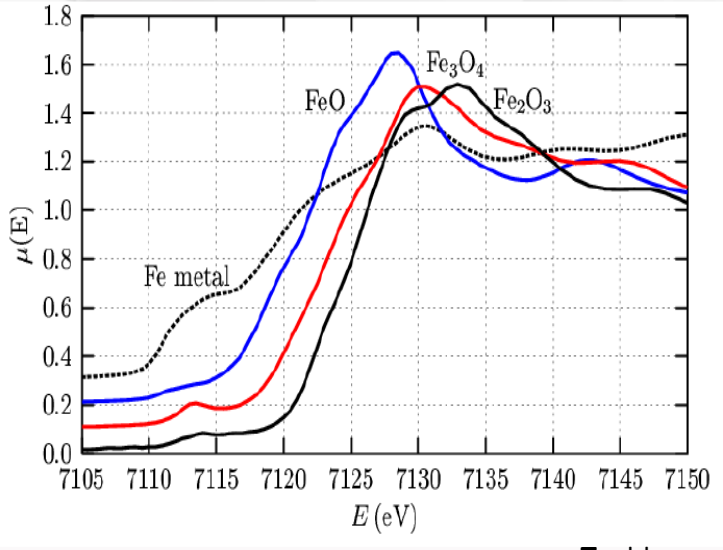

Higher the oxidation state

=

Higher the edge energy

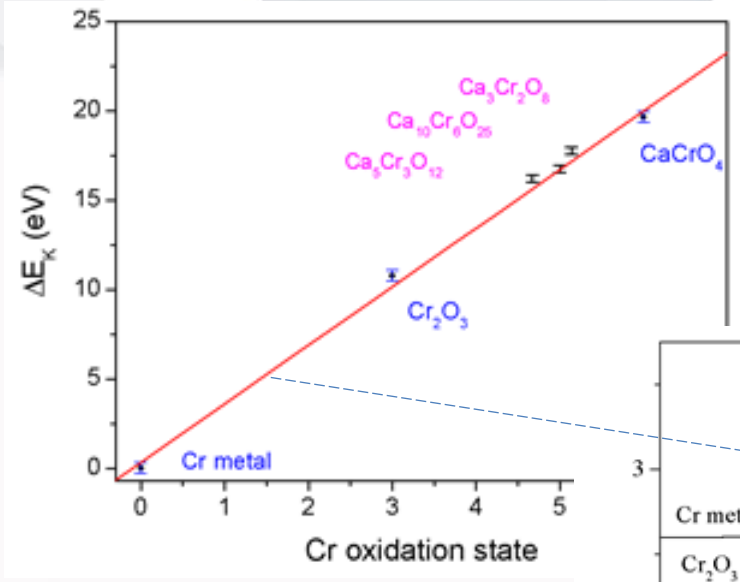

Cr K edge

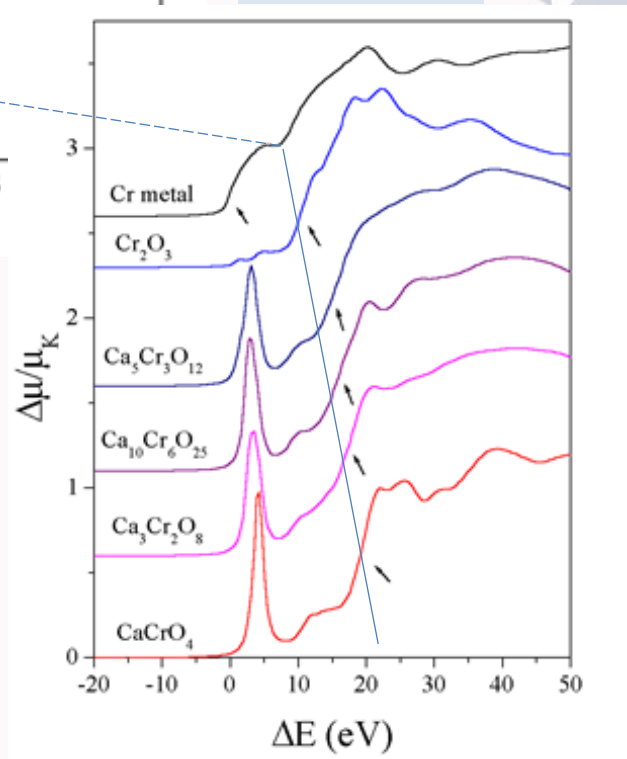

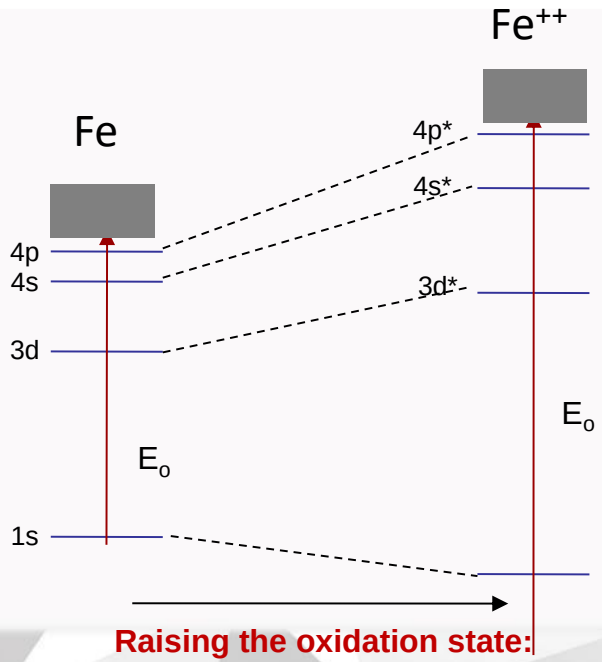

Raising the oxidation state:

1) destabilizes the antibonding (**empty**) levels

Raising the oxidation state shortens the bond length

2) decreases the screening stabilizing the core level

$L_{2,3}$ edge white lines: *a probe for occupancy of d band in nd elements (n=3, 4, 5)*

$L_{2,3}$: transitions $p \rightarrow d$ states

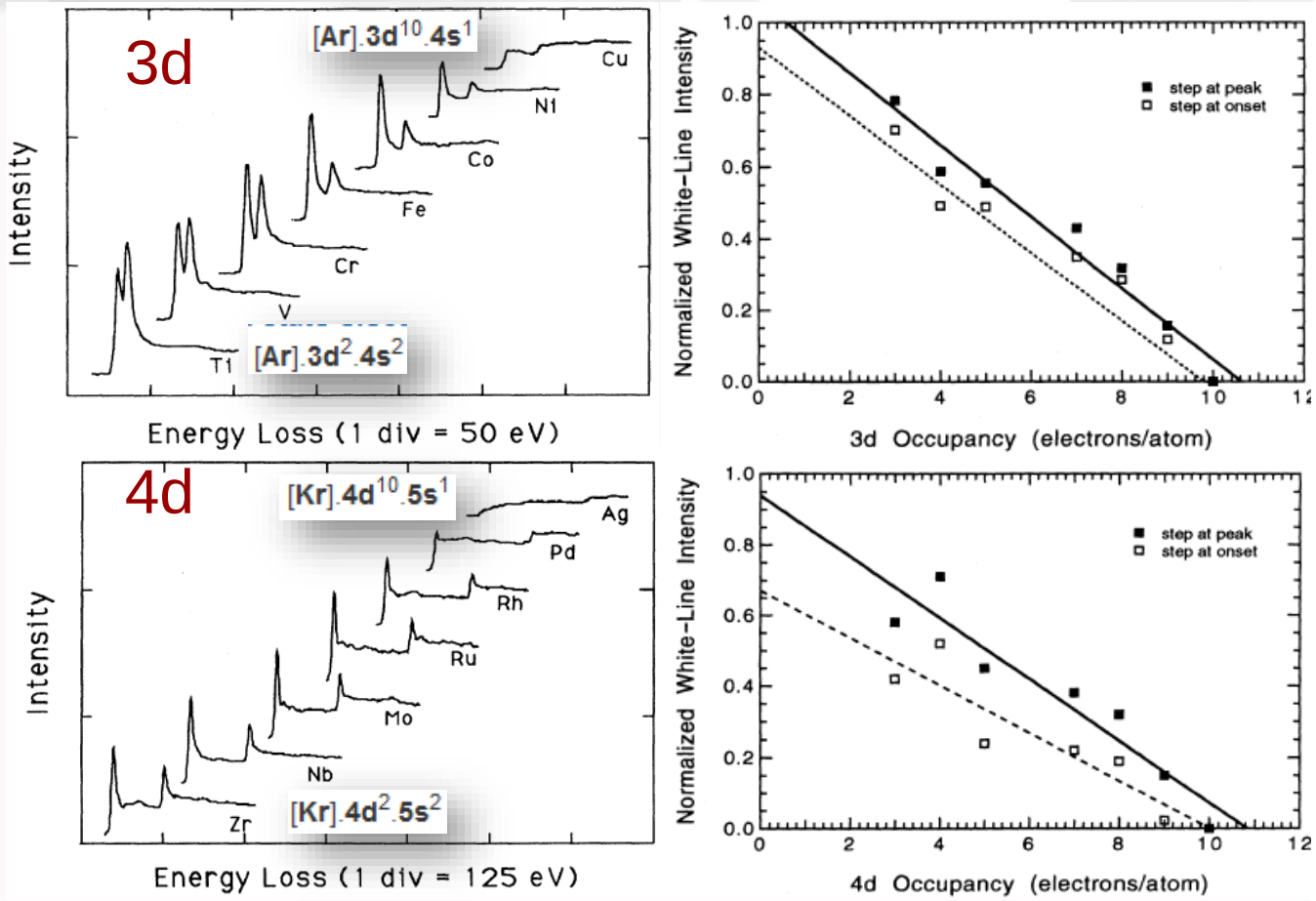

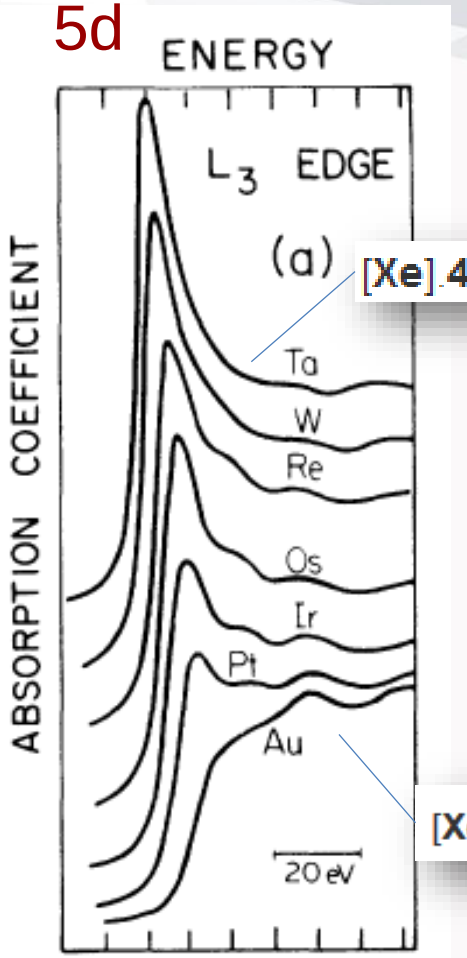

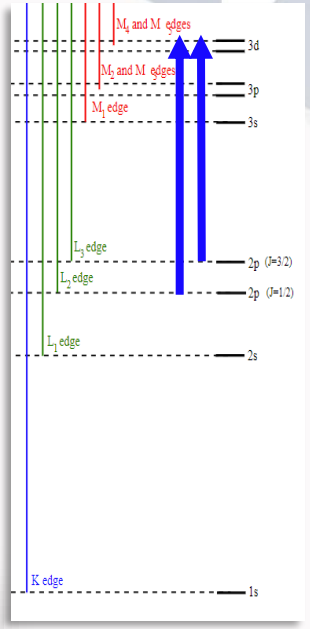

PHYSICAL REVIEW B VOLUME 47, NUMBER 14 1 APRIL 1993-II

White lines and *d*-electron occupancies for the 3*d* and 4*d* transition metals

D. H. Pearson,* C. C. Ahn, and B. Fultz

Examples

Pt L_2 edge white line in Pt_xGe_y intermetallic compounds

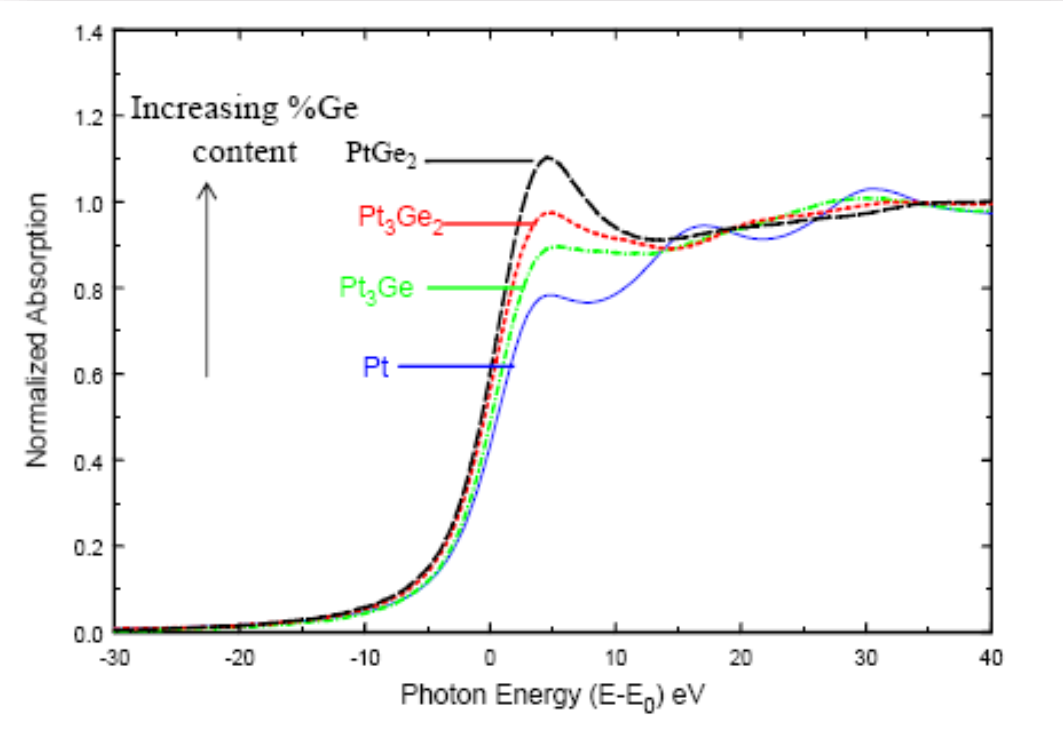

- Transition is $2p$ to $5d$: Pt d-band full, so "no" intensity at edge.
- PtGe intermetallics: charge transfer from d-band of Pt to Ge, resulting in significant intensity at edge.
- Use as signature of Pt-Ge intermetallic formation.

Charge transfer in Cu-Au thin film alloys

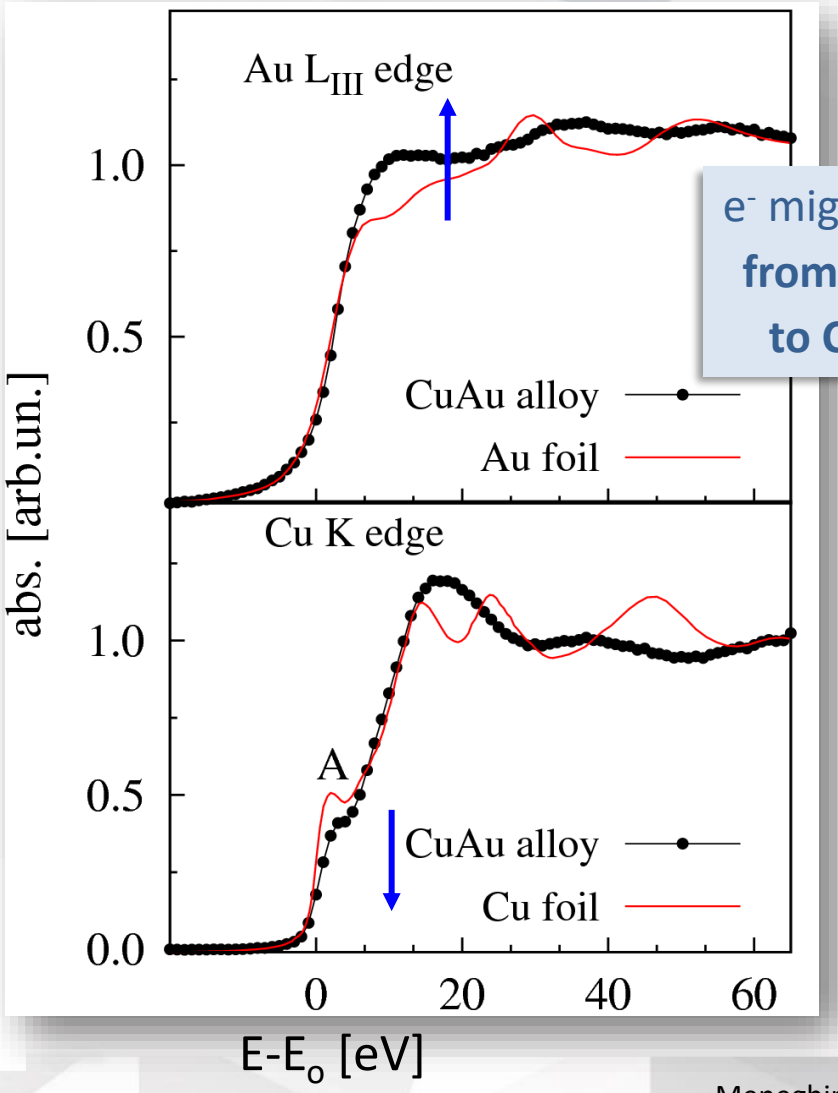

e⁻ migrate
from Au (more empty states)
to Cu (fewer empty states)

Meneghini et al. Corrosion effects in CuAu thin films (unpublished)

Edge region: fingerprints of chemical species

Chemical shift = oxidation state

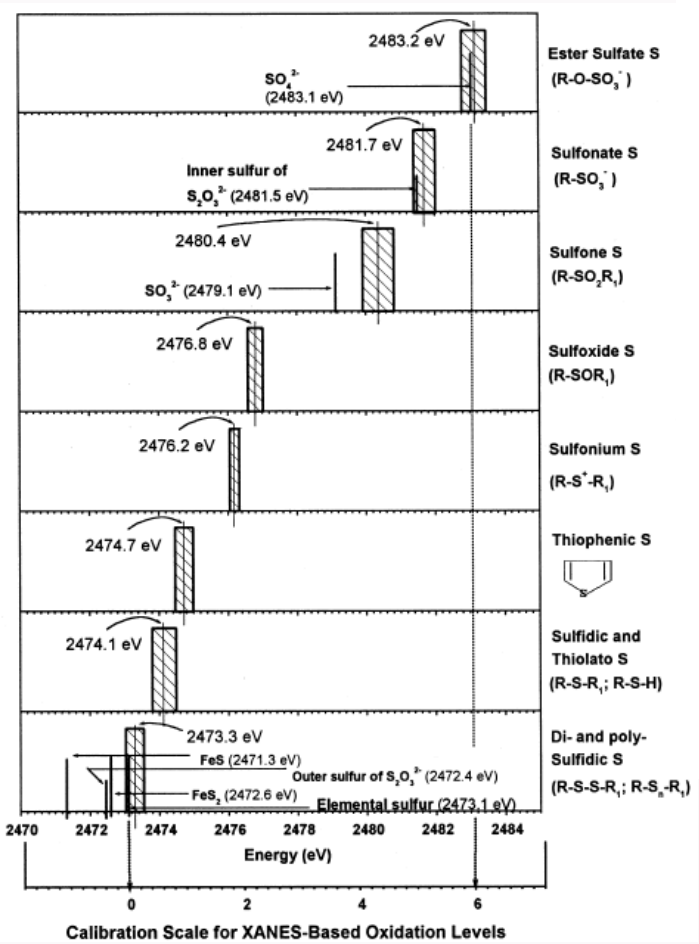

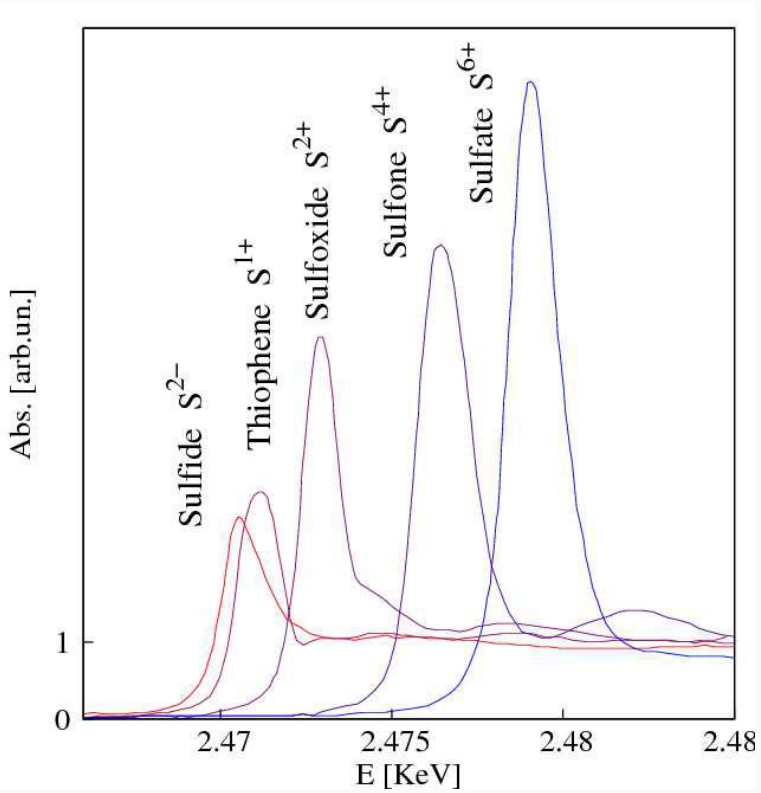

Edge shape = chemical environment

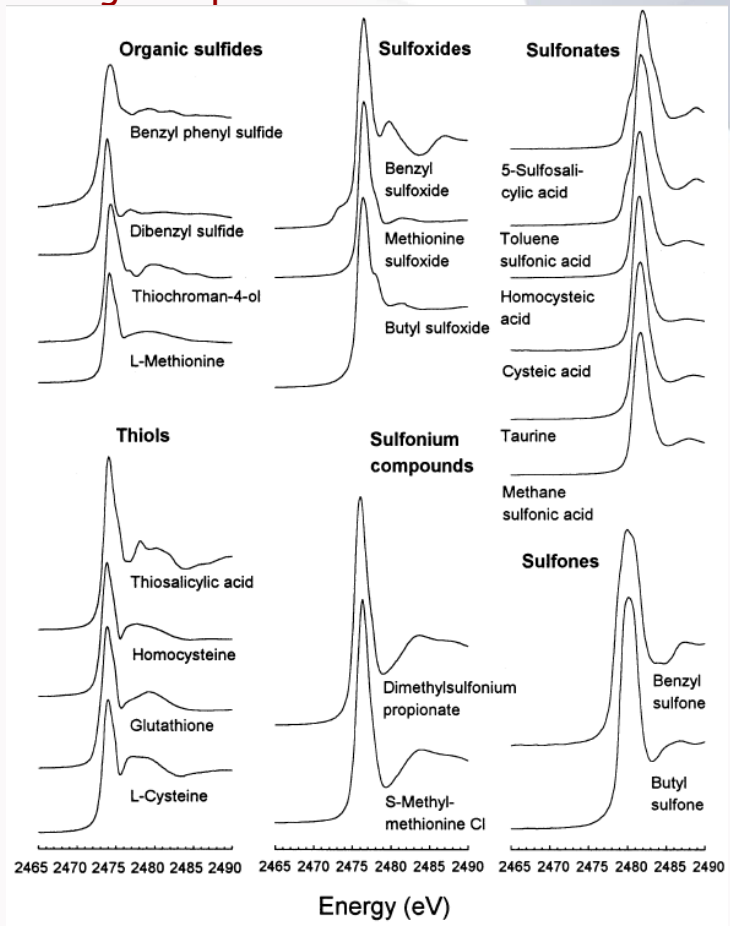

A. Vairavamurthy / Spectrochimica Acta Part A 54 (1998) 2009–2017

features of the edge region…

reveal chemical species in mixtures

Environmental sciences

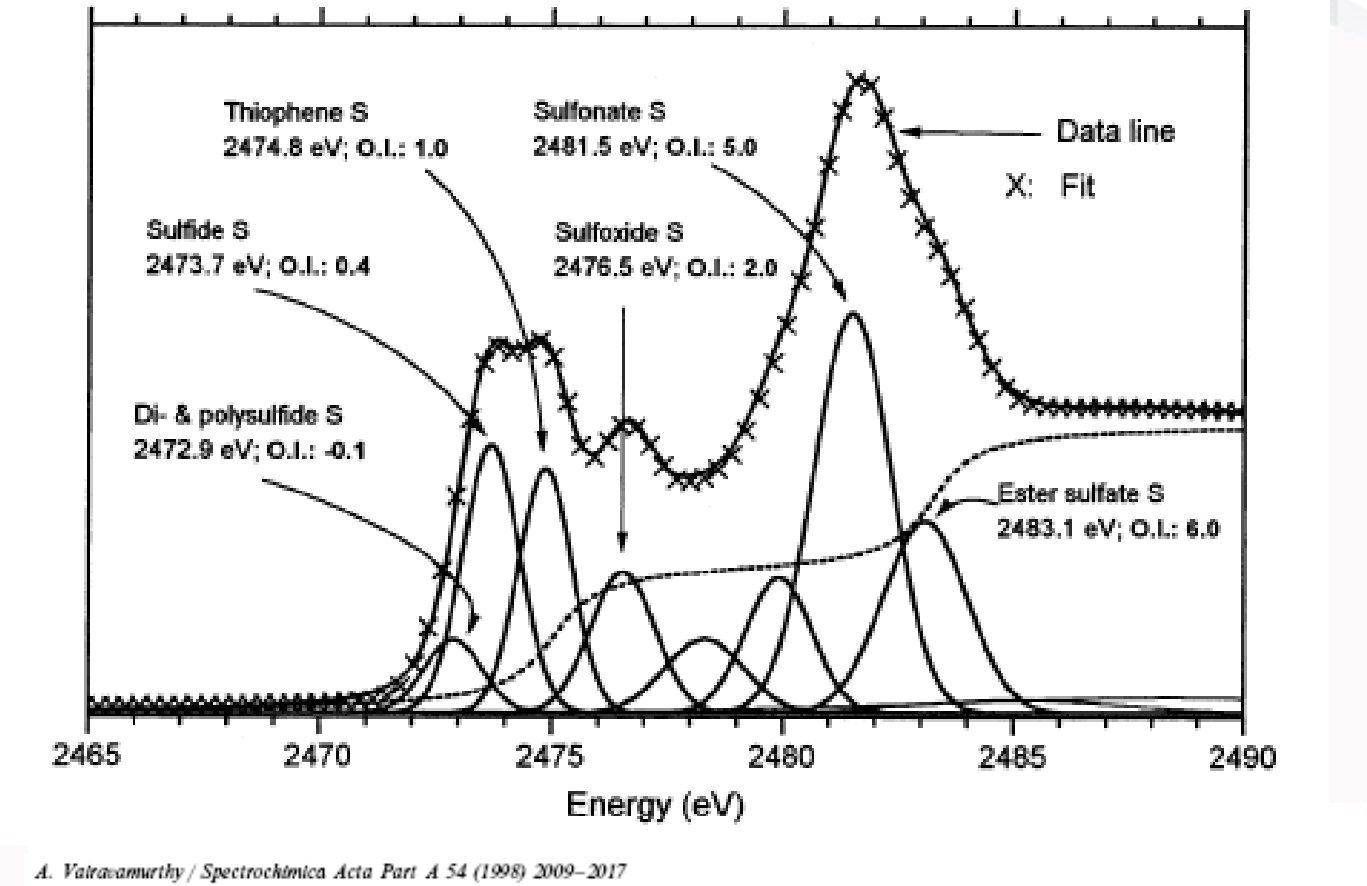

A. Vairavamurthy / Spectrochimica Acta Part A 54 (1998) 2009–2017

chemical speciation of Sulphur in humic substances

Chemical speciation in Natural samples: the problem

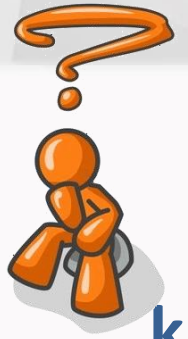

Natural samples are intrinsically **disordered**, **multiphase**, **poorly know composition** chemical species

natural sciences: biology, geology, medicine, cultural heritage, chemistry (catalysis, reactions…), …

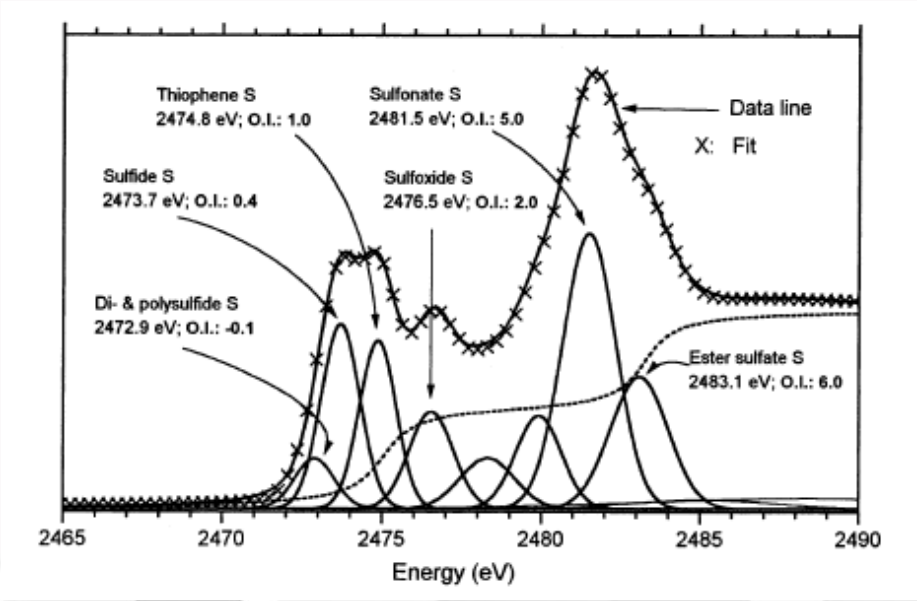

- Chemical lab: Elemental analysis
- XRD blind to the amorphous phases, local disorder, chemical defects, grain boundaries…

The XANES features are fingerprints for specific compounds

Analysis of mixtures: Linear Combination Analysis (LCA)

Environmental sciences

The XANES features are fingerprints for specific compounds

$$\mu^{th} = \sum_j \alpha_j \mu^{ref_j}$$

$$R^2 = \sum_i \left(\mu^{exp}(E_i) - \mu^{th}(E_i)\right)^2$$

α_j = atomic fraction of the chemical specie j

F. Bardelli et al. Geoch. & cosmochem. acta 2011

As adsorption in Natural Calcite samples

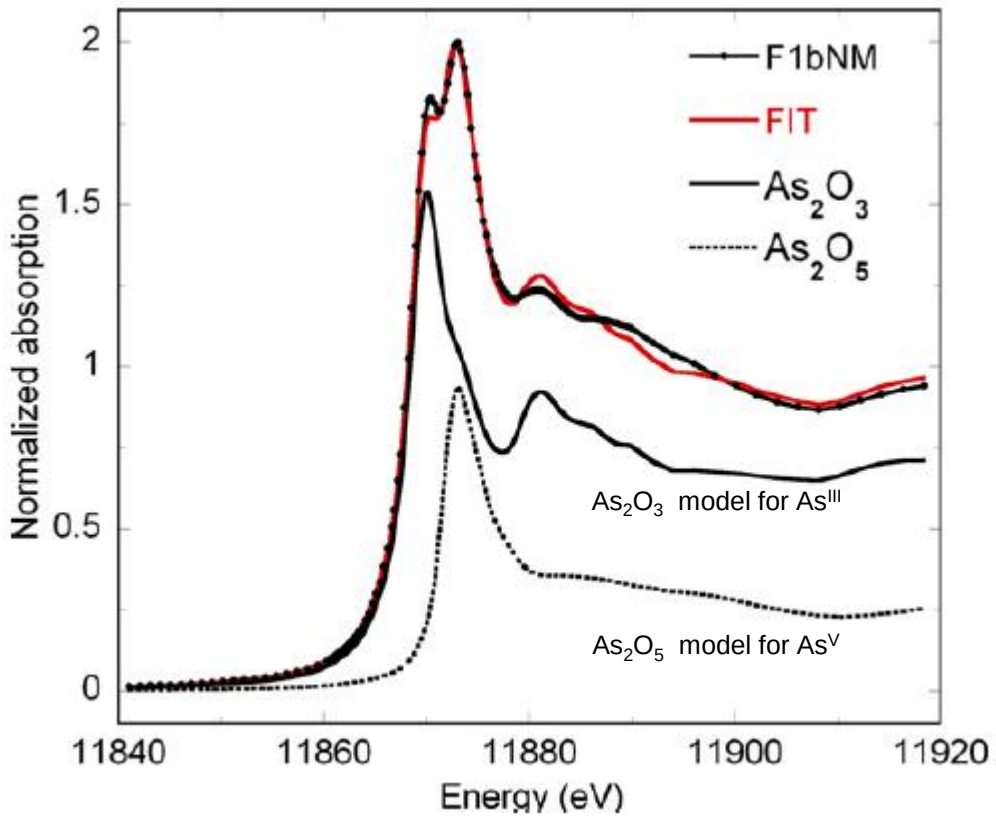

also: ***Linear Combination Fit (LCF)***

XANES - LCA for Catalysis

chemistry

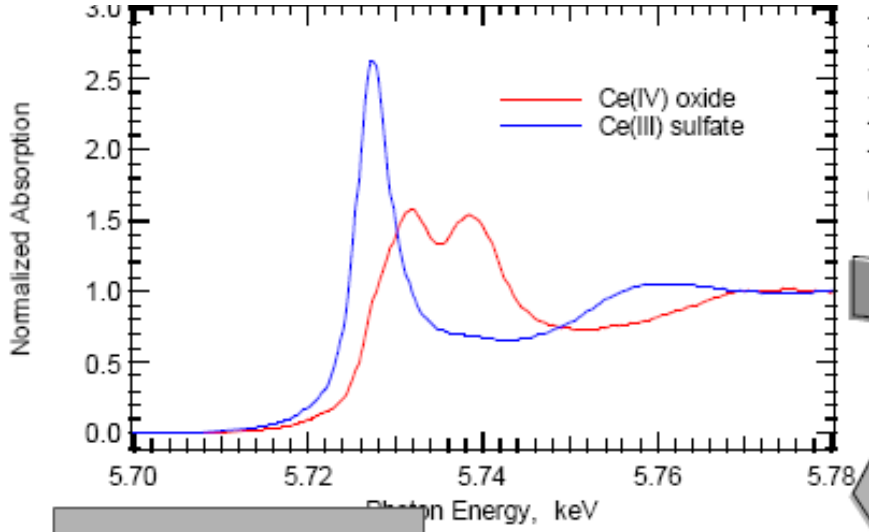

Fit experimental data to linear combination of known reference compounds

TPR-XANES of *in situ* reduction of $Ce_{0.7}Zr_{0.3}$ oxide

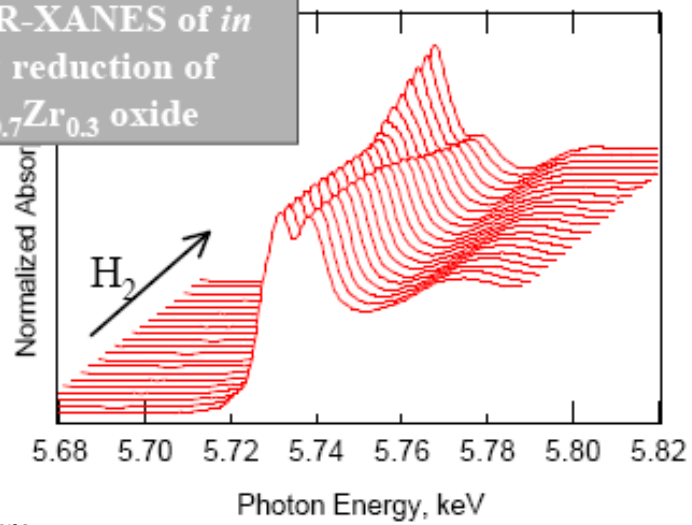

LC-XANES fit to determine amount of Ce(III) and Ce(IV) present as function of temperature

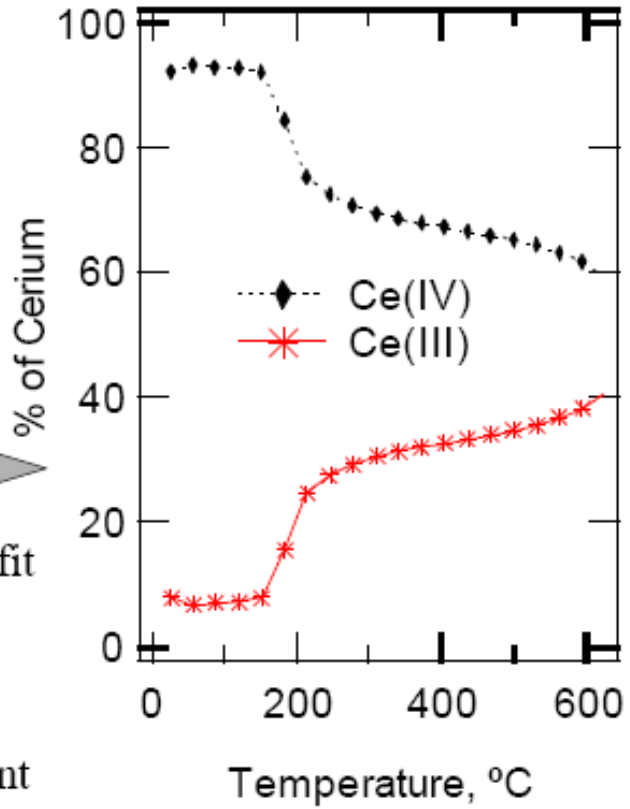

Simon R. Bare

Advanced materials: looking for magneto-electric coupling

Material sciences

$$\mu^{th} = \sum_j \alpha_j \mu^{ref_j}$$

$$R^2 = \sum_i \left(\mu^{exp}(E_i) - \mu^{th}(E_i)\right)^2$$

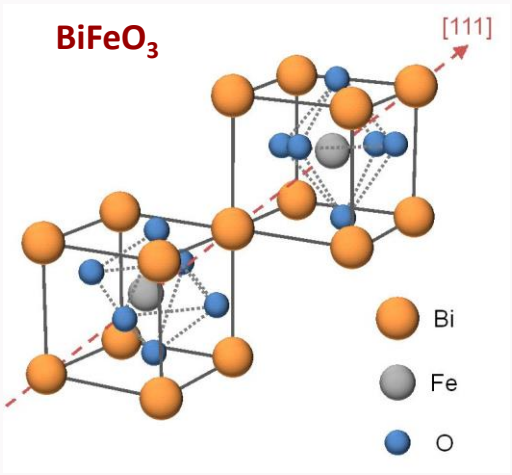

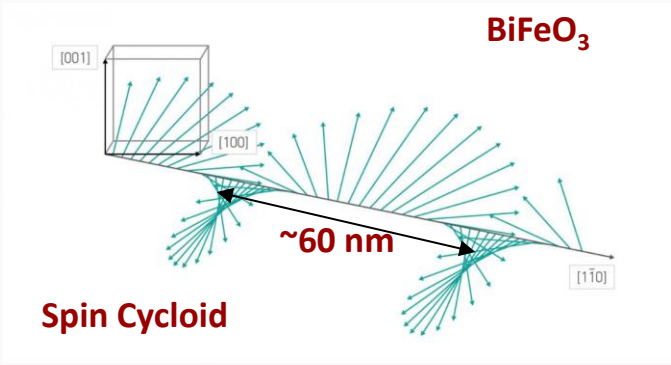

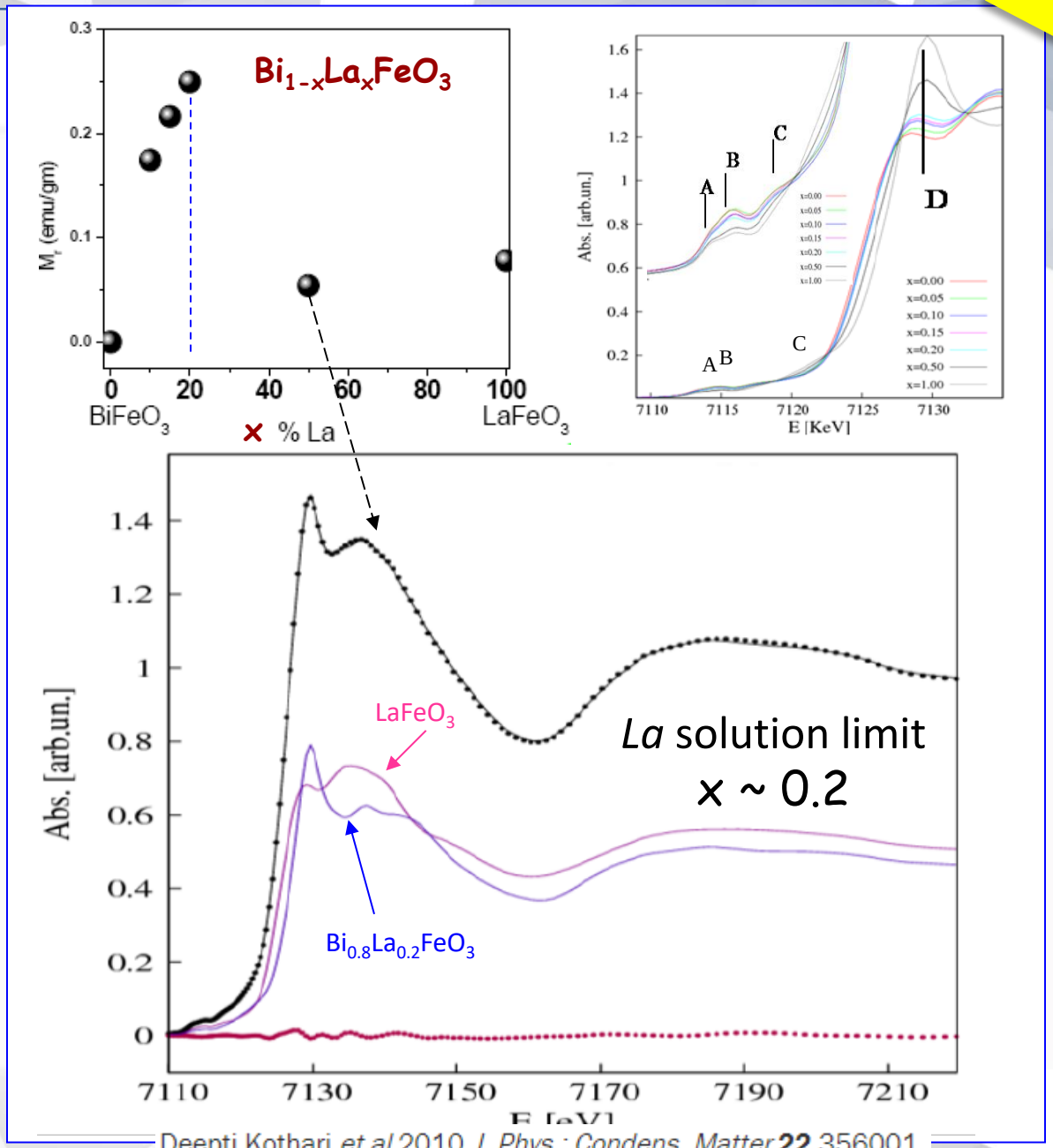

Deepti Kothari *et al* 2010 *J. Phys.: Condens. Matter* **22** 356001

Advanced materials: looking for diluted magnetic units

$BaTiO_3$

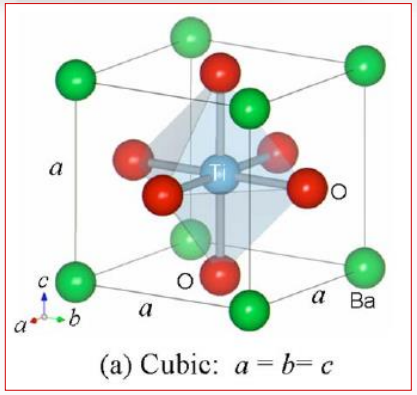

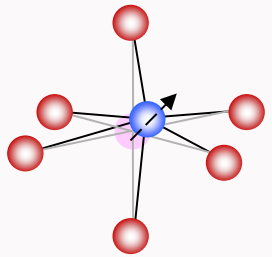

$BaTiO_3$ is **ferroelectric**: off center displacement of Ti^{4+} ions produces a **permanent electric dipole** in TiO_6 molecules

$BaTi_{1-x}Fe_xO_{3-\delta}$

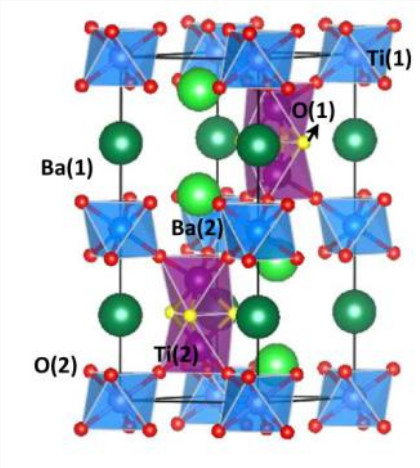

doping with magnetic ions (Fe) may provide some magnetoelectric coupling and stabilize the ferroelectric phase

$BaTi_{0.95}Fe_{0.05}O_{3-X}$

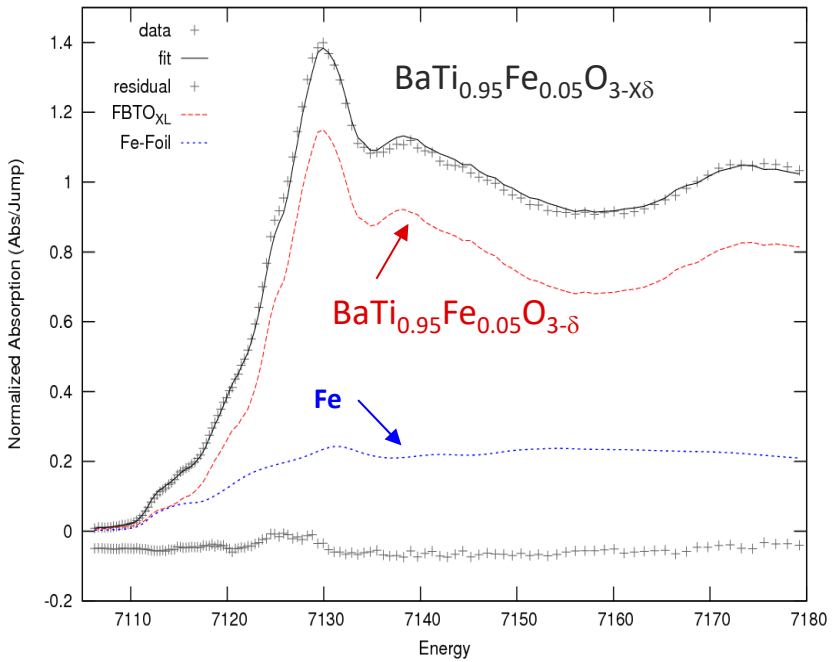

Large Oxygen vacancies causes the Fe ions segregating as metallic Fe^0 phase, the sample is no more homogeneous at the short-range scale, wrong magneto-electric understanding

Note: XRD can't show Fe crystalline phase because of low (≪ 1%) Fe metal

T. Chakraborty, C. Meneghini, G. Aquilanti, S. Ray, J. Phys.: Condens. Matter 25 (2013) 23600
T. Chakraborty, C. Meneghini, G. Aquilanti, S. Ray, Advanced Functional Materials (2014)

Special Applications of XANES spectroscopy: μ-XANES & mapping

XAS vs XRF
XRF= elemental sensitivity
XAS= **elemental sensitivity + chemical speciation**

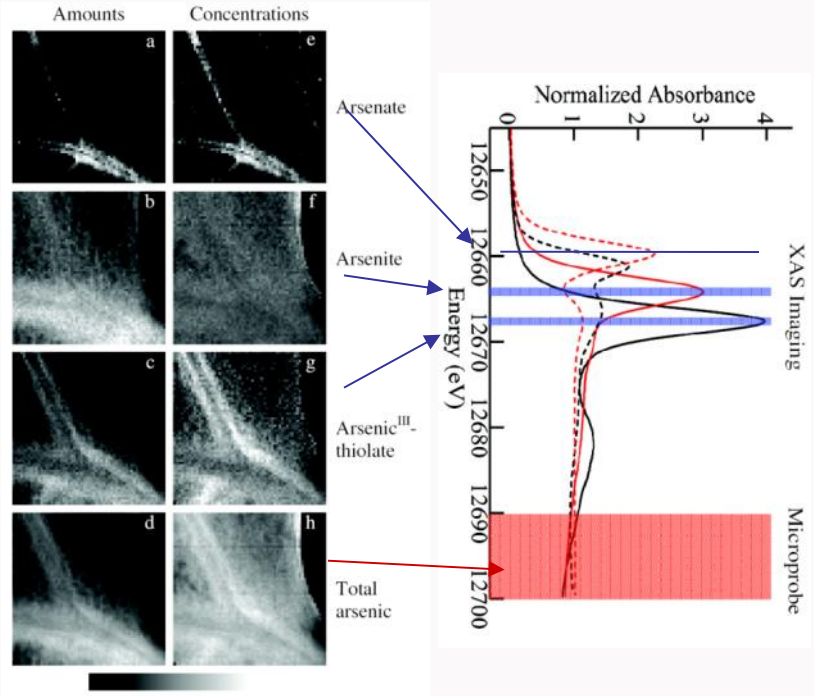

I. J.Pickering & G. N. George Proc. XAFS13 conference (2006)

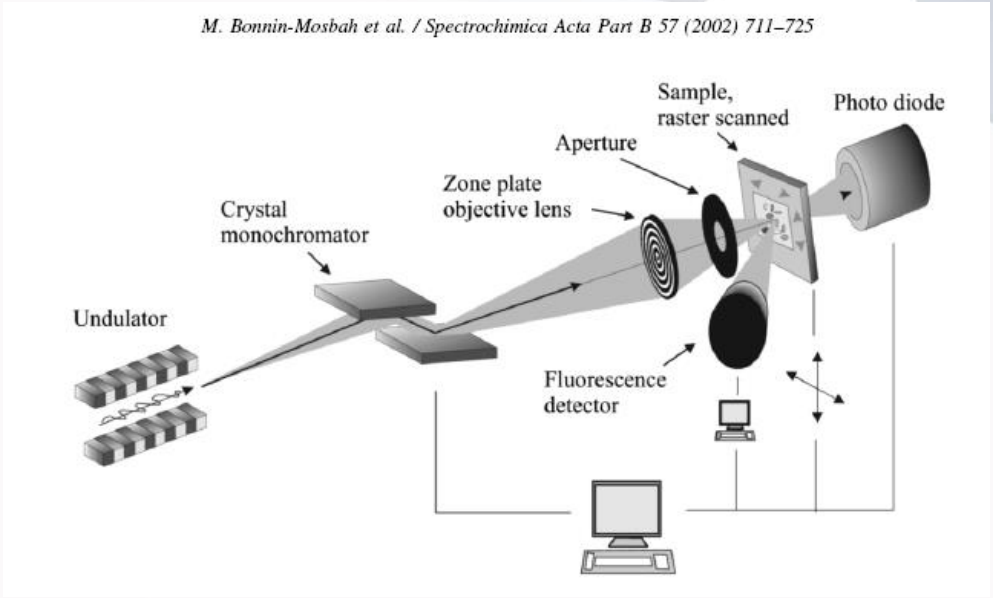

NOTE: X-ray lenses and zone plates work in a reduced energy window, therefore the EXAFS region is often not accessible to micro and nano probes

Cultural heritage

CdS yellow colour in oil paints may degrade if exposed to light giving rise to white spots.

Chemical transformations giving rise to colour changes are mapped by μXANES

Anal. Chem. **XXXX,** *xxx,* 000–000

Characterization of a Degraded Cadmium Yellow (CdS) Pigment in an Oil Painting by Means of Synchrotron Radiation Based X-ray Techniques

Geert Van der Snickt,† Joris Dik,‡ Marine Cotte,§,|| Koen Janssens,*,† Jakub Jaroszewicz,† Wout De Nolf,† Jasper Groenewegen,‡ and Luuk Van der Loeff⊥

"Still Life with Cabbage" by James Ensor (ca.1921

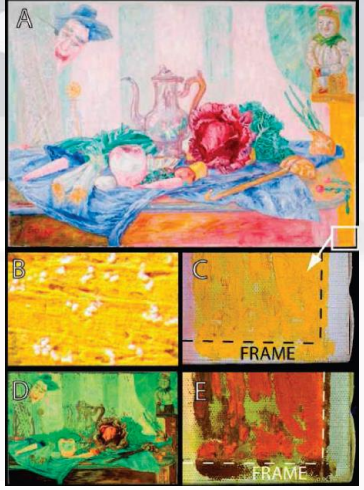

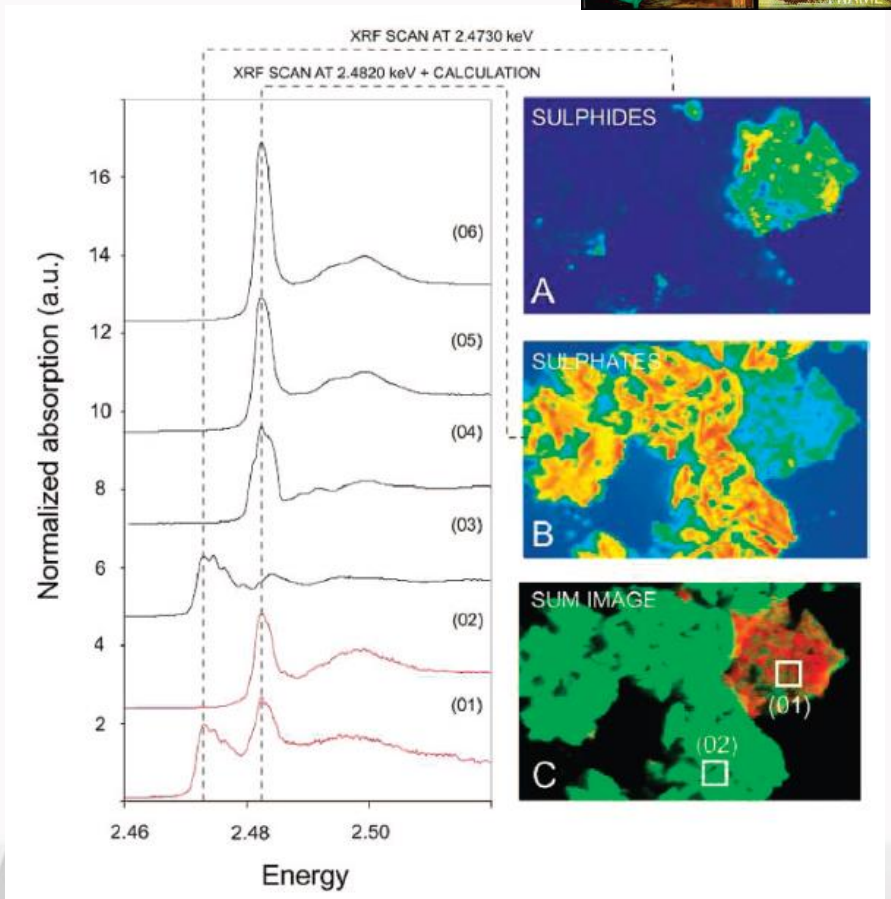

(01) yellow paint in sample, (02) white/transparent globules in sample, (03) CdS, (04) anglesite ($PbSO_4$), (05) $CdSO_4$, (06) $CdSO_4 \cdot H_2O$

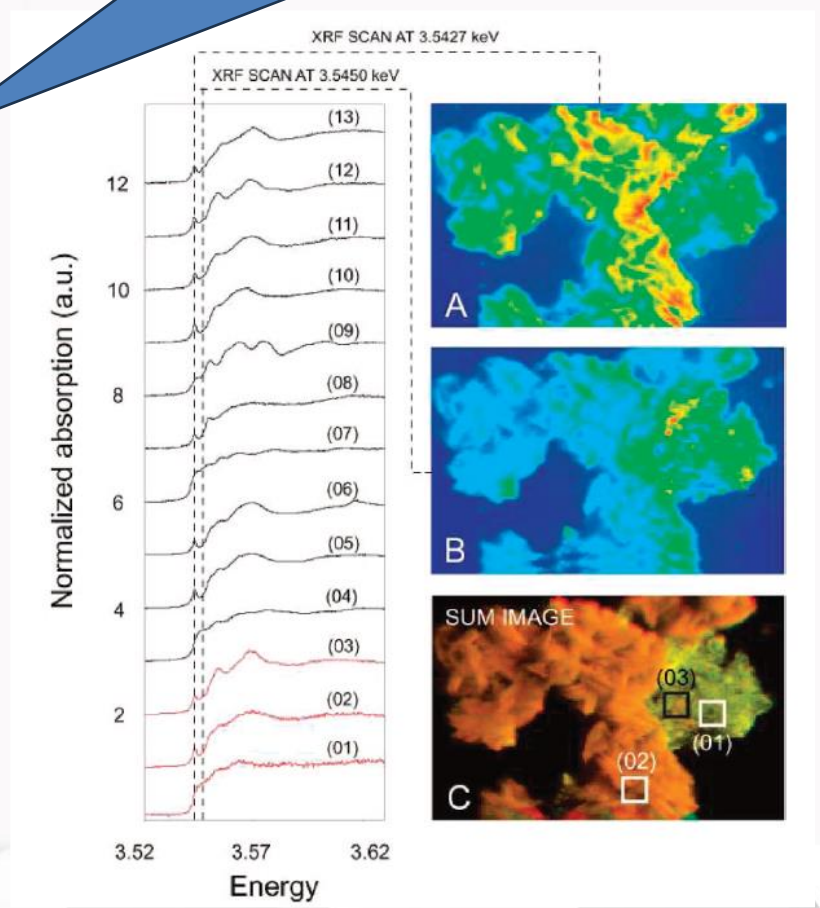

powders: (01) yellow paint in the sample, (02) white/transparent globules in the sample, (03) Cd-rich, S- and Pb-poor area inside the yellow paint of the sample, (04) CdS, (05) $CdSO_4$, (06) hydrated $CdSO_4$, (07) metallic Cd, (08) $CdCl_2$, (09) CdO, (10) $CdNO_3$, (11) Cd formate ($(CHO2)_2Cd$), (12) Cd acetate ($Cd(CH_3COO)_2 \cdot 2H_2O$), (13) $CdCO_3$. Right column: Cd chemical mappings obtained by μ-XRF scanning near the Cd L_{III} edge,

ID21-ID16B ESRF Microfocus beamline

Cultural heritage

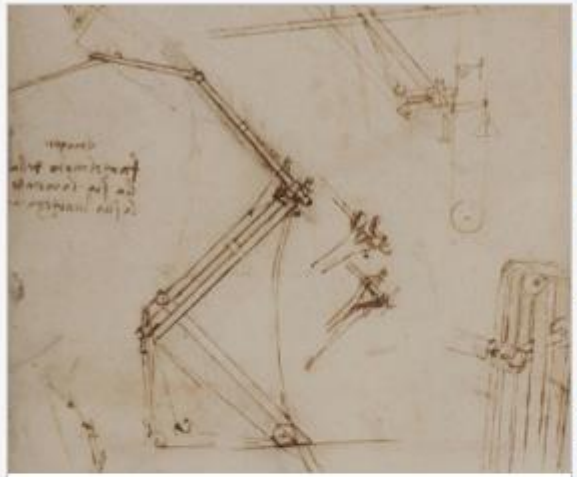

13-06-2023

Revealing new insights into black stains on the passepartout of Leonardo da Vinci's Codex Atlanticus

→ *Read more*

Link.html

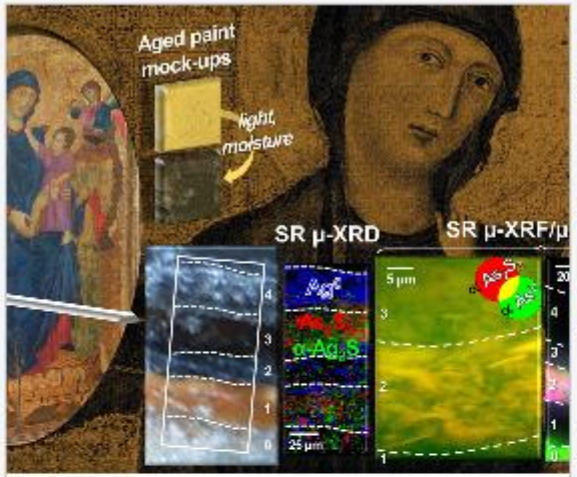

16-12-2021

Revealing the causes of darkening of "fake-gold" decorations on medieval paintings

→ *Read more*

Link.html

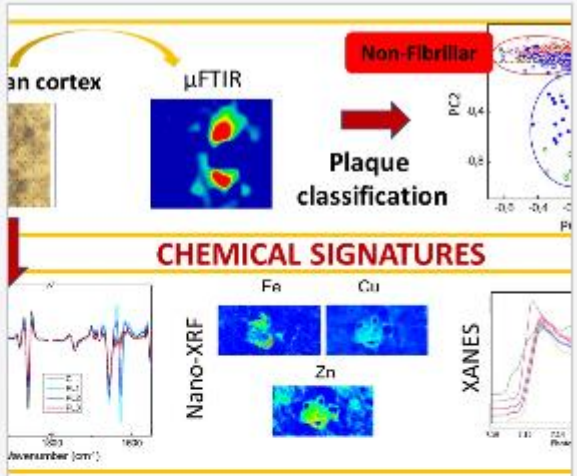

14-06-2021

Characterising amyloid plaques in Alzheimer's disease

→ *Read more*

Link.html

Bio-Remediation or: how to use Plants and (micro-)organisms employed to regulate pollutant mobility (i.e. heavy metals) within the ecosystems

Bio/Geo sciences

Elphidium

Quinquenoculina

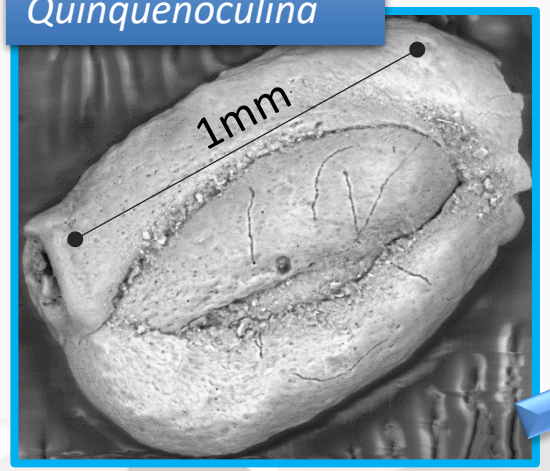

XANES

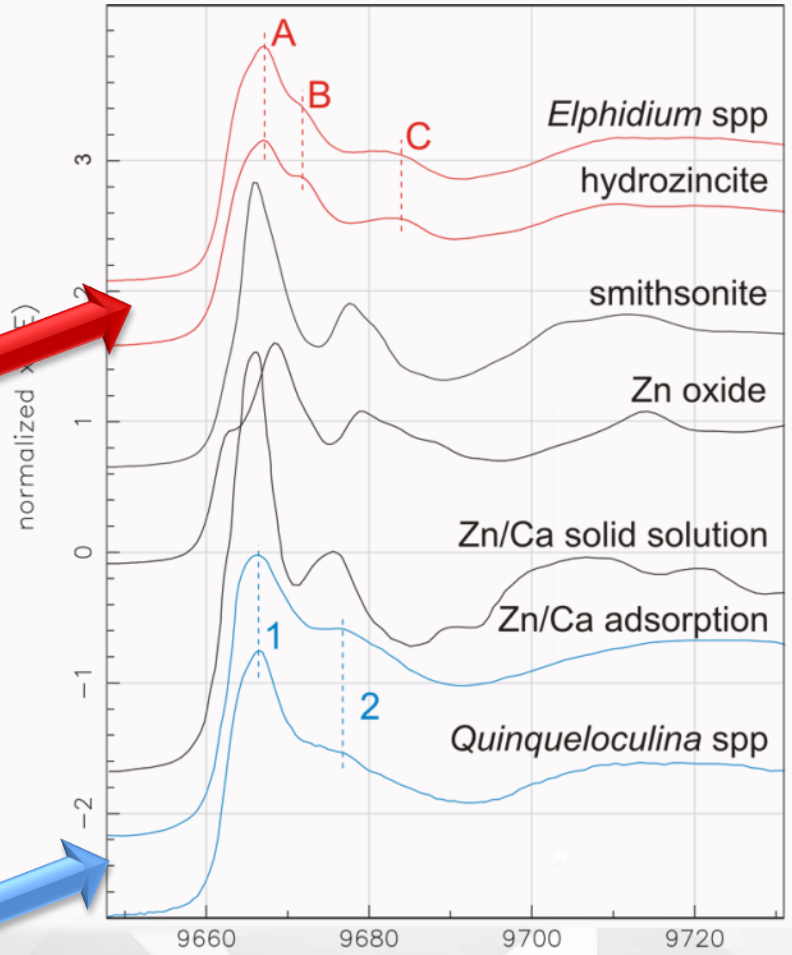

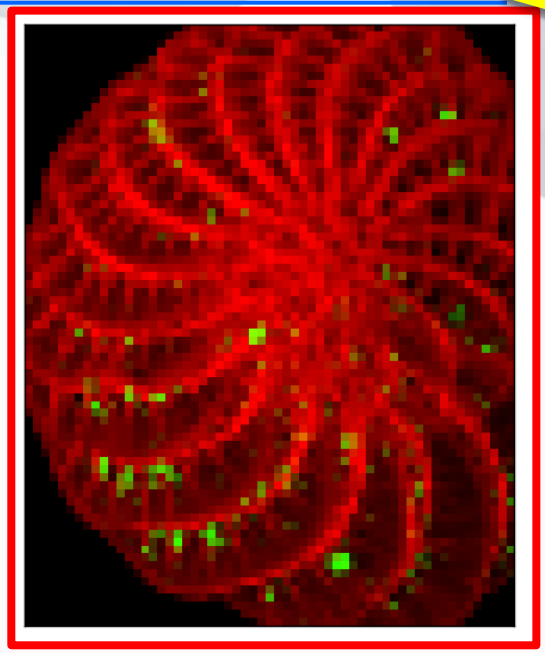

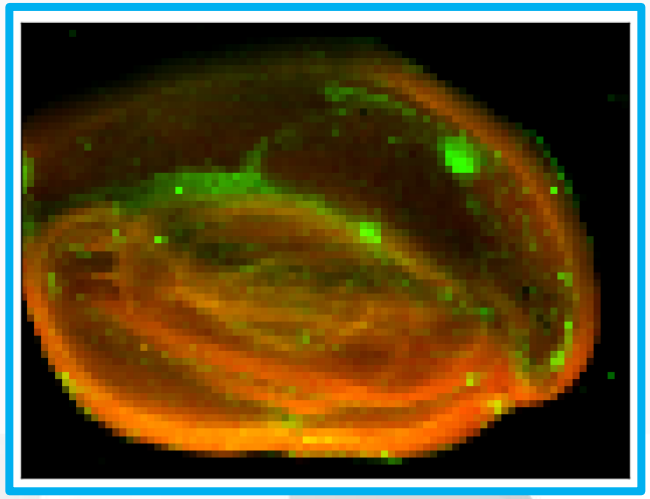

Chemical Geology 477 (2018) 100–111

Bio-Remediation or: how to use Plants and (micro-)organisms employed to regulate pollutant mobility (i.e. heavy metals) within the ecosystems

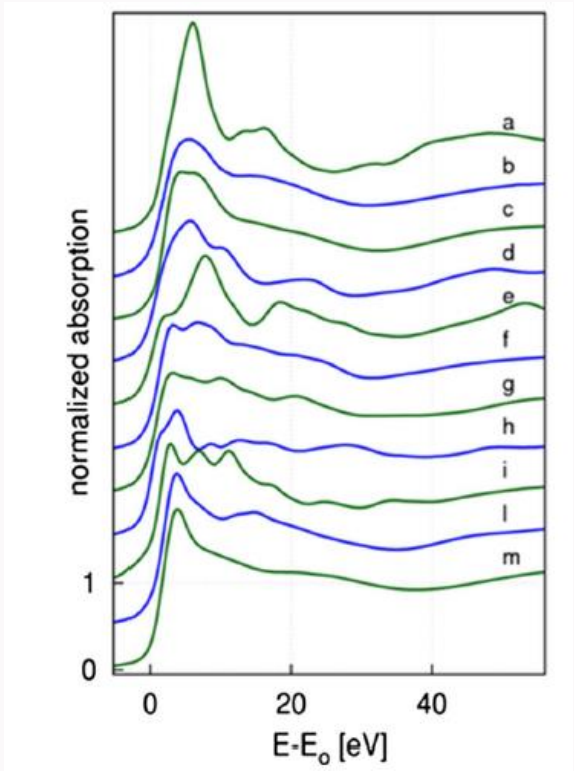

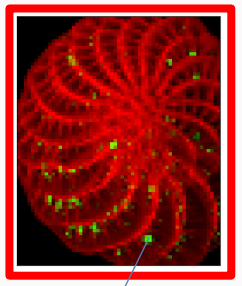

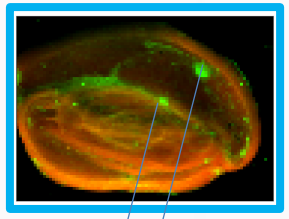

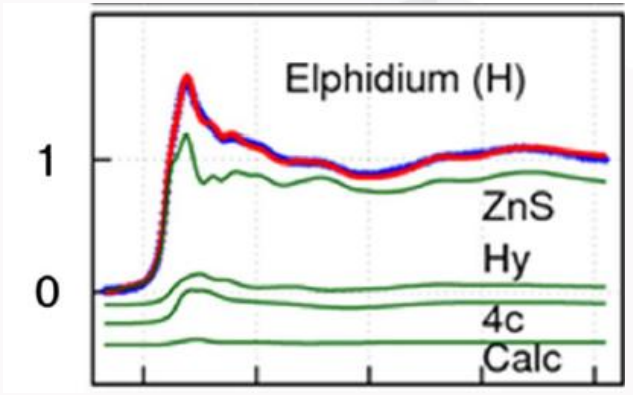

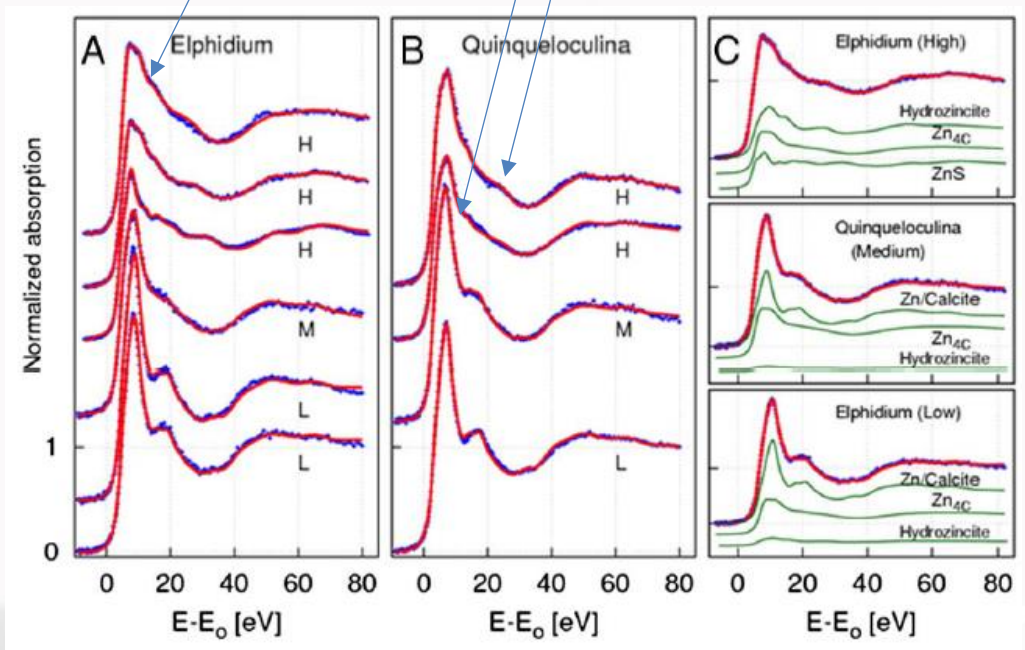

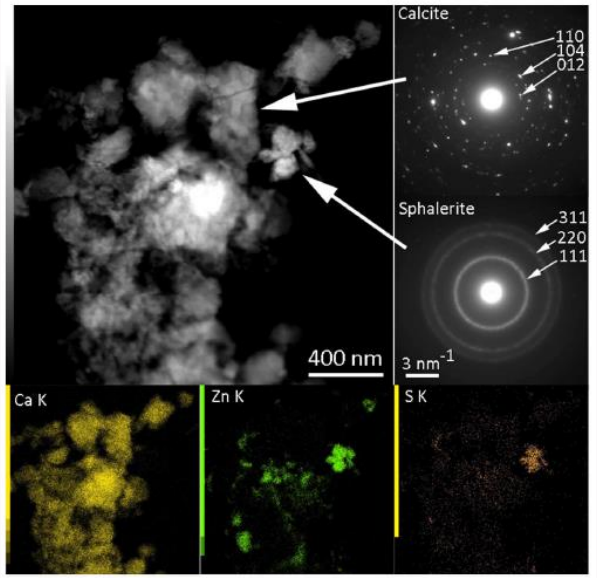

G. De Giudici, D. Medas, P. Lattanzi, C. Meneghini, et al. to be submitted (Scienze)

New instruments → new data analysis methods

fast data collection →
huge datasets

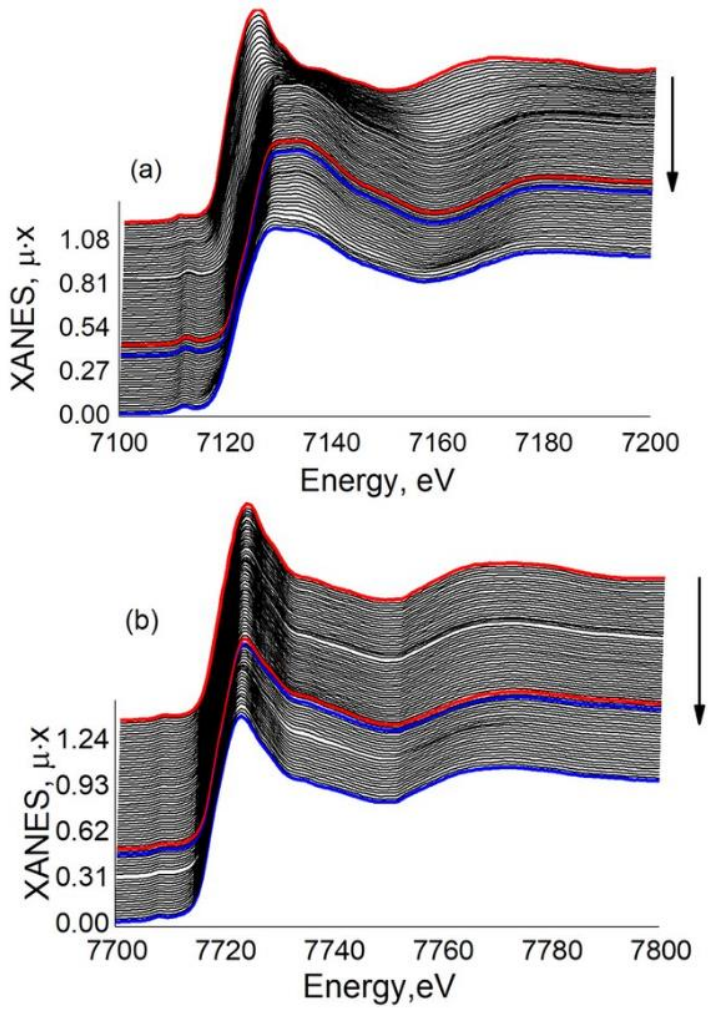

High data quality →
search for tiny effects

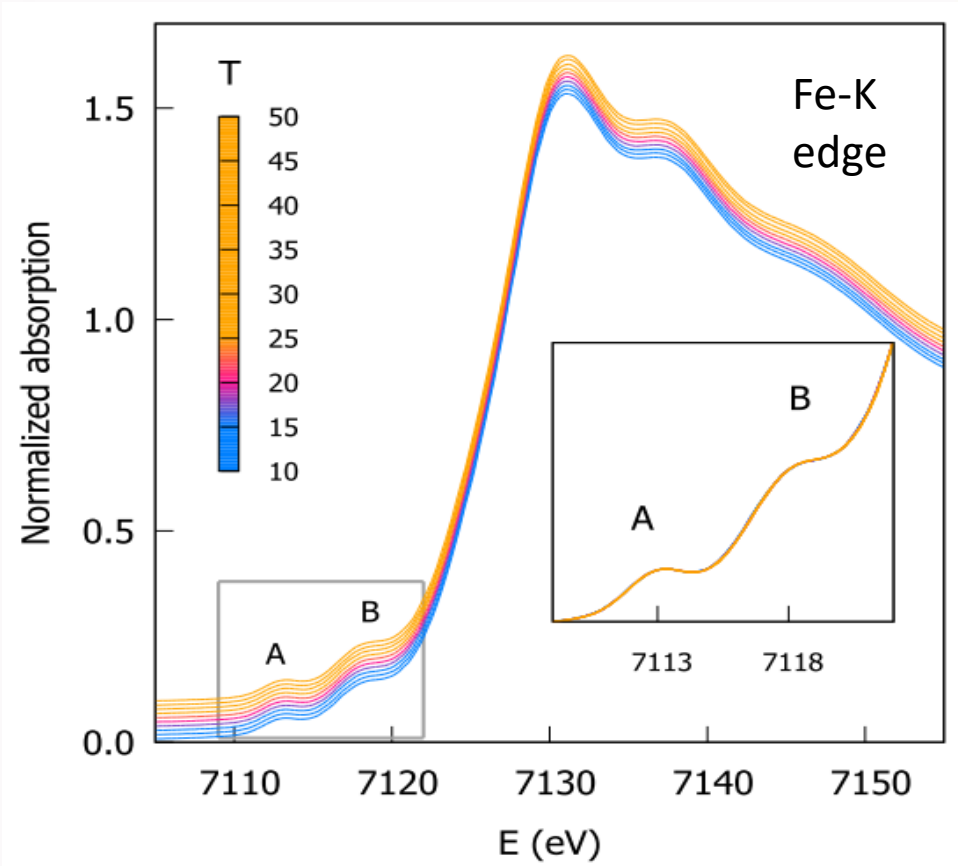

Principal Component Analysis

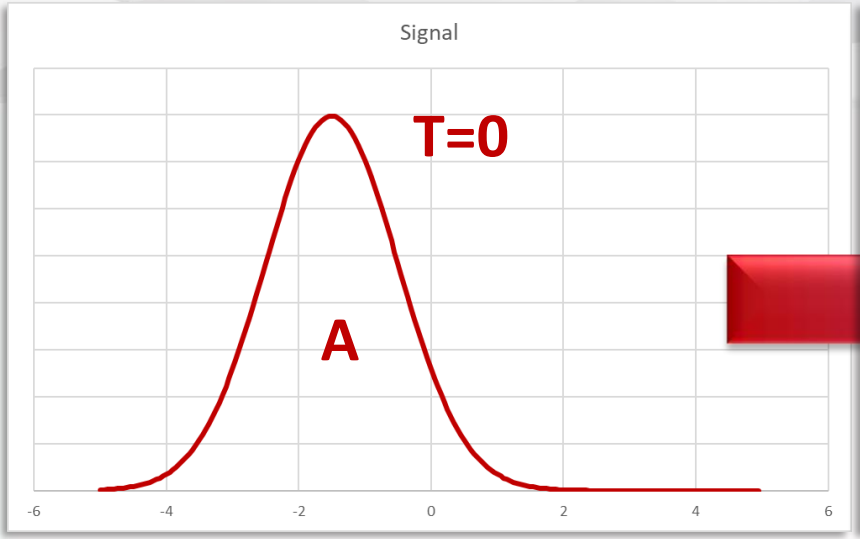

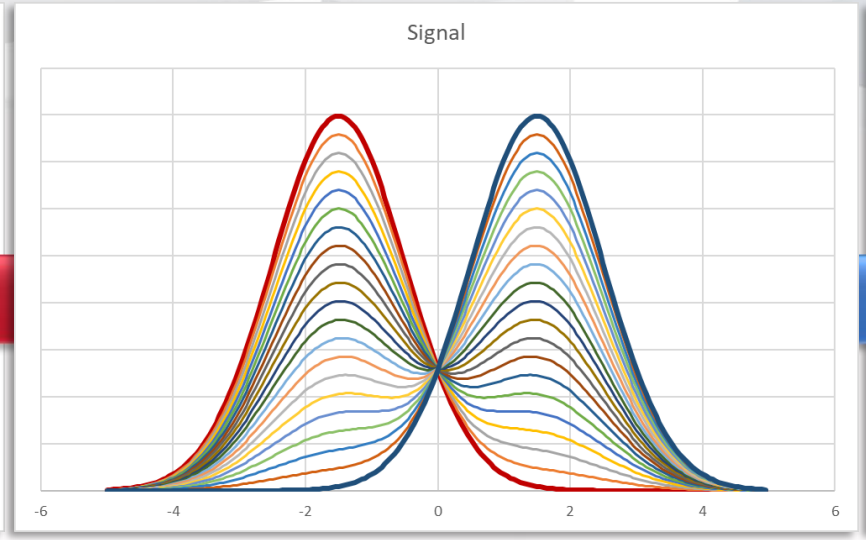

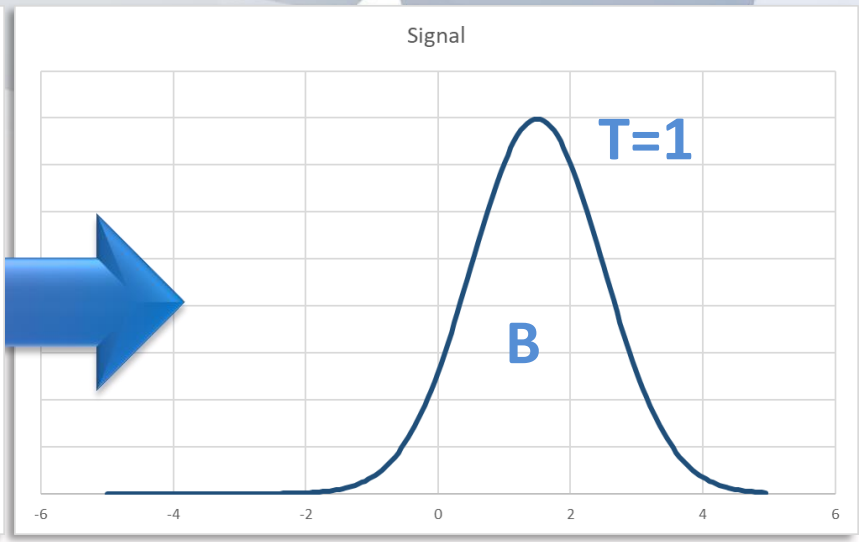

$$f(x,T) = \bar{f}(x) + \sum_i \alpha_i(T) C_i(x)$$

$C_i(x)$ = Eigenvectors of the covariance matrix

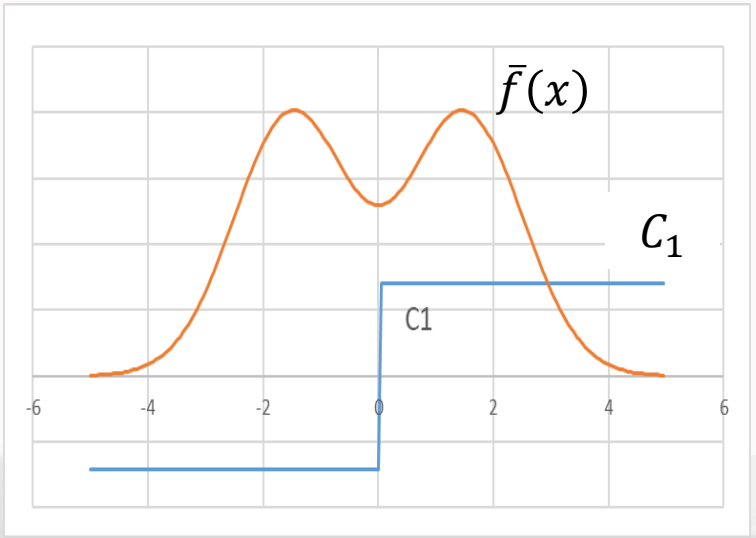

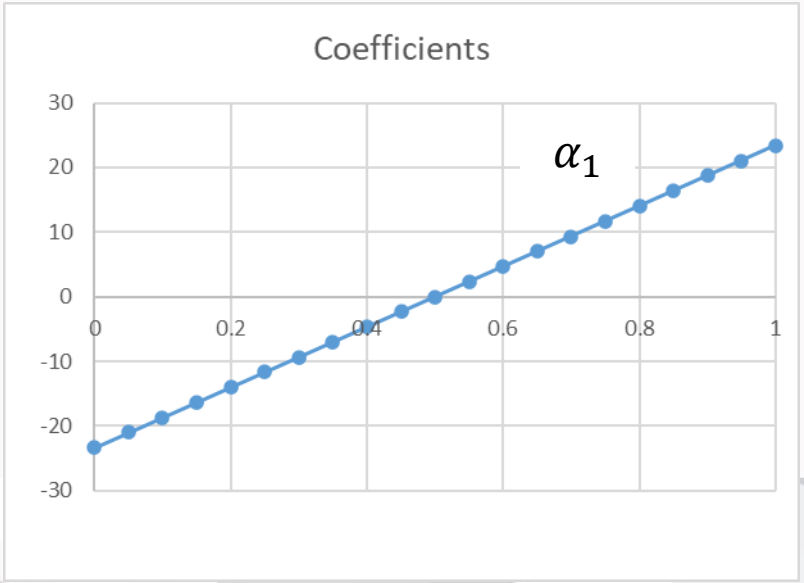

Principal Component Analysis

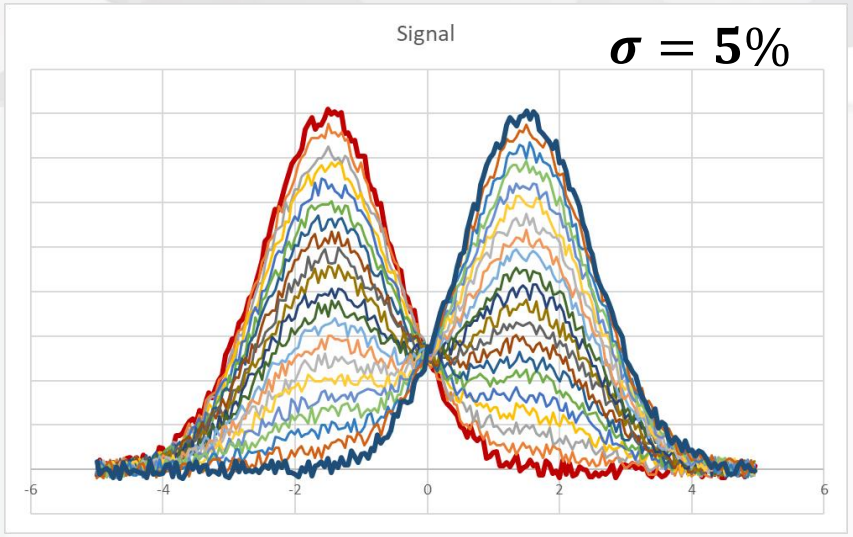

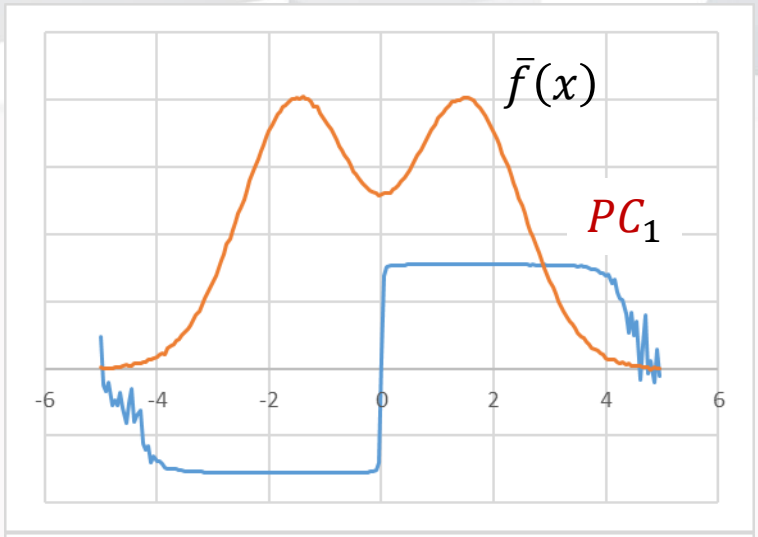

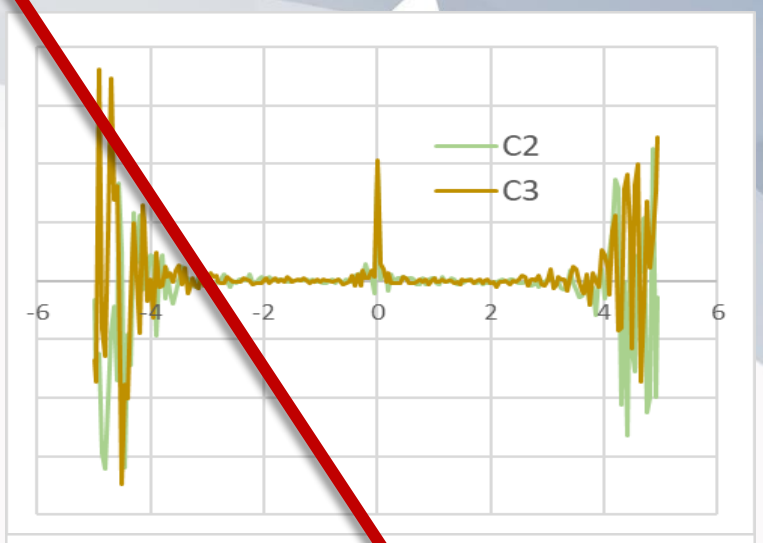

$$f(x,T) \simeq \bar{f}(x) + \sum_i \alpha_i(T) PC_i(x)$$

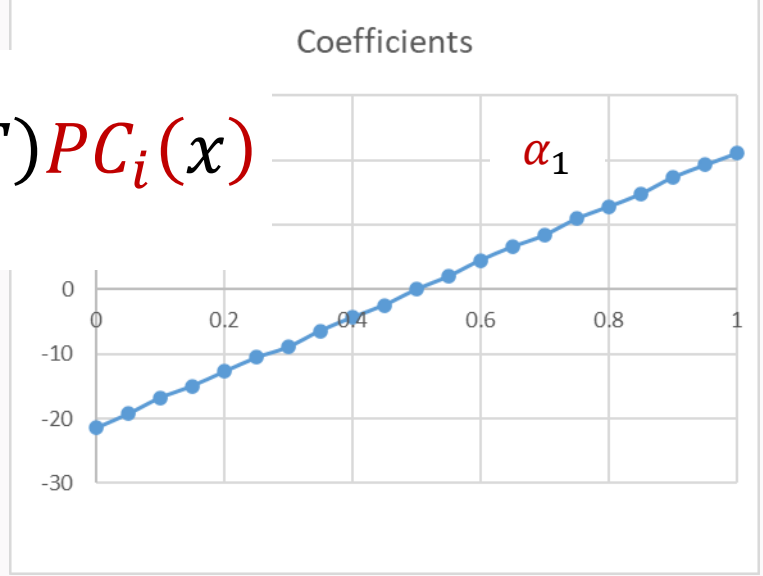

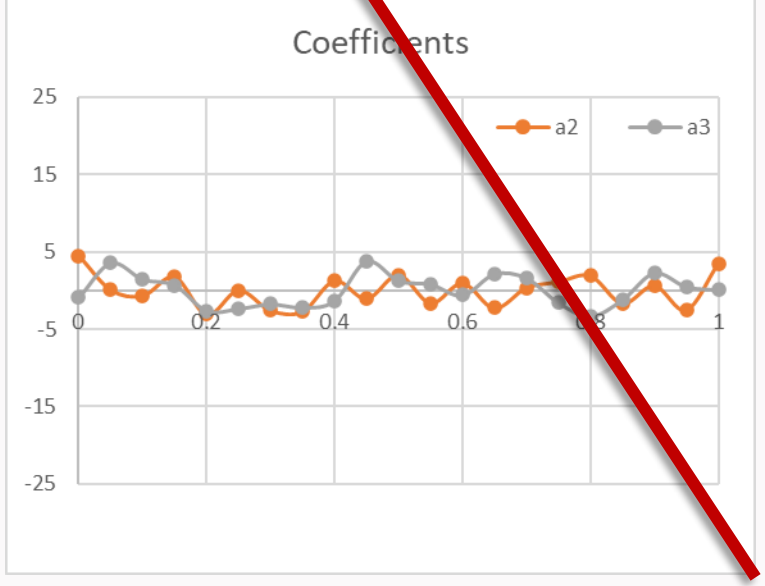

Principal Component Analysis

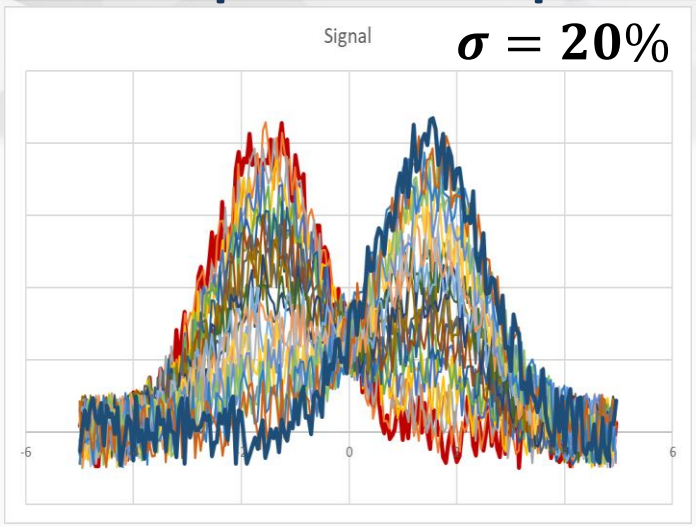

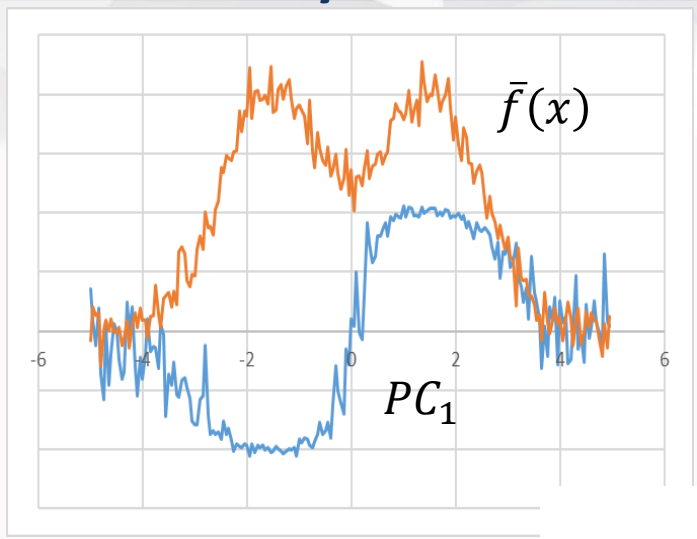

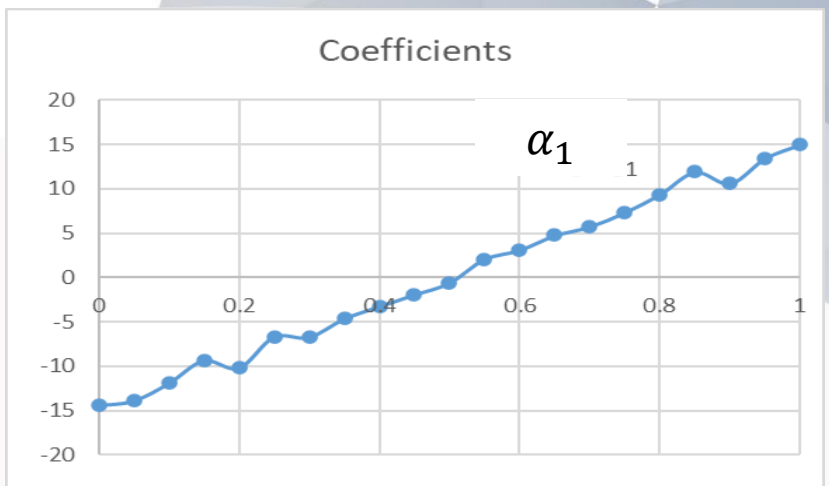

$$f(x,T) \simeq \bar{f}(x) + \sum_i \alpha_i(T) PC_i(x)$$

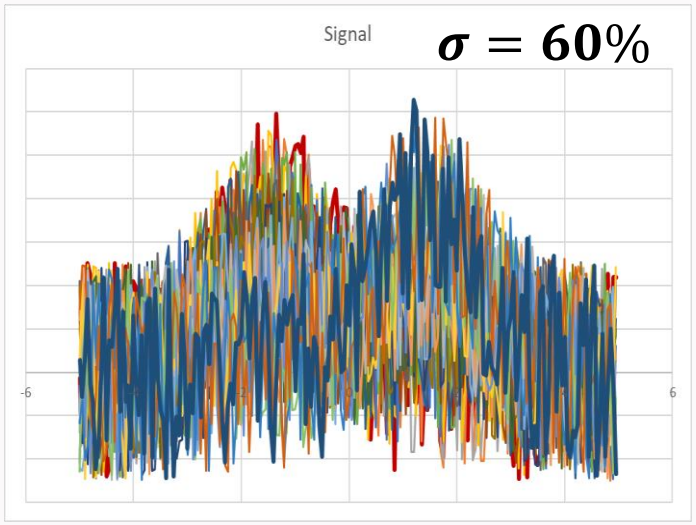

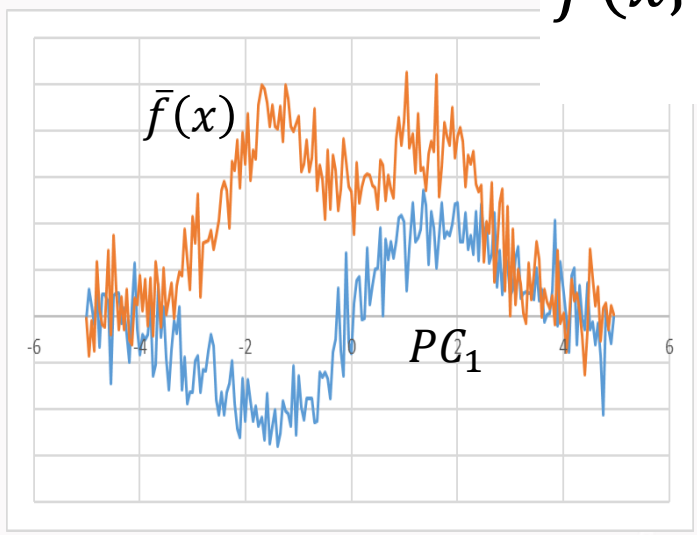

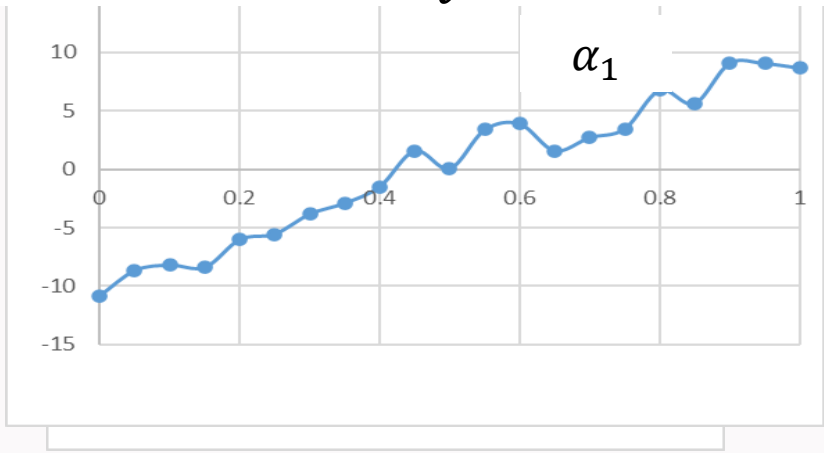

Chemical reactions

Chemistry

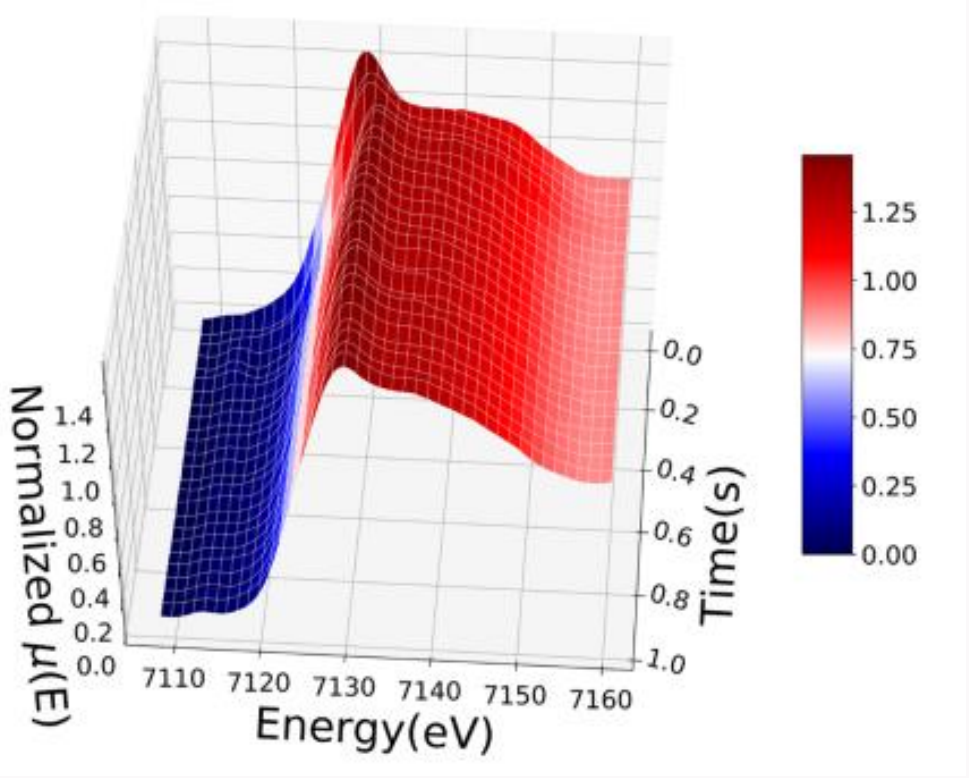

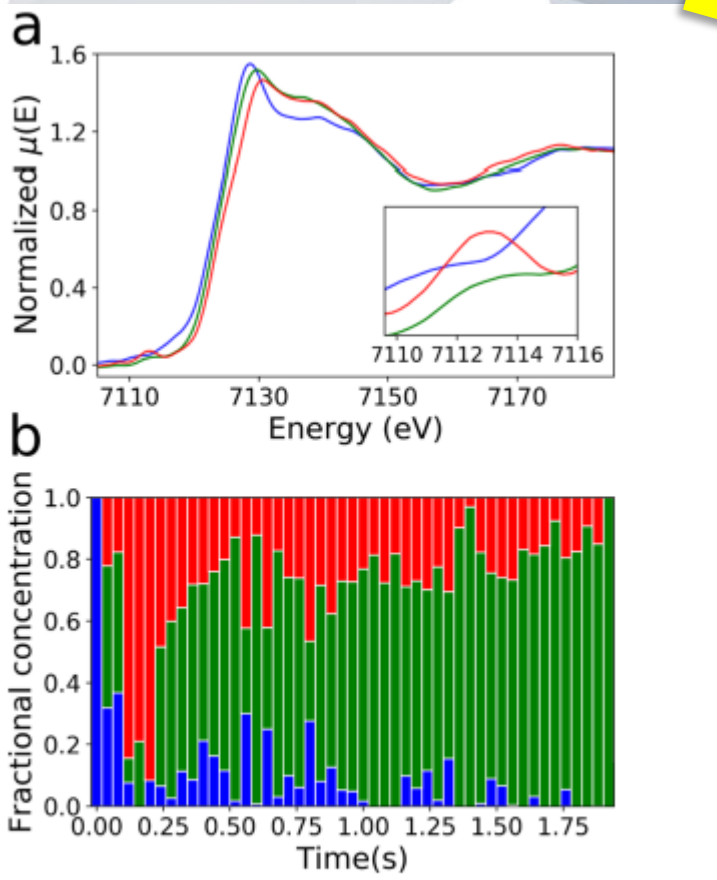

Figure 4. Fe K-edge XANES spectra (a) and fractional concentration profiles (b) extracted by using the transformation matrix-based decomposition.

Inorg. Chem. 2020, 59, 9979 – 9989

Direct Mechanistic Evidence for a Nonheme Complex Reaction through a Multivariate XAS Analysis

Francesco Tavani,* Andrea Martini, Giorgio Capocasa, Stefano Di Stefano, Osvaldo Lanzalunga, and Paola D'Angelo*

https://pubs.acs.org/action/showCitFormats?doi=10.1021/acs.inorgchem.0c01132&ref=pdf

Multiferroicity and Local structure in $FeVO_4$

Fundamental material science

JOURNAL OF SOLID STATE CHEMISTRY 4, 29–37 (1972)

Crystal Structure and Mössbauer Effect Investigation of $FeVO_4$

B. ROBERTSON
Division of Natural Sciences and Mathematics, University of Saskatchewan, Regina, Saskatchewan, Canada
AND
E. KOSTINER
Baker Laboratory of Chemistry, Cornell University, Ithaca, New York 14850

PHYSICAL REVIEW B 80, 220402(R) (2009)

Multiferroicity and spiral magnetism in $FeVO_4$ with quenched Fe orbital moments

A. Daoud-Aladine,[1,*] B. Kundys,[2] C. Martin,[2] P. G. Radaelli,[1,3] P. J. Brown,[4] C. Simon,[2] and L. C. Chapon[1]

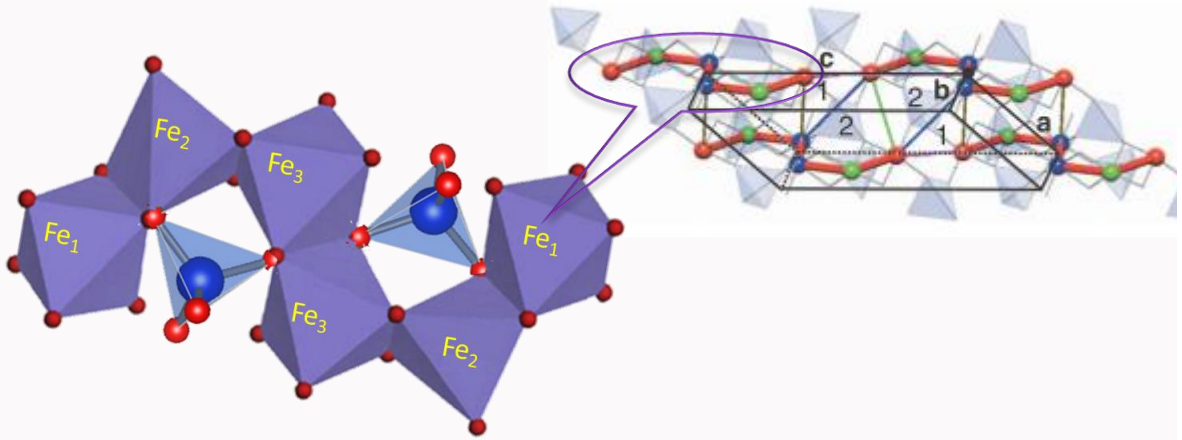

Magnetic transitions at $T_{N_1} = 22\text{K}$ and $T_{N_2} = 15\text{K}$
Ferroelectric below 15 K

Which is the role of role of local atomic structure?

Heat capacity

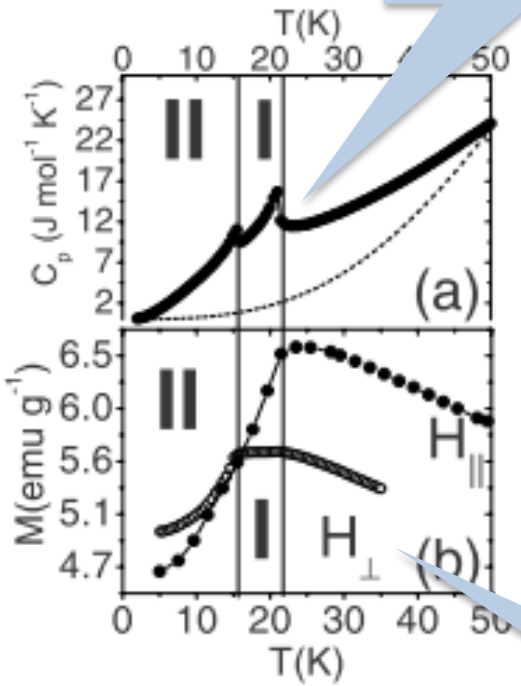

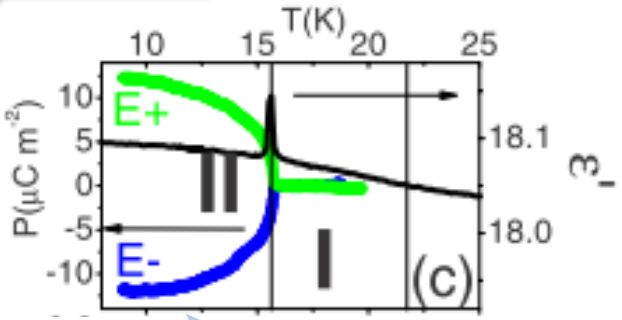

Electric polarization for sample cooled in a positive E^+ or negative E^- electric field (ϵ: dielectric constant)

Magnetization

Multiferroicity and Local structure in $FeVO_4$

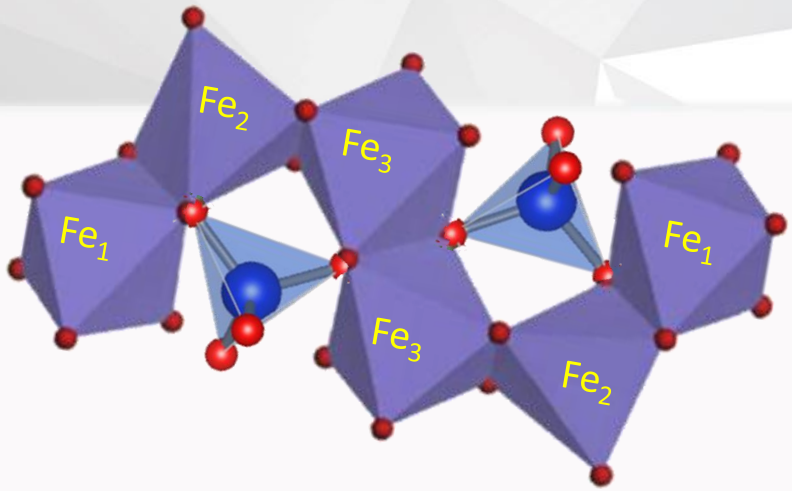

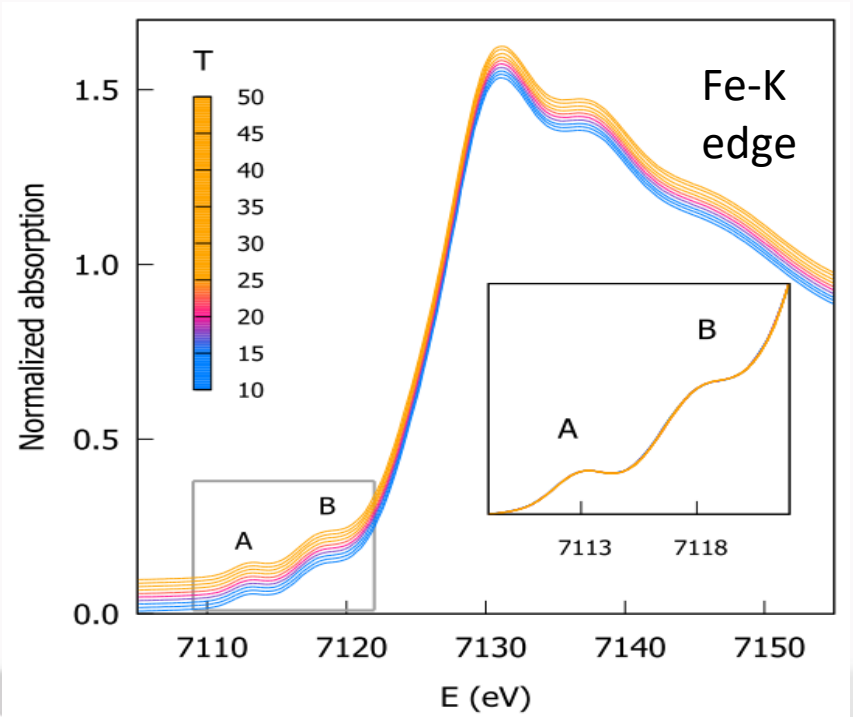

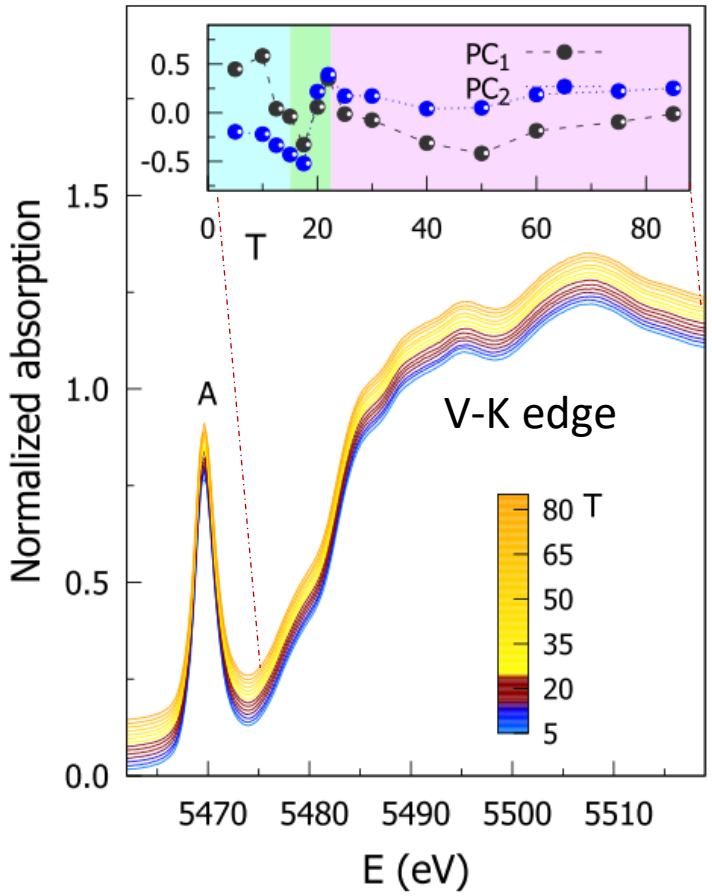

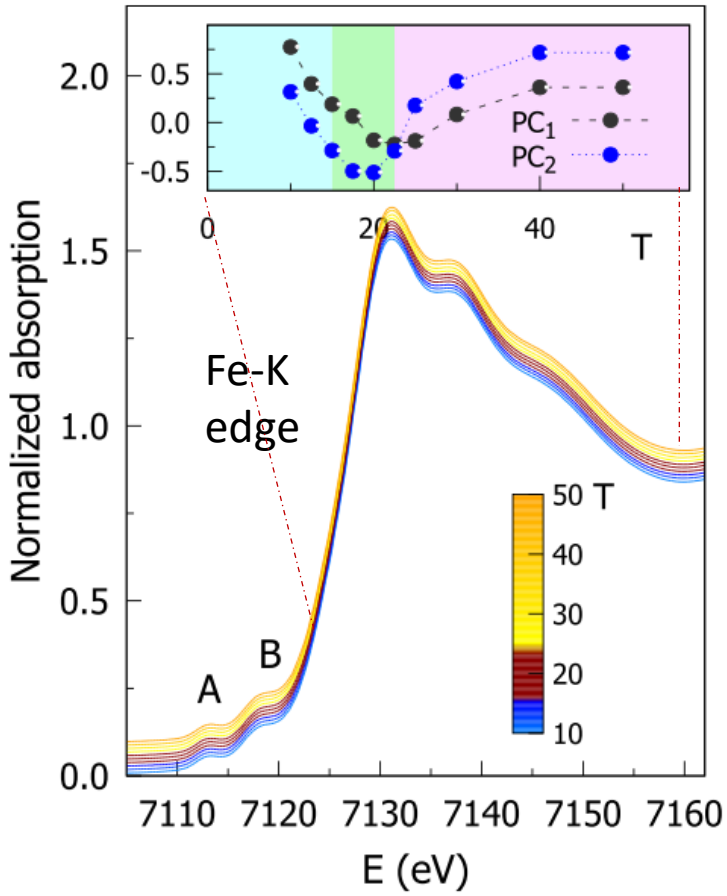

microstructural distortions reveal changes in the SSE interactions along the $Fe^{3+}OV^{5+}OFe^{3+}$ pathways

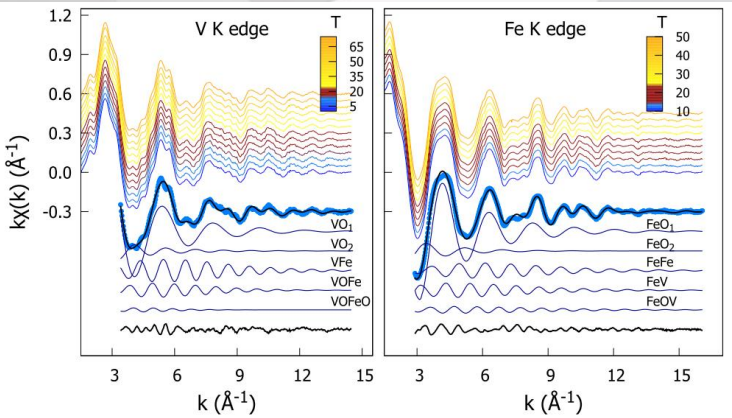

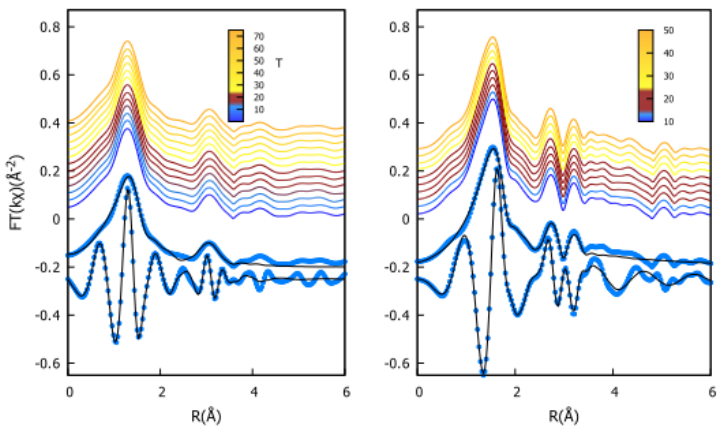

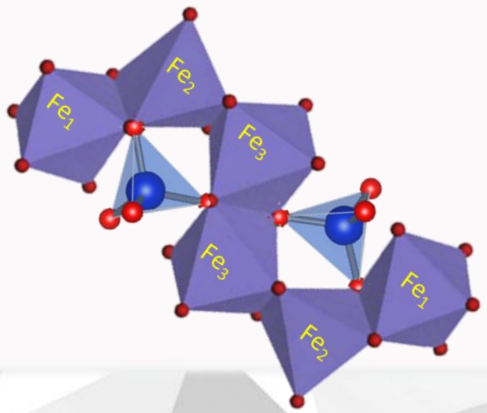

No changes in the FeO_6 or VO_4 units

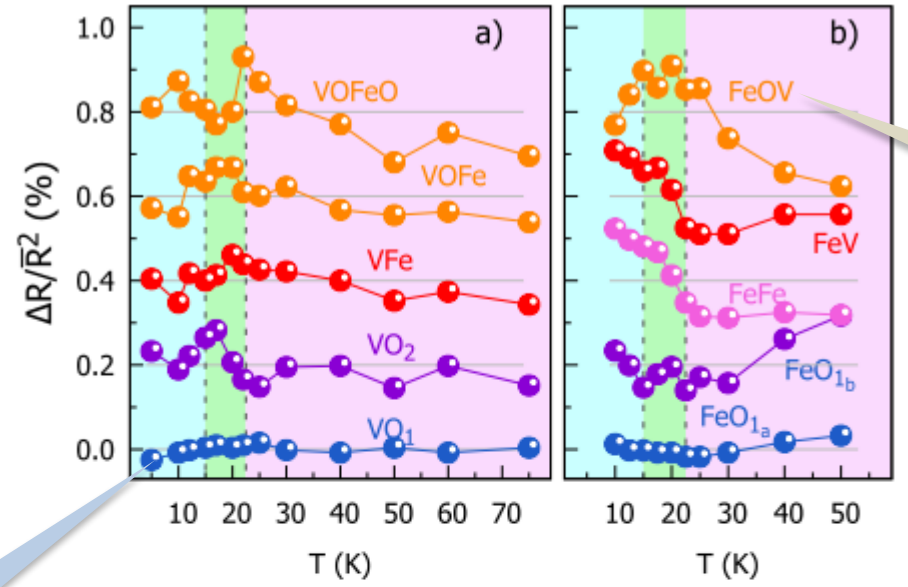

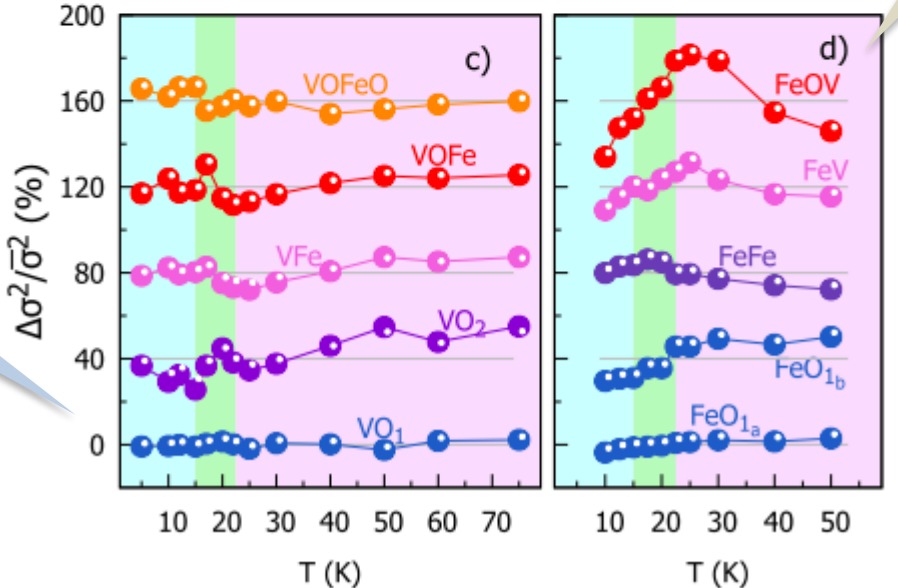

Changes of $FeO_6 - VO_4$ connectivity

Medium range order and ferroelectricity in $Bi_5FeTi_3O_{15}$ ceramics

PCA XANES **PCA pre-edge**

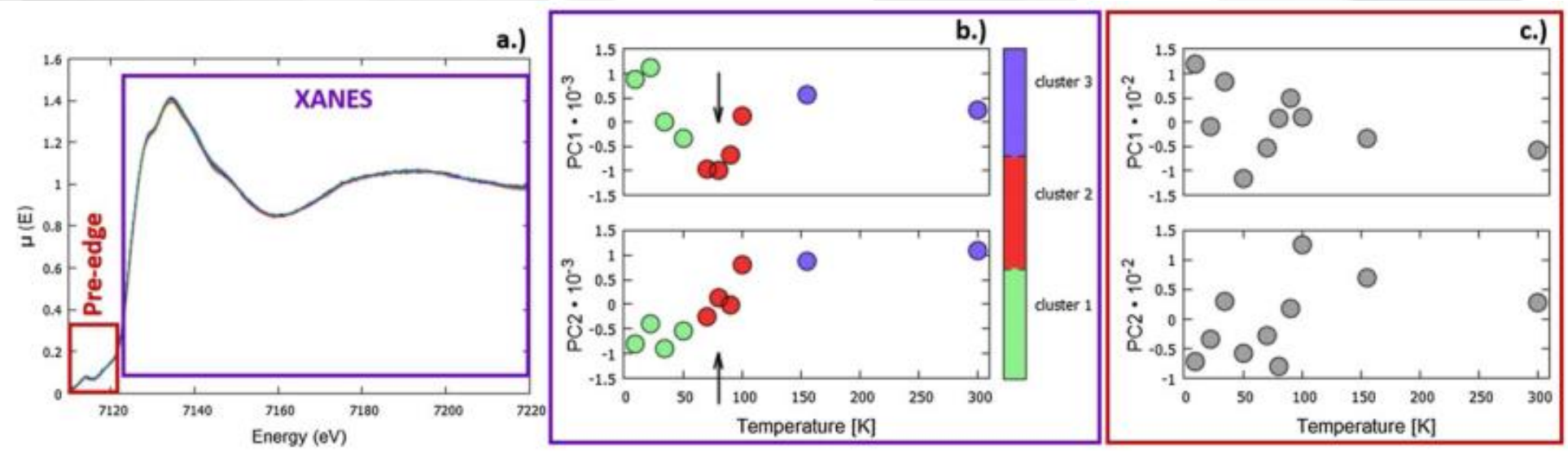

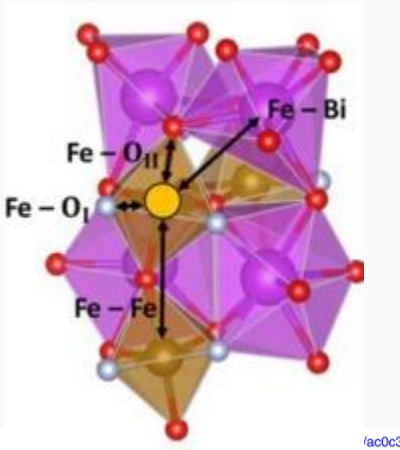

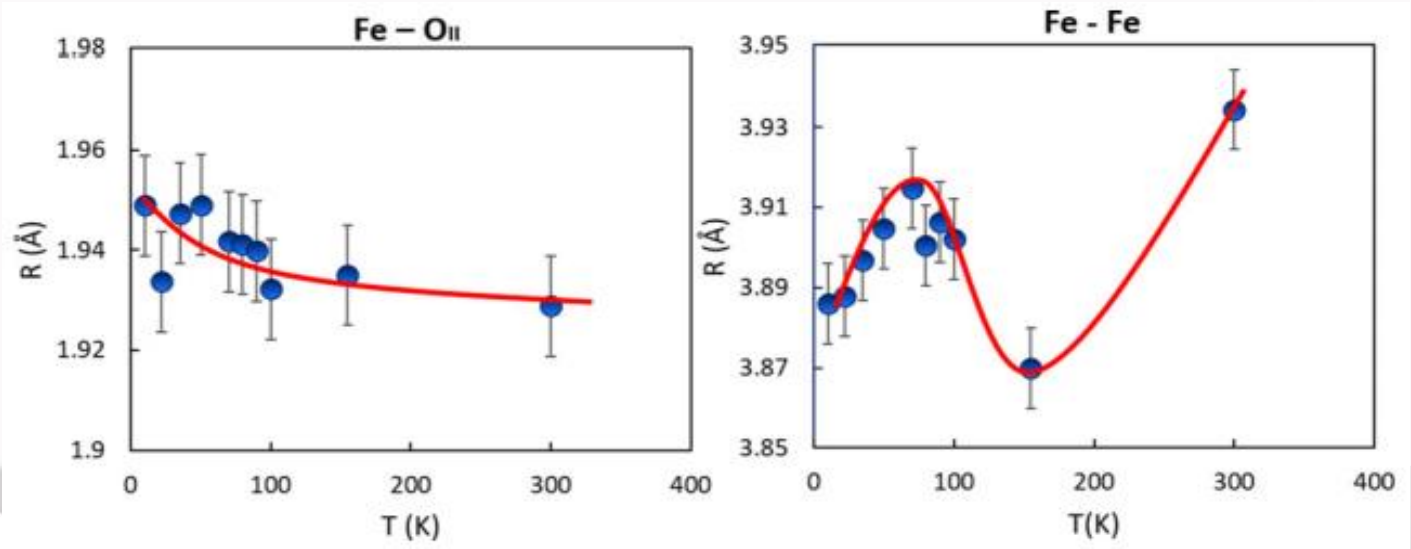

J. Phys.: Condens. Matter **0** (2021) 000000 (11pp)

Lattice assisted dielectric relaxation in four-layer Aurivillius $Bi_5FeTi_3O_{15}$ ceramic at low temperatures

Deepak Prajapat[1], Akash Surampalli[1], Irene Schiesaro[2], S D Kaushik[3], Carlo Meneghini[2], Archna Sagdeo[4,5], V G Sathe[1], V Siruguri[3], Edmund Welter[6] and V Raghavendra Reddy[1]

Thanks for…

Carlo Meneghini

carlo.meneghini@uniroma3.it